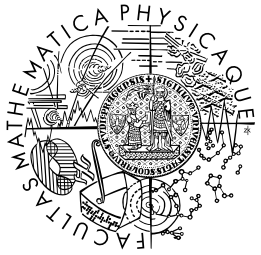

FACULTY
OF MATHEMATICS
AND PHYSICS
Charles University

DOCTORAL THESIS

Tereza Uhlířová

Violation and Conservation of Symmetries in Atomic Systems

Department of Chemical Physics and Optics

Supervisor of the doctoral thesis: doc. Mgr. Jaroslav Zamastil, Ph.D.

Study programme: Physics

Study branch: Biophysics, Chemical and Macromolecular Physics

Prague 2023

I declare that I carried out this master thesis independently, and only with the cited sources, literature and other professional sources. It has not been used to obtain another or the same degree.

I understand that my work relates to the rights and obligations under the Act No. 121/2000 Sb., the Copyright Act, as amended, in particular the fact that the Charles University has the right to conclude a license agreement on the use of this work as a school work pursuant to Section 60 subsection 1 of the Copyright Act.

In Prague, 3. 2. 2023 Tereza Uhlířová

I wish to thank my supervisor, doc. Mgr. Jaroslav Zamastil, Ph.D., for his patient and devoted guidance, encouragement and valuable advice during the research and both my master and PhD studies. I am also grateful to my family and friends for their unceasing support not only throughout my whole studies.

Title: Violation and Conservation of Symmetries in Atomic Systems

Author: Tereza Uhlířová

Department: Department of Chemical Physics and Optics

Supervisor: doc. Mgr. Jaroslav Zamastil, Ph.D., Department of Chemical Physics and Optics

Abstract:

This thesis focuses on the three pillars of any high-precision *ab initio* calculation: on the Hartree-Fock (HF) model, on the choice of a suitable basis set, and on the inclusion of electron correlation.

We start with a study of singular properties of the HF model. Specifically, we systematically investigate the stability of all atomic closed-shell systems up to xenon using a symmetry-adapted Thouless stability matrix. To obtain a global view on the stability of a particular isoelectronic sequence, we employ high-order perturbative method and then analyze the obtained series. This allows us to determine onsets of spin and orbital symmetry breaking. In addition, we also propose a physical meaning of the instabilities.

In the next part of this thesis, we focus on the use of the Sturmian basis set for relativistic calculations. We propose a numerically stable algorithm for the evaluation of one- and two-electron matrix elements. Thus we defeat the major impediment of a wider use of this basis set in precise atomic structure calculations. The use of the proposed method and its significance is illustrated on a series of calculations. For instance, we evaluate the so-called parity non-conserving amplitude for cesium; this is a second-order property and thus greatly depends on the accuracy of the used wave functions.

The last part of this thesis deals with the inclusion of electron correlation. We use the well-known coupled cluster (CC) method for closed shells and a combined configuration interaction-CC (CI-CC) method for one-electron open shells. We take advantage of the spherical symmetry of atoms and propose a symmetry-adapted form of the CC and CI-CC approaches; this idea significantly reduces the number of terms to be evaluated as well as the number of equations to be solved. This method is illustrated on the ionization energies of I.A elements.

Keywords: Hartree-Fock, Dirac-Hartree-Fock, coupled cluster method, configuration interaction, electron correlation, symmetry breaking, adaptation to symmetry

Contents

List of Abbreviations

BS	broken-symmetry
CC	coupled cluster
CCD	coupled cluster doubles
CCSD	coupled cluster singles and doubles
EOM-CC	equation-of-motion coupled cluster
CG	Clebsch-Gordan
CI	configuration interaction
FCI	full configuration interaction
DFT	density functional theory
DHF	Dirac-Hartree-Fock
EM	electromagnetic
EW	electroweak
HF	Hartree-Fock
RHF	Restricted Hartree-Fock
UHF	Unrestricted Hartree-Fock
PNC	parity non-conservation
SA	symmetry-adapted
SC (SCF)	self-consistent (self-consistent field)
SI	Supplementary Information
SM	Standard Model
lhs	left-hand side
rhs	right-hand side

Notation

In Chapters 2 – 5, we will use the following notation:

Z, $z = 1/Z$	nuclear charge, inverse of nuclear charge
N	number of electrons
$\|a\rangle$, $\|A\rangle$	spin-orbitals, orbitals, or shells
$\hat{\mathsf{z}}$	one-particle operator
$\hat{\mathsf{v}}$	two-particle operator
$\hat{\mathsf{f}}$	Fock operator
$\hat{\mathsf{h}}_0$	one-particle Hamiltonian for an electron moving in a potential field due to a nucleus
$\hat{\mathsf{r}}_{12}$	distance between two electrons
ε	spin-orbital (or orbital) (Dirac-)Hartree-Fock energy
E	total energy
E_{HF}	total (Dirac-)Hartree-Fock energy
ΔE	correlation energy
$\mathsf{\Lambda}$, λ	stability matrix, its eigenvalue
$\hat{\mathbf{S}}$, $\hat{\mathsf{S}}_z$, $\hat{\mathsf{S}}^2$	spin operator, its z-component, and its square
$\hat{\mathbf{L}}$, $\hat{\mathsf{L}}_z$, $\hat{\mathsf{L}}^2$	angular momentum operator, its z-component, and its square
$\hat{\mathbf{J}}$, $\hat{\mathsf{J}}_z$, $\hat{\mathsf{J}}^2$	total angular momentum operator, its z-component, and its square
$\hat{\mathsf{\Pi}}$	parity operator
$\hat{\mathsf{K}}$	relativistic parity operator
$\hat{\mathsf{G}}$	G operator
$\mathcal{P}_{12}$	permutation of 1 and 2
$\mathcal{A}_{ab}$, $\mathcal{A}^{ab}$	antisymmetrization of a and b
$\mathcal{A}_{abc}$, $\mathcal{A}^{abc}$	antisymmetrization of a, b and c, even permutations only
$\mathcal{P}_{abc}$, $\mathcal{P}^{abc}$	antisymmetrization of a, b and c, all permutations
α	fine-structure constant, $\alpha = 1/137.0359991$ [1]

Introduction

In his 1991 speech during a workshop on electron correlation, J. Čížek, the father of the well-known coupled cluster method and one of the most prominent figures of the 20th century quantum chemistry, remembers: "Around 1960 there were three outstanding problems in the quantum theory of atoms and molecules: the calculation of molecular integrals, seeking a satisfactory solution of the Hartree-Fock problem for molecules and the problem of the correlation energy." [2] Nowadays, more than sixty years later and after a gigantic boom of the computational power, these three problems seem to have been more or less resolved. The Gaussian functions have become a prevalent basis for very cheap evaluation of atomic and molecular integrals. Calculations on the Hartree-Fock (HF) level are now a dime a dozen. Post-HF methods such as the coupled clusters (CC) or configuration interaction (CI) for the inclusion of correlation energy have become commonplace as well. In addition, the current quantum chemistry world is rife with other not fully *ab initio* approaches such as the density functional theory (DFT) or semi-empirical methods.

While the above-mentioned solutions may be satisfactory for mundane problems, once we near the high-precision frontiers of modern physics and chemistry, we will discover that we are still facing the very same three obstacles. The Gaussian functions are not suitable for a correct description of the behavior of orbital wave functions at large distances from the nucleus, and hence for the description of excited states. The hydrogen-like Slater functions are sometimes used as an alternative; however, they retain the other major drawback inherent in the Gaussian functions: they are non-orthogonal and thus plagued with linear dependence. The non-linearity of the HF equations does not guarantee the unambiguity of the obtained solution (e.g., Is it the true energy minimum?). Yet a stable HF solution is essential for further post-HF calculations. Current implementations and truncations, mostly due to the limited computational resources, of the CC and CI methods do not allow one to always account for the electron correlation to satisfactory accuracy. Therefore, clearly, further methodological development is still necessary.

One of such cutting-edge and very difficult challenges of contemporary high-precision science is the study of the Standard Model (SM) and physics beyond it. One can, for example, perform extremely precise measurement and *ab initio* calculation of a very subtle effect known as parity violation. The combination of such measurement and calculation then yields one of the most stringent tests of the SM. However, the journey towards outstanding results is pathed with many obstacles and it usually takes several years to complete it; both experimentally and theoretically. In this thesis, we will focus on the latter and show how one can defeat the formidable challenges.

This thesis is structured as follows. In Chapter 1 we start with a brief introduction to the SM and electroweak (EW) theory. We explain parity violation in atoms and show how one can measure and calculate this effect. In the next Chapter 2 we introduce two concepts that will appear throughout this thesis: the well-known HF model and the so-called Sturmian functions. In Chapter 3 we study the HF model, which is the starting point of almost all high-quality *ab initio*

calculations, and focus on HF solutions and on their existence and properties. In the next part of this thesis, we head towards the development of new methodological tools for precise relativistic atomic structure calculations. In Chapter 4 we present an algorithm for numerically stable evaluation of one- and two-electron integrals between the Sturmian functions. This basis set of hydrogen-like functions allows for the most accurate calculations ever. In Chapter 5 we then continue to explore the world of electron correlation and the CC and CI methods while taking advantage of the atomic spherical symmetry.

The aim of this thesis is to present the problems and our contribution to its solution in a readable manner for a wider audience; details and mathematical derivations may be found in our pertinent papers [3, 4]. These two papers (both already published) are attached to this thesis. The content of Chapter 5 forms the basis for our next publication and will be submitted in few months. Some of the parts of the theoretical background and description of our specific approach were copied from the pertinent papers [3, 4] or its Supplementary Information (SI) as we believe that there we succeeded in formulating them in the best possible way.

A Fortran 2009 program called PASC (Precise Atomic Structure Calculations) has been developed from the scratch as a part of this thesis. This program is available from the authors upon reasonable request. The first part of the program, which includes the algorithm for the evaluation of one- and two-electron matrix elements in the Sturmian basis for both relativistic and non-relativistic calculations, the non-relativistic HF and relativistic Dirac-HF (DHF) procedures, and procedures for evaluation of the PNC amplitude and other atomic properties, see Chapter 4, is also accessible via the *Comput. Phys. Commun.* repository, see [4]. The second part of this program containing the CC and CI procedures is expected to be submitted also to the *Comput. Phys. Commun.* journal and added to their repository.

1. Motivation

1.1 The Standard Model and Beyond

In 1973, when the current formulation of the SM of fundamental constituents and interactions was finalized, only eight particles were known experimentally: electron and its neutrino, muon and its neutrino, three quarks (u, d, s), and photon. The SM predicted the existence of nine other particles: tauon and its neutrino, another three quarks (c, t, b), $W^{\pm}$ bosons, Z^0 boson, and the famous Higgs boson. All of them were experimentally discovered (mostly with predicted properties) in the succeeding years; the last one was the Higgs boson in 2012.

Unfortunately, the much celebrated discovery of the Higgs boson also marked the beginning of what is sometimes called the "nightmare scenario at the LHC". We are certain that the SM is incomplete as, for example, neutrino oscillations and dark matter indicate. However, high-energy collision experiments have not lead to anything new after the great Higgs discovery. Moreover, we even lack bright theoretical ideas as what type of experiments to conduct or at what energy scale to look for new physics. Yet the cost of the construction and upkeep of large accelerators is astronomical. For example, the CERN proposal for a new supercollider asks for more than 21 billion euros [5].

In this situation, precise low-energy tests of the SM offer one of the viable possibilities how to proceed further in our exploration of fundamental physical laws. Nowadays, these are most notably rare decays of B-mesons and K-mesons (see, e.g., [6]) and violation of discrete symmetries in atomic spectroscopy (see, e.g., [7, 8, 9]), such as parity.

1.2 Parity Violation

In quantum mechanics, parity describes the symmetry of a wave function under the parity transformation, i.e., under the inversion of the coordinates: $\hat{\mathcal{P}} : \mathbf{r} \to -\mathbf{r}$. This transformation may be thought of as a replacement of the original state by its mirror image. If the wave function does not change the sign under this transformation, $\hat{\mathcal{P}} |\Psi\rangle = + |\Psi\rangle$, it is said to be of even parity; if it changes the sign, $\hat{\mathcal{P}} |\Psi\rangle = - |\Psi\rangle$, it is said to be of odd parity. Note that the square of the parity operator, regardless of the parity of the wave function, always gives the original state: $\hat{\mathcal{P}}^2 |\Psi\rangle = + |\Psi\rangle$. Thus, the physical observables, which depend on the square of the wave function, remain unchanged under parity transformations.

To illustrate the parity property, consider the spherical harmonics $Y_{l,m}(\mathbf{n})$ for example. As is usual, l denotes the orbital quantum number and m its possible projections $m = -l, -l+1, \ldots, l-1, l$, and $\mathbf{n}$ is the unit direction vector. The parity of $Y_{l,m}$ is $(-1)^l$ (see, e.g., [10] or any other textbook on quantum mechanics). Thus, for instance, as one can easily imagine recalling the orbital shapes from high-school chemistry, the spherical s-orbitals, for which $l = 0$ and hence the parity $(-1)^0 = 1$, do not change the sign under the coordinate inversion (i.e., are even), while the p-orbitals, for which $l = 1$ and hence the parity $(-1)^1 = -1$, do change the sign and thus are odd.

It had been long believed that the parity of an isolated system is conserved. However, in 1956 Lee and Young made the Nobel prize-winning suggestion that the parity may not be conserved in weak interactions [11]. The first experimental proof was provided by Wu et al. [12] one year later as her team observed anisotropic distribution of the electrons emitted in the β-decay of polarized ^{60}Co nuclei.

The theory was gradually completed in the 1960s by Glashow and Weinberg and is now known as the theory of EW interactions. It unites the electromagnetic (EM) and weak interactions and constitutes a part of the SM. It predicts the existence of three types of forces: the well-known EM interactions mediated by photons, the weak interactions mediated by the charged $W^{\pm}$ bosons, and the EW interactions mediated by neutral Z^0 bosons.

One of the predictions of this EW theory is that an electron and a nucleus of an atom exchange a Z^0 boson, see Fig. 1.1 for illustration. This interaction gives rise to an observable effect known as *atomic parity violation* or more often termed *atomic parity non-conservation* (PNC) and is quantified via a so-called PNC amplitude $\mathcal{E}_{\rm PNC}$.

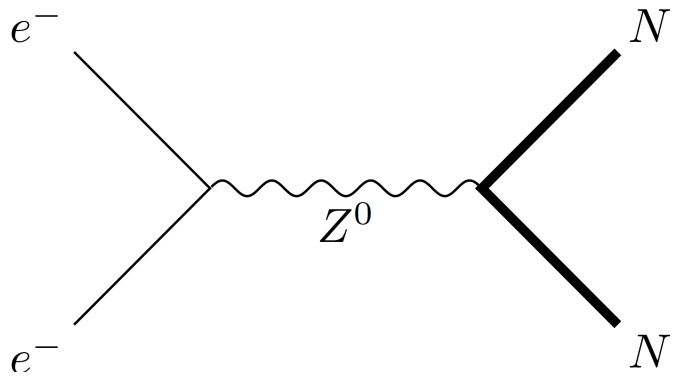

Figure 1.1: Exchange of a Z^0 boson between an electron (e^-) and a nucleus (N).

The PNC effect has been firmly experimentally established in several heavy atoms, see Chapter 1.3. When these experiments are accompanied by very precise theoretical calculations, see Chapter 1.4, they yield the most precise low energy tests of the SM. This in turn puts strong lower bounds on masses of additional hypothetical particles mediating the PNC interactions. If the SM is established on some level of accuracy, the precise theory and experiment yield hitherto unknown aspects of nuclear properties such as neutron skin and parity violating nuclear interactions, see, e.g., [7, 8, 9].

For example, the combination of a precise measurement and precise atomic structure calculation allows us to "weigh" the $W^{\pm}$ and Z^0 bosons. From the comparison of the experiment and theory one can deduce the value of the so-called weak nuclear charge Q_W and hence of the weak mixing angle ϑ (also known as the Weinberg angle), see Chapter 1.4. Note that ϑ is the only parameter of the EW theory (unlike, for instance, the many parameters of the once famous string theory). The currently best calculation [13] and measurement [14, 15] of the PNC amplitude for cesium give

$$\sin^2\vartheta = 0.2356(20)\,.$$

This in turn yields the masses of the $W^{\pm}$ and Z^0 bosons:

$$m_W = \sqrt{\frac{\alpha\pi}{\sqrt{2}G_\beta \sin^2\vartheta}} \simeq 79\,\mathrm{GeV}\,,$$
$$m_Z = \frac{m_W}{\cos\vartheta} \simeq 90\,\mathrm{GeV}\,.$$

Here, G_β is the Fermi constant determined from the neutron lifetime, $\sqrt{2}$ comes from the historical definition of G_β, and α is the fine-structure constant. Note that this simple result is correct up to corrections at the order of α (and higher) [16]. This spectroscopic "weighing" can be then compared with the masses of the $W^{\pm}$ and Z^0 bosons that were determined from the positions of resonances in high-energy electron-positron annihilation experiments, $m_W \simeq 80\,\mathrm{GeV}$ and $m_Z \simeq 91\,\mathrm{GeV}$. As Fig. 1.2 illustrates, there is still a large discrepancy among the high-energy results. Therefore, clearly, a low-energy input, which is completely independent of the high-energy experiments, could help to settle this issue.

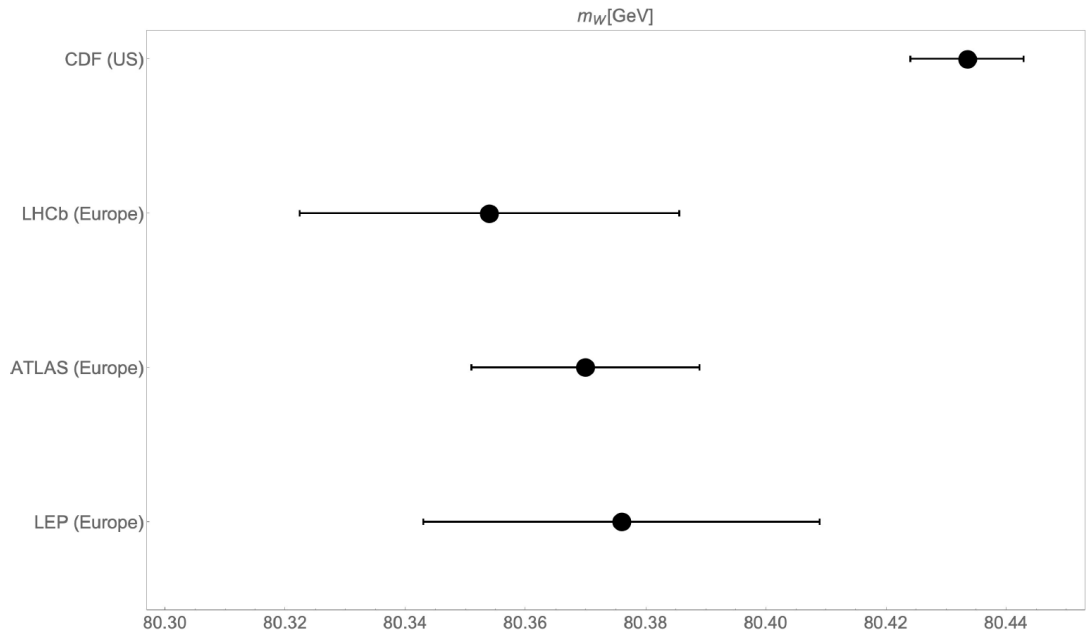

Figure 1.2: Determination of the mass of the $W^{\pm}$ bosons, m_W, in a variety of high-energy collision experiments. Clearly, the exact value of m_W is still uknown. This figure was taken from [17].

1.3 Measurement of PNC

The PNC effect has been successfully measured only on a few 6th-row heavy elements: Cs [14, 15, 18], Yb [19, 20, 21], Tl [22, 23], Pb [24, 25, 26] and Bi [27], and experimental detection of the PNC in chiral molecules is still to be achieved. This subtle effect is usually measured using Stark interference (Cs, Yb) or so-call optical rotation (Bi, Pb, Tl) technique. We will focus here on the former approach, which yielded the so far most accurate result (for cesium). For an overview of the latter, see, e.g., the review [7] or directly the cited papers.

The most famous is the experiment of the C. Wieman group at CU Boulder from 1997 [15], see also [14]. After 7 years of apparatus development and 5 years of studying potential systematic errors, they obtained the so far most precise measurement on the cesium atom. The experimental set up is shown in Fig. 1.3. A beam of cesium atoms leaves the cavity and enters the interaction region, where there are mutually perpendicular static homogeneous magnetic **B** and electric **E** fields[1]. The cesium atoms are excited from their ground $6S$ state to the $7S$ state by a dye laser with polarization $\boldsymbol{\epsilon}$ and one then detects the number of photons from the spontaneous decay via the $6P_{1/2}$ and $6P_{3/2}$ states, see the scheme with the cesium energy levels in Fig. 1.4. One detects the photons with wavelengths 852 nm and 894 nm.

The thus obtained signal is a combination of a very strong Stark contribution, very weak magnetic dipole transition, and an even more subtle PNC contribution. The amplitude for the transition is, cf. Chapter 1.4,

$$|\mathcal{A}_{6S\to 7S}|^2 \simeq E^2\beta^2\epsilon_z^2 \pm 2E\beta\left(\mathcal{E}_{\rm PNC}^{\rm exp}\epsilon_z\epsilon_x + M\epsilon_z^2\right) ; \tag{1.1}$$

E is the strength of the external electric field **E**, β the vector transition polarizability, here M the magnetic dipole moment, and $\mathcal{E}_{\rm PNC}^{\rm exp}$ the PNC amplitude, see the next Chapter 1.4 for precise definition. We can see from this expression that the biggest experimental challenge is the elimination of the magnetic transition which mimics the true PNC contribution. This is achieved by changing the polarization ϵ_x of the standing wave laser. To eliminate additional potential systematic errors, one also reverses the direction of the magnetic and electric fields and changes the Zeeman levels from which and to which one excites. Finally, the PNC signal is observed as modulation of the obtained signal (this is the ratio of the second to the first term on the rhs of Eq. (1.1)):

$$\Delta_{PNC} = 2\frac{\epsilon_x\mathcal{E}_{\rm PNC}^{\rm exp}}{E\epsilon_z\beta} .$$

Note that the experiment provides us with the ratio $\mathcal{E}_{\rm PNC}^{\rm exp}/\beta$, so one needs to determine β to be able to extract the PNC amplitude. So far the most accurate value, $\beta = 26.957(51)a_{\rm B}^3$ (where $a_{\rm B}$ is the Bohr radius), comes from [28, 29], see also [30, 31, 32]. Typical experimental conditions were $E = 2.5$ kV/cm, $B = 70$ G and $\epsilon_x/\epsilon_z = 0.94$ giving $\Delta_{\rm PNC}$ of $(1-2)\times 10^{-6}$. Note that the detection of these very few photons is like looking for a needle in a haystack.

1.4 Calculation of PNC

In the theoretical treatment, the description of the EW interactions amounts to adding an extra potential term to the one-particle Dirac Hamiltonian (in natural units):

$$\hat{\mathsf{H}}_{\rm PNC} = \frac{G_\beta}{\sqrt{8}}\rho_W(\mathbf{r})\gamma_5 , \tag{1.2}$$

[1]The electric field is applied to allow the otherwise highly forbidden $6S \to 7S$ transition and to enhance the PNC effect via interference. The magnetic field is introduced to break the degeneracy in the projection of the total angular momentum M of the atomic states. The PNC contribution depends on M, and thus if the energy levels were degenerate, the net contribution would be zero.

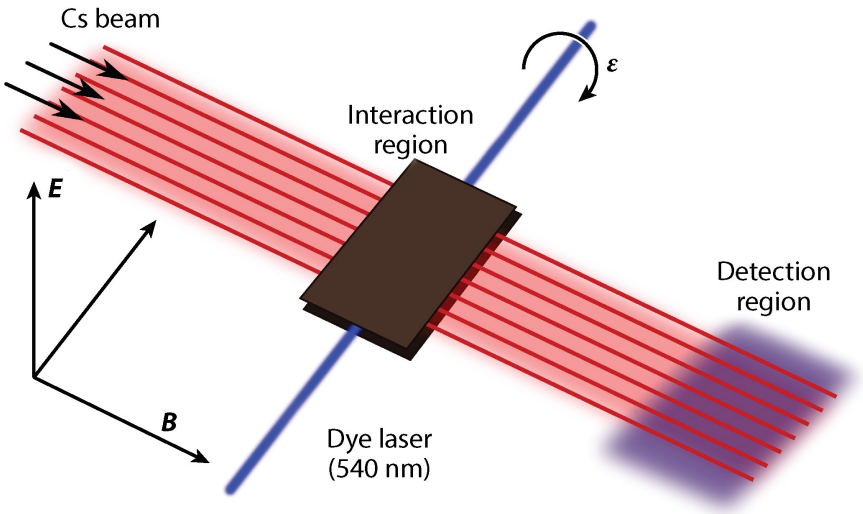

Figure 1.3: Experimental set up for the measurement of the PNC amplitude on Cs via Stark interference (Fig. 3 in [7]).

γ_5 is the Dirac matrix. ρ_W is the so-called weak charge density and is given in terms of the proton and neutron densities, ρ_Z and ρ_N, respectively:

$$\rho_W(\mathbf{r}) = \rho_Z(\mathbf{r})(1 - 4\sin^2\vartheta) - \rho_N(\mathbf{r})\,.$$

If, in the first approximation, we consider the above densities to be given by the nuclear density $\rho(\mathbf{r})$ as

$$\rho_Z(\mathbf{r}) = Z\rho(\mathbf{r})\,, \quad \rho_N(\mathbf{r}) = N\rho(\mathbf{r})\,, \quad \rho_W(\mathbf{r}) = Q_W\rho(\mathbf{r})\,,$$

where clearly Z is the nuclear charge and N the number of the neutrons, the above expression reduces to

$$Q_W = Z(1 - 4\sin^2\vartheta) - N\,. \tag{1.3}$$

We can see the two main features of this interaction now. First, it is parity violating; that is, it mixes states of different parity, namely an S-state and a $P_{1/2}$ state. Second, the interaction is really weak. Changing to atomic units in (1.2), we find that the interaction is proportional to

$$Q_W G_\beta m_e^3 (Z\alpha)^4 \simeq m_e(Z\alpha)^2 \left[10^{-5}\left(\frac{m_e}{m_p}\right)^2 \alpha^2\right] Q_W Z^2\,,$$

where we substituted $G_\beta \simeq 1 \times 10^{-5} m_p^{-2}$. m_e is the electron mass, m_p the proton mass and $m_e/m_p \simeq 10^{-3}$, and $\alpha = 1/137.0359991$ is the fine-structure constant [1]. The factor in the square brackets on the rhs is thus of the order 10^{-15}. However, given that $Q_W \approx Z$, there is an enhancement of the interaction strength by the factor Z^3 for heavy atoms. Indeed, as already mentioned, this effect has been observed only on the heavy 6th-row elements.

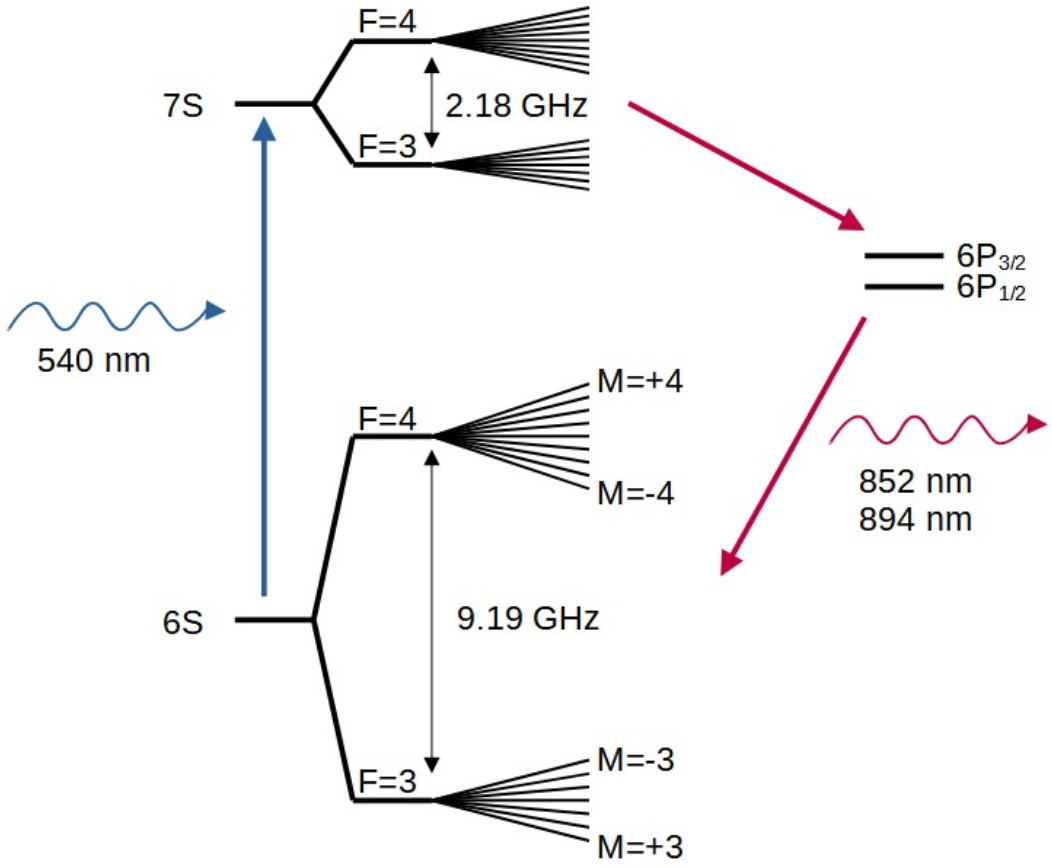

Figure 1.4: Energy levels in cesium with hyperfine structure and weak-field Zeeman structure. Cesium atoms are excited from the $6S$ to the $7S$ states by a dye laser (in blue). Photons from the decay via $6P_{3/2}$ and $6P_{1/2}$ states to the $6S$ ground state (in red) are detected. Scheme adapted from [14].

The expression for the PNC amplitude is obtained as follows, see, e.g., [14]. We consider a dipole transition from an intial state $|\mathrm{I}\rangle$ to a final state $|\mathrm{F}\rangle$; the amplitude of such a transition is proportional to

$$\mathcal{A}_{\mathrm{FI}}^{\mathrm{dip}} = \mathcal{A}_{\mathrm{FI}}^{\mathrm{el}} + \mathcal{A}_{\mathrm{FI}}^{\mathrm{mag}} = -\langle \mathrm{F}| \boldsymbol{\epsilon} \cdot \hat{\mathbf{d}} |\mathrm{I}\rangle - \langle \mathrm{F}| (\boldsymbol{\eta} \times \boldsymbol{\epsilon}) \cdot \hat{\boldsymbol{\mu}} |\mathrm{I}\rangle \ . \tag{1.4}$$

Two terms describe the electric $\mathcal{A}_{\mathrm{FI}}^{\mathrm{el}}$ and magnetic $\mathcal{A}_{\mathrm{FI}}^{\mathrm{mag}}$ contributions, respectively. $\hat{\mathbf{d}}$ stands for the electric dipole operator and $\hat{\boldsymbol{\mu}}$ for magnetic dipole moment. $\boldsymbol{\epsilon}$ is the polarization of EM radiation inducing the transition, $\boldsymbol{\eta}$ the direction of propagation of the EM wave.

Now, we use the perturbative theory: the non-perturbed Hamiltonian $\hat{\mathsf{H}}_0$ is the Hamiltonian $\hat{\mathsf{H}}_{\mathrm{at}}$ of a free atom (i.e., with no external field),

$$\hat{\mathsf{H}}_0 = \hat{\mathsf{H}}_{\mathrm{at}} \, .$$

Its eigenstates are the (total) states of a free atom $|F, I, J, M_F\rangle$. They are defined by the combined spin and orbital angular momentum of the electrons, $\hat{\mathbf{J}} = \hat{\mathbf{S}} + \hat{\mathbf{L}}$ (hence the quantum number J), the spin of the nucleus, $\hat{\mathbf{I}}$ (hence I), and the

total angular momentum state of the electrons and the nucleus, $\hat{\mathbf{F}} = \hat{\mathbf{J}} + \hat{\mathbf{I}}$ (hence F and M_F). Here, we will label the states $\left|\mathrm{I}^{(0)}\right\rangle$ and $\left|\mathrm{F}^{(0)}\right\rangle$ for simplicity;

$$\hat{\mathsf{H}}_{\mathrm{at}} \left|\mathrm{I}^{(0)}\right\rangle = E_{\mathrm{I}}^{(0)} \left|\mathrm{I}^{(0)}\right\rangle$$

and similarly for the final state $\left|\mathrm{F}^{(0)}\right\rangle$.

The perturbative term $\hat{\mathsf{H}}_1$ comprises the Stark interaction with the external static electric field with intensity $\mathbf{E}$ and the PNC interaction with the nucleus, Eq. (1.2),

$$\hat{\mathsf{H}}_1 = -\mathbf{E} \cdot \hat{\mathbf{d}} + \hat{\mathsf{H}}_{\mathrm{PNC}} \,.$$

The first-order correction to the wave function of the initial state is thus

$$|\mathrm{I}\rangle \simeq \left|\mathrm{I}^{(0)}\right\rangle + \left|\mathrm{I}^{(1)}\right\rangle \,, \tag{1.5}$$

$$\left|\mathrm{I}^{(1)}\right\rangle = -\frac{1}{\hat{\mathsf{H}}_{\mathrm{at}} - E_{\mathrm{I}}^{(0)}} \hat{\mathsf{H}}_1 \left|\mathrm{I}^{(0)}\right\rangle \,, \tag{1.6}$$

and similarly for the final state $|\mathrm{F}\rangle$.

For the electric part $\mathcal{A}_{\mathrm{FI}}^{\mathrm{el}}$ of the amplitude (1.4) we consider the expansion to the first order, Eqs. (1.5) and (1.6); we thus obtain

$$\mathcal{A}_{\mathrm{FI}}^{\mathrm{el}} = \left\langle \mathrm{F}^{(0)} \right| \left[\hat{\mathsf{H}}_1 \frac{1}{\hat{\mathsf{H}}_{\mathrm{at}} - E_{\mathrm{F}}^{(0)}} \boldsymbol{\epsilon} \cdot \hat{\mathbf{d}} + \boldsymbol{\epsilon} \cdot \hat{\mathbf{d}} \frac{1}{\hat{\mathsf{H}}_{\mathrm{at}} - E_{\mathrm{I}}^{(0)}} \hat{\mathsf{H}}_1 \right] \left| \mathrm{I}^{(0)} \right\rangle \,.$$

We can separate the Stark and the PNC contribution $\mathcal{A}_{\mathrm{FI}}^{\mathrm{el}} = \mathcal{A}_{\mathrm{FI}}^{\mathrm{Stark}} + \mathcal{A}_{\mathrm{FI}}^{\mathrm{PNC}}$,

$$\mathcal{A}_{\mathrm{FI}}^{\mathrm{Stark}} = -E_i \epsilon_j \left\langle \mathrm{F}^{(0)} \right| \left[\hat{\mathsf{d}}_i \frac{1}{\hat{\mathsf{H}}_{\mathrm{at}} - E_{\mathrm{F}}^{(0)}} \hat{\mathsf{d}}_j + \hat{\mathsf{d}}_j \frac{1}{\hat{\mathsf{H}}_{\mathrm{at}} - E_{\mathrm{I}}^{(0)}} \hat{\mathsf{d}}_i \right] \left| \mathrm{I}^{(0)} \right\rangle \,, \tag{1.7}$$

$$\mathcal{A}_{\mathrm{FI}}^{\mathrm{PNC}} = \epsilon_i \left\langle \mathrm{F}^{(0)} \right| \left[\hat{\mathsf{H}}_{\mathrm{PNC}} \frac{1}{\hat{\mathsf{H}}_{\mathrm{at}} - E_{\mathrm{F}}^{(0)}} \hat{\mathsf{d}}_i + \hat{\mathsf{d}}_i \frac{1}{\hat{\mathsf{H}}_{\mathrm{at}} - E_{\mathrm{I}}^{(0)}} \hat{\mathsf{H}}_{\mathrm{PNC}} \right] \left| \mathrm{I}^{(0)} \right\rangle \,, \tag{1.8}$$

The expression for the Stark amplitude (1.7) is parametrized

$$\mathcal{A}_{\mathrm{FI}}^{\mathrm{Stark}} = -\frac{\alpha}{3} \mathbf{E} \cdot \boldsymbol{\epsilon} \delta_{\mathrm{FI}} - i\beta \left(\boldsymbol{\epsilon} \times \mathbf{E} \right) \cdot \left(\boldsymbol{\sigma} \right)_{\mathrm{FI}} \,;$$

α is the scalar polarizability, β the vector polarizability (see also Chapter 1.3), and $(\boldsymbol{\sigma})_{\mathrm{FI}}$ elements of the Pauli matrices between the final and initial atomic states, $(\boldsymbol{\sigma})_{\mathrm{FI}} = \left\langle \mathrm{F}^{(0)} \right| \boldsymbol{\sigma} \left| \mathrm{I}^{(0)} \right\rangle$. This parametrization is motivated by the fact that the term in the brackets in the expression for the Stark amplitude (1.7) is a tensor T_{ij} and can be decomposed into irreducible elements (a sum of a scalar, a vector and a tensor part, respectively)

$$T_{ij} = \frac{T}{3} \delta_{ij} + \frac{1}{2} \left(T_{ij} - T_{ji} \right) + \left[\frac{1}{2} \left(T_{ij} + T_{ji} \right) - \frac{T}{3} \delta_{ij} \right] \,.$$

The vector part can be further rewritten $1/2 \left(T_{ij} - T_{ji} \right) = 1/2 \epsilon_{ijk} V_k$; ϵ_{ijk} is the Levi-Civita symbol. The tensor part does not contribute.

The expression for the PNC contribution, Eq. (1.8), is parametrized as

$$\mathcal{A}_{\mathrm{FI}}^{\mathrm{PNC}} = i \, \mathrm{Im} \mathcal{E}_{\mathrm{PNC}} \, \boldsymbol{\epsilon} \cdot \left(\boldsymbol{\sigma} \right)_{\mathrm{FI}} \,. \tag{1.9}$$

Here, $\mathrm{Im}\mathcal{E}_{\mathrm{PNC}}$ (a number) is the quantity known as the PNC amplitude that we want to calculate.

The magnetic dipole contribution, see Eq. (1.4), which is already very weak, is considered only in the lowest order of the perturbative method. Further, the magnetic dipole is parametrized $\hat{\boldsymbol{\mu}} = M\boldsymbol{\sigma}$ (M is a number, see also Eq. (1.1)). We thus obtain

$$\mathcal{A}_{\mathrm{FI}}^{\mathrm{mag}} = -M\,(\boldsymbol{\eta}\times\boldsymbol{\epsilon})\cdot(\boldsymbol{\sigma})_{\mathrm{FI}}\,.$$

The whole expression (1.4) for the transition amplitude thus becomes

$$\mathcal{A}_{\mathrm{FI}}^{\mathrm{dip}} = -\frac{\alpha}{3}\mathbf{E}\cdot\boldsymbol{\epsilon}\delta_{\mathrm{FI}} - i\beta\,(\boldsymbol{\epsilon}\times\mathbf{E})\cdot(\boldsymbol{\sigma})_{\mathrm{FI}} + i\ \mathrm{Im}\mathcal{E}_{\mathrm{PNC}}\ \boldsymbol{\epsilon}\cdot(\boldsymbol{\sigma})_{\mathrm{FI}} - M\,(\boldsymbol{\eta}\times\boldsymbol{\epsilon})\cdot(\boldsymbol{\sigma})_{\mathrm{FI}}\,. \tag{1.10}$$

This is the parametrization used by the experimentalists.

Now, we consider the experimental set up, see Chapter 1.3 and Fig. 1.3. The external electric field $\mathbf{E}$ is oriented along the x axis:

$$\mathbf{E} = (E,0,0)\,.$$

The exciting laser propagates along the y axis and is elliptically polarized

$$\begin{aligned}\boldsymbol{\eta} &= (0,1,0)\,,\\ \boldsymbol{\epsilon} &= (i\epsilon_x,0,\epsilon_z)\,.\end{aligned}$$

The expression for the amplitude, Eq. (1.10), thus becomes:

$$\begin{aligned}\mathcal{A}_{\mathrm{FI}}^{\mathrm{dip}} =& -\frac{\alpha}{3}E\epsilon_z\delta_{\mathrm{FI}} - i\beta\epsilon_z E\,(\sigma_y)_{\mathrm{FI}} +\\ &+\ \mathrm{Im}\mathcal{E}_{\mathrm{PNC}}\ \Big[-\epsilon_x\,(\sigma_x)_{\mathrm{FI}} + i\epsilon_z\,(\sigma_z)_{\mathrm{FI}}\Big] -\\ &- M\Big[\epsilon_z\,(\sigma_x)_{\mathrm{FI}} - i\epsilon_x\,(\sigma_z)_{\mathrm{FI}}\Big]\end{aligned}$$

Further, we consider only transitions with $M_{\mathrm{F}} = M_{\mathrm{I}} \pm 1$ (as chosen in the experiment). The above expression consequently simplifies to

$$\mathcal{A}_{\mathrm{FI}}^{\mathrm{dip}} = -i\beta\epsilon_z E\,(\sigma_y)_{\mathrm{FI}} -\ \mathrm{Im}\mathcal{E}_{\mathrm{PNC}}\ \epsilon_x\,(\sigma_x)_{\mathrm{FI}} - M\epsilon_z\,(\sigma_x)_{\mathrm{FI}}$$

The probability is then (we neglect the very small terms involving only PNC or magnetic dipole contributions)

$$\begin{aligned}\left|\mathcal{A}_{\mathrm{FI}}^{\mathrm{dip}}\right|^2 =& \beta^2\epsilon_z^2E^2\,(\sigma_y)_{\mathrm{FI}}\,(\sigma_y)_{\mathrm{IF}} +\\ &+ i\epsilon_x\epsilon_z E\beta\ \mathrm{Im}\mathcal{E}_{\mathrm{PNC}}\ \Big[(\sigma_y)_{\mathrm{IF}}\,(\sigma_x)_{\mathrm{FI}} - (\sigma_x)_{\mathrm{IF}}\,(\sigma_y)_{\mathrm{FI}}\Big] +\\ &+ i\epsilon_z^2E\beta M\Big[(\sigma_y)_{\mathrm{IF}}\,(\sigma_x)_{\mathrm{FI}} - (\sigma_x)_{\mathrm{IF}}\,(\sigma_y)_{\mathrm{FI}}\Big]\end{aligned}$$

The terms for the Pauli matrices can be expressed via $\sigma_\pm$ matrices (as usual, these matrices are defined $\sigma_\pm = \sigma_x \pm i\sigma_y$):

$$\begin{aligned}(\sigma_y)_{\mathrm{IF}}\,(\sigma_x)_{\mathrm{FI}} - (\sigma_x)_{\mathrm{IF}}\,(\sigma_y)_{\mathrm{FI}} &= \frac{1}{2}\Big[\,(\sigma_+)_{\mathrm{IF}}\,(\sigma_-)_{\mathrm{FI}} - (\sigma_-)_{\mathrm{IF}}\,(\sigma_+)_{\mathrm{FI}}\,\Big]\,,\\ (\sigma_y)_{\mathrm{IF}}\,(\sigma_y)_{\mathrm{FI}} &= \frac{1}{4}\Big[\,(\sigma_+)_{\mathrm{IF}}\,(\sigma_-)_{\mathrm{FI}} + (\sigma_-)_{\mathrm{IF}}\,(\sigma_+)_{\mathrm{FI}}\,\Big]\,.\end{aligned}$$

The first terms on the rhs describe the transition with $M_\mathrm{F} = M_\mathrm{I} - 1$ and the second terms the transitions with $M_\mathrm{F} = M_\mathrm{I} + 1$. The final theoretical expression for the observed signal is thus

$$\begin{aligned}\left|\mathcal{A}_\mathrm{FI}^\mathrm{dip}\right|^2 =& \frac{1}{4}\beta^2\epsilon_z^2 E^2\Big[M_\mathrm{I}\delta_{M_\mathrm{F},M_\mathrm{I}-1} + (M_\mathrm{I}+1)\,\delta_{M_\mathrm{F},M_\mathrm{I}+1}\Big] + \\ &+ \frac{1}{2}\epsilon_z E\beta\Big(\ \mathrm{Im}\mathcal{E}_\mathrm{PNC}\ \epsilon_x + M\epsilon_z\Big)\Big[M_\mathrm{I}\delta_{M_\mathrm{F},M_\mathrm{I}-1} - (M_\mathrm{I}+1)\,\delta_{M_\mathrm{F},M_\mathrm{I}+1}\Big]\,.\end{aligned}$$

In the case of ^{133}Cs, see Fig. 1.4, the atomic states are $\left|I^{(0)}\right\rangle = |6S\rangle$ and $\left|F^{(0)}\right\rangle = |7S\rangle$. The nuclear spin is $I = 7/2$; hence the total angular momenta are $F = 3$ with projections $M = -3, ..., +3$ and $F = 4$ with $M = -4, ..., +4$. We consider transitions between the extreme levels (as, again, dictated by the experiment), i.e., $M_\mathrm{I} = \pm 3 \to M_\mathrm{F} = \pm 4$ or $M_\mathrm{I} = \pm 4 \to M_\mathrm{F} = \pm 3$. The above expression for the transition amplitude thus becomes, cf. Eq. (1.1),

$$\left|\mathcal{A}_{6S\to 7S}^\mathrm{dip}\right|^2 = \beta^2\epsilon_z^2 E^2 \pm 2\epsilon_z E\beta\Big(\ \mathrm{Im}\mathcal{E}_\mathrm{PNC}\ \epsilon_x + M\epsilon_z\Big)\,. \tag{1.11}$$

1.5 Recent Theoretical Works and their Shortcomings

As mentioned at the beginning of Chapter 1.3, the PNC amplitude has been successfully measured on only five atoms. Theoretical calculations have been accomplished for all of them: Cs [13, 33, 34, 35, 36, 37, 38], Yb [39, 40], Tl [41, 42], Pb [43], and Bi [43]. However, if we take a look at the relative errors in the theoretical and experimental determination of the PNC amplitude, see Tab. 1.1 (adapted from [7]), we can see that – with the exception of ytterbium where the experiment is still ongoing – the incertainty in the theory is much larger than the experimental one. Therefore, clearly, further development on the theoretical side is necessary.

Table 1.1: Relative error of the theoretical and experimental, respectively, determination of the PNC amplitude in various atoms. Adapted from [7].

Atom	Theory [%]	Experiment [%]
Cs	0.9	0.3
Yb	10	26
Tl	2.5	1.1
Pb	8	1.2
Bi	10	2

We focus on the cesium atom here. The PNC amplitude $\mathrm{Im}\mathcal{E}_\mathrm{PNC}$, see Eqs. (1.8) and (1.9) and also Eq. (1.11), to be evaluated is defined as

$$i\mathrm{Im}\mathcal{E}_\mathrm{PNC} = \langle 7s|\left[\hat{\mathsf{H}}_\mathrm{PNC}\frac{1}{\hat{\mathsf{H}}_\mathrm{at} - E_{7s}}\hat{\mathsf{d}}_z + \hat{\mathsf{d}}_z\frac{1}{\hat{\mathsf{H}}_\mathrm{at} - E_{6s}}\hat{\mathsf{H}}_\mathrm{PNC}\right]|6s\rangle\ , \tag{1.12}$$

where, recall, $\hat{\mathsf{H}}_{\mathrm{PNC}}$ is given in Eq. (1.2) and $\hat{\mathsf{H}}_{\mathrm{at}}$ is the Hamiltonian of a free atom. $\hat{\mathsf{d}}_z$ is the z-component of the electric dipole operator. $\langle 7s|$ and $|6s\rangle$ are one-particle atomic states (in contrast to the total states $6S$, $7S$ used by the experimentalists). Note that, as is common, we dropped the $1/2$ subscript in $s_{1/2}$ as the composition of s-states with $l = 0$ and spin $s = 1/2$ can yield only total angular momentum $j = 1/2$. In literature, this PNC amplitude is usually reported in the units of $iea_{\mathrm{B}}(-Q_W/N) \cdot 10^{-11}$; e denotes the elementary charge.

From Eq. (1.12) one can see the probably greatest challenge in the evaluation of the PNC amplitude: due to the presence of the dipole operator $\hat{\mathsf{d}}_z = \sum e_i z_i$ and of the EW term $\sim \rho(R)$, we have to obtain the needed wave functions (for s and $p_{1/2}$ states) with great accuracy *both* far away from the nucleus (due to the former term) as well as very near the nucleus (due to the latter term).

There were several attempts on the theoretical evaluation of the PNC amplitude in cesium, the most notable are the works [13, 33, 34, 35, 36, 37, 38], and on the development of high-precision methods for atomic systems in general, see, e.g., [44, 45, 46, 47]. The best calculation (as of 2022) was achieved by S. G. Porsev, K. Beloy and A. Derevianko in 2010 [13]. In their sophisticated calculation, they started with the DHF model and then employed the CC method with singles, doubles and valence triples (see later Chapter 5.3) and a few other corrections, see [13] for details.

However, as good as [13] is, it has several shortcomings. First of all, it is not truly *ab initio* calculation; see the sentence "In this approach, the valence singles, S_v, are rescaled by the ratio of experimental and theoretical energies", *op. cit.* p. 4 before Eq. (12). Second, the error of the theoretical determination of the ionization energy of the normal state of Cs in [13] is 0.3 %, while that of the normal state of Au in [48] is only 0.03 %. Needless to say that the electronic structure of Au is much more complicated than that of Cs. The reason behind this is that the present calculations of PNC amplitudes (summarized in [7, 8, 9]) do not squeeze all the fruit of modern CC methodology (see, e.g., [49]). This methodology uses single-reference CC method for calculation of the ground state of closed-shell systems and equation-of-motion CC (EOM-CC) for calculation of the excited states and simple open shells, see Chapter 5.

2. Preliminaries

Before we turn to our work, let us introduce two important concepts that will appear throughout the next chapters of this thesis. First, we summarize here the well-known HF model in its general spin-orbital formulation. Later, this model will be used for the non-relativistic (see Chapter 3) and relativistic (see Chapter 4) closed-shell atomic systems. The specific forms of the HF model will be introduced in the respective chapters. Second, we define here the Sturmian functions and show their basic properties. This basis set is used for all presented calculations.

2.1 Hartree-Fock Model

To derive the HF equations, we start with the expression for HF energy of a system constituted by N electrons moving in the electrostatic potential of a nucleus (or nuclei in the case of molecules) and of other electrons

$$E_{\mathrm{HF}} = \sum_{a=1}^{N} \langle a| \hat{\mathsf{z}} |a\rangle + \frac{1}{2} \sum_{a=1}^{N} \sum_{b=1}^{N} \langle a|_1 \langle b|_2 \hat{\mathsf{v}} (1 - \mathcal{P}_{12}) |a\rangle_1 |b\rangle_2 \,. \tag{2.1}$$

Here, $|a\rangle$ and $|b\rangle$ are normalized spin-orbitals in the abstract notation. $\hat{\mathsf{z}}$ and $\hat{\mathsf{v}}$ are one- and two-particle operators, respectively. $\mathcal{P}_{12}$ exchanges the coordinates of the two electrons. Next, we vary this expression (2.1) with respect to each spin-orbital, subjected to normalization constraint $\langle a|a\rangle = 1$, and set it equal to zero. We thus obtain the well-known HF equations (where $a = 1, \ldots, N$):

$$\hat{\mathsf{f}} |a\rangle = \varepsilon_a |a\rangle \,. \tag{2.2}$$

The Fock operator $\hat{\mathsf{f}}$ is given by

$$\hat{\mathsf{f}} = \hat{\mathsf{z}} + \sum_{b=1}^{N} \langle b|_2 \hat{\mathsf{v}} (1 - \mathcal{P}_{12}) |b\rangle_2 \,. \tag{2.3}$$

ε_a are one-particle (spin-orbital) energies. These non-linear coupled equations are then solved (usually iteratively) and we obtain the HF wave functions, i.e., spin-orbitals, spin-orbital energies and total energy. The total energy is related to the orbital energies

$$E_{\mathrm{HF}} = \frac{1}{2} \sum_{a=1}^{N} \left[\varepsilon_a + \langle a| \hat{\mathsf{z}} |a\rangle \right] .$$

Note that all these relations are completely general and hold regardless of the specific forms of the one- and two-particle operators $\hat{\mathsf{z}}$ and $\hat{\mathsf{v}}$ and spin-orbitals a.

2.2 Sturmian Basis Set

The Sturmian basis system is found as follows, see, e.g., [10, 50, 51]. Consider the well-known eigenproblem for the radial hydrogenic Hamiltonian,

$$\left[\frac{\hat{\mathsf{p}}_r^2}{2} + \frac{l(l+1)}{2r^2} - \frac{1}{r} \right] R^{\mathrm{h}}_{n,l}(r) = -\frac{1}{2n^2} R^{\mathrm{h}}_{n,l}(r) \,; \tag{2.4}$$

r is the radial coordinate, $\hat{\mathsf{p}}_r$ the radial momentum

$$\hat{\mathsf{p}}_r = -i\left(\frac{\partial}{\partial r} + \frac{1}{r}\right) , \tag{2.5}$$

and n and l principal and orbital quantum numbers, respectively. We make an energy-dependent scaling $r \to rn$ and multiply the Eq. (2.4) by r. Rearranging the terms, we transform eigenproblem (2.4) to the eigenproblem

$$\hat{\mathsf{T}}_3 R_{n,l}(r) = nR_{n,l}(r) , \quad \hat{\mathsf{T}}_3 = \frac{r}{2}\left[\hat{\mathsf{p}}_r^2 + \frac{l(l+1)}{r^2}\right] + \frac{r}{2} . \tag{2.6}$$

The functions $R_{n,l}(r)$ are the Sturmian functions; they are related to hydrogenic functions by simple relation

$$R^{\mathrm{h}}_{n,l}(r) = \frac{1}{n^2} R_{n,l}\left(\frac{r}{n}\right) .$$

The advantage of the Sturmian over hydrogenic functions is that the former form a complete discrete basis set, while the latter do not. This is most easily seen by noting the existence of the ladder operators

$$\hat{\mathsf{T}}_\pm = \frac{r}{2}\left[\hat{\mathsf{p}}_r^2 + \frac{l(l+1)}{r^2}\right] - \frac{r}{2} \pm ir\hat{\mathsf{p}}_r , \quad [\hat{\mathsf{T}}_3, \hat{\mathsf{T}}_\pm] = \pm\hat{\mathsf{T}}_\pm . \tag{2.7}$$

By a procedure completely analogous to that used for angular momentum, one can show, see, e.g., [10], that n has to be a positive integer greater than $l+1$ and that

$$\hat{\mathsf{T}}_\pm R_{n,l} = \sqrt{(n \mp l)[n \pm (l+1)]}\, R_{n\pm1,l} . \tag{2.8}$$

It is worth noting that the operator $\hat{\mathsf{T}}_3$ is Hermitian with respect to the inner product with weight r. Consequently, the eigenfunctions $R_{n,l}(r)$ of the operator $\hat{\mathsf{T}}_3$ are orthonormal with weight r

$$(n_1, l|n_2, l) = \int_0^\infty r R_{n_1,l}(r) R_{n_2,l}(r)\mathrm{d}r = \delta_{n_1,n_2} . \tag{2.9}$$

The inner product defined in the last equation is to be contrasted with the ordinary inner product in the space of the radial functions

$$\langle n_1, l|n_2, l\rangle = \int_0^\infty r^2 R^{\mathrm{h}}_{n_1,l}(r) R^{\mathrm{h}}_{n_2,l}(r)\mathrm{d}r = \delta_{n_1,n_2} . \tag{2.10}$$

Thus, we have two kinds of inner products, Eqs. (2.9) and (2.10). Notice that we distinguish them by using different brackets.

We can further improve this basis set by considering screened radial functions $R_{n,l}(\xi, r)$ instead of the ordinary ones $R_{n,l}(r)$, Eq. (2.6), see [50]. The screening functions are obtained from the ordinary ones by the energy-independent scaling $r \to \xi r$ and multiplication by ξ (to ensure proper normalization, see Eq. (2.9))

$$R_{n,l}(\xi, r) = \xi R_{n,l}(r\xi) . \tag{2.11}$$

The use of screened functions is motivated by the fact that electrons in an atom see the nuclear charge differently. Consider a two-electron system, for example. The electron that is closer to the nucleus is indeed effected by the true nuclear charge Z. However, the other electron, which is further from the nucleus (i.e., in a higher state), sees an effective nuclear charge $Z-1$ as the nuclear charge Z is screened by the electron in the lower state.

3. Symmetry Breaking of the Hartree-Fock Model

This chapter focuses on the well-known HF approximation (see Chapter 2.1) and studies its singular behavior at critical regions. This work was published as [3] (attached), see also [52]. Note that the notation in this chapter slightly differs from the rest of this work; we have decided to follow the notation of the herein referenced paper [3] for the sake of clarity.

3.1 Introduction

3.1.1 Hartree-Fock Method

The HF model is nowadays a cheap and a well-established approximation and is widely used as the starting point for further accurate *ab initio* calculations. Its key idea in the description of two-electron interactions is to consider each electron to be moving in an average potential due to all other electrons. This way we neglect a significant part of the electron correlation (we usually obtain around 95 % of the exact energy), but, unlike the DFT method for example, we can account for the missing correlation contribution via one of the post-HF methods and *systematically* improve the accuracy of the result.

Within the HF approximation, we distinguish generally between restricted (RHF) and unrestricted (UHF) models. A non-relativistic atomic electron wave function consists typically of three separable contributions: a radial part, an angular part and a spin part. In the strictest case, we assume that the radial part is identical for all possible angular and spin parts. Consider a $2p$ orbital, for example. In fact, it represents six different electronic wave functions, but we usually consider the radial part to be the same for all six functions. This is the RHF model and its solutions is termed symmetry-adapted (SA). If we lift any of these spin or orbital restrictions, for example we do not *a priori* assume that the radial parts are identical for $2p_x$, $2p_y$ and $2p_z$ orbitals, we obtain an orbital UHF model; similarly for a spin UHF model. If we indeed obtain different radial wave functions and lower energy than for the RHF approach, $E(\mathrm{BS}) < E(\mathrm{SA})$, we call the solution of the UHF equations as broken-symmetry (BS).

The HF approximation leads to a system of coupled non-linear equations that cannot be solved exactly. They are usually solved via the iterative self-consistent field (SCF) method. In most standard situations no problems arise. However, there is generally no guarantee that the method will indeed converge; it can, for example, oscillate between two or more non-physical solutions or numerically "explode". One encounters these convergence problems predominantly due to one of the following two reasons:

(i) The system cannot exist, i.e., we are trying to find a non-existing solution.

(ii) The system features strong electron correlation. The RHF solution is a poor approximation to the ground state, multiple HF solutions may lie close one to another, and instabilities appear. Their presence implies the existence of another, BS, solution with lower energy. However, as stated by Pulay [53],

especially in complicated systems, the SCF algorithm tends to converge to a SA solution even if its energy lies above a BS solution.

Therefore, it would be of much help if one knew *a priori* what type of solution to look for and whether any exists, for that matter.

3.1.2 Properties of HF Solutions

The first step towards the investigation of the existence of and the relation between SA and BS solutions was undertaken by Thouless in 1960 in the context of nuclear physics [54, 55]. His bright idea was to apply tools from mathematical analysis.

The HF equations arise from the requirement that the first variation of energy in the space of monoexcitations vanishes. However, this requirement does not ensure that the found solution is indeed a local minimum; $\delta^{(1)}E = 0$ leads to any extremal point, i.e., also to (local) maxima and saddle points. To determine whether the found solution is indeed a minimum, we could calculate the so-called Hessian (a matrix of second derivatives) and find its eigenvalues. If all the eigenvalues are positive, the found SA solution is indeed a minimum and is said to be stable. Conversely, if there is at least one negative eigenvalue, another BS solution of lower energy exists and the found SA solution is said to be unstable.

In atomic and molecular physics, the investigation of HF solutions and their stability was initiated by Paldus and Čížek by a series of studies in the late 1960s and early 70s [56, 57, 58, 59, 60, 61, 62]. For the first time, a connection between HF instabilities and symmetry breaking was pointed out and a classification of the instabilities according to spin symmetry was proposed. They introduced a concept of singlet and non-singlet (triplet) instabilities in the case of closed-shell systems and doublet and non-doublet instabilities for open-shell systems, and studied (spin) symmetry breaking in many molecular systems. A more complete classification of instabilities was provided later by Fukutome [63] and Stuber and Paldus [64, 65]. Symmetry breaking and the UHF problem were then revisited by Pulay and coworkers during the development of an inexpensive quantum-chemical method, named UNO-CAS (unrestricted natural orbital – complete active space) method, which should be capable of describing strongly correlated systems and has been successfully applied to systems such as polyenes, aromatic molecules and transition metal compounds [53, 66, 67].

There is a great variety of topics that still have not been fully understood. For instance, despite several attempts on clarification, e.g., [63, 68], the physical and chemical significance of symmetry breaking and BS wave functions remains not fully concluded. Likewise, the question of survival of the symmetry breaking once the electron correlation is accounted for [69] is still unresolved. Also, as of now, there is still no clear deterministic method for the localization of a BS solution. There were various attempts (if interested the reader may look into the cited papers), such as a method of the steepest descent by Paldus and Čížek [56, 62], a direct energy minimization algorithm by Stuber and Paldus [64, 65], a method by Tóth and Pulay [70] in the context of a search for an automatic determination of active space for strongly correlated systems. We also proposed a method for obtaining a BS solution once we have a SA solution (and showed how one can always obtain a SA solution), see [52].

Given the practical importance of the knowledge whether, for a given system, a SA or a SB solution is the energy minimum, whether a HF solution exists at all, and how one can obtain a HF solution, we have decided to systematically investigate all closed-shell atomic systems of the Mendeleev periodic table. This work aims to obtain the stability matrix for those systems, to classify the found instabilities and to ascribe a physical meaning to them.

3.2 Theory

The general formulation of the HF model was presented in Chapter 2.1. Here, we will focus on closed-shell atomic systems in the non-relativistic approximation and present the pertinent expressions. We will also introduce the standard formulation of the stability matrix.

3.2.1 Restricted Hartree-Fock Model

In the non-relativistic RHF model for atoms, we put N electrons into N spin-orbitals labeled by A. These spin-orbitals are successively put in accordance with the Bohr Aufbau principle into ν shells labeled by a. Each shell is characterized by the orbital angular momentum l_a and principal quantum number n_a. In a given shell, there are $2(2l_a + 1)$ states of the type

$$\langle \mathbf{r}|a\rangle = \phi_{n_a,l_a}(r)Y_{l_a,m}(\mathbf{n})\,|s\rangle \tag{3.1}$$

where $\phi_{n,l}(r)$ are radial functions and n is the principal quantum number of the pertinent atomic shell, $Y_{l,m}(\mathbf{n})$ are spherical harmonics and magnetic quantum number m runs from $-l$ to l by 1 (hence the factor $2l_a + 1$), and $|s\rangle = \left|\frac{1}{2}, \pm\frac{1}{2}\right\rangle$ are the spin states (hence the additional factor 2). This is commonly referred to as the central field or shell model, see Chapter 4.3.1 for the relativistic model. Note in passing that the shells are uniquely labeled either by a natural number a, or by a pair of quantum numbers $\{n_a, l_a\}$. For instance, a neon-like atom has three filled shells: $1s, 2s, 2p$; thus the correspondence is $1 \leftrightarrow (1,0)$, $2 \leftrightarrow (2,0)$ and $3 \leftrightarrow (2,1)$. Henceforth, we will use both labelings interchangeably.

In the non-relativistic case, the one-particle operator $\hat{\mathsf{z}}$ is the one-electron Hamiltonian for the kinetic energy of the electron and its potential energy in the Coulomb field of the nucleus with charge Z (in atomic units),

$$\hat{\mathsf{z}} = \hat{\mathsf{h}}_0 = \frac{\hat{\mathsf{p}}^2}{2} - \frac{Z}{\hat{\mathsf{r}}}$$

and the two-electron operator is simply the inverse distance between two electrons

$$\hat{\mathsf{v}} = \hat{\mathsf{r}}_{12}^{-1}\,.$$

Assuming spin and orbital restriction, we can integrate out the pertinent degrees of freedom. Then by means of the multipole expansion of the Coulomb potential and the Wigner-Eckart theorem for angular integrations, see, e.g., [10, 71], the expression for the RHF energy for N electrons in ν shells, Eq. (2.1),

becomes (we scaled the electronic coordinates $\mathbf{r}^{(i)} \to \mathbf{r}^{(i)}/Z$)

$$\frac{E_{\mathrm{HF}}}{Z^2} = 2\sum_{a=1}^{\nu}(2l_a+1)\,\langle a|\,\hat{\mathsf{h}}_0^{l_a}\,|a\rangle + \\ + \frac{1}{Z}\sum_{a=1}^{\nu}\left[\sum_{b=1}^{a-1}(2l_a+1)(2l_b+1)\,\langle a|_1\langle b|_2\left(4\hat{\mathsf{v}}_c\,|a\rangle_1|b\rangle_2 - 2\hat{\mathsf{v}}_e\,|b\rangle_1|a\rangle_2\right) + \right. \\ \left. + (2l_a+1)^2\,\langle a|_1\langle a|_2(2\hat{\mathsf{v}}_c - \hat{\mathsf{v}}_e)\,|a\rangle_1|a\rangle_2\right].$$

Here, $|a\rangle$ and $|b\rangle$ are the radial orbitals in the abstract notation; their projections onto the coordinate basis are the radial functions $\langle r|a\rangle = \phi_{n_a,l_a}(r)$, cf. (3.1). $\hat{\mathsf{h}}_0^l$ is the radial part of the hydrogenic Hamiltonian, see Eqs. (2.4) and (2.5),

$$\hat{\mathsf{h}}_0^l = \frac{1}{2}\left[\hat{\mathsf{p}}_r^2 + \frac{l(l+1)}{r^2}\right] - \frac{1}{r}\,,$$

and the radial operators of the Coulomb and exchange interaction read

$$\hat{\mathsf{v}}_c = r_>^{-1}\,, \quad \hat{\mathsf{v}}_e = \sum_{l=|l_a-l_b|}^{l_a+l_b}\frac{r_<^l}{r_>^{l+1}}\frac{(l_a,0,l_b,0|l,0)^2}{2l+1}\,, \tag{3.2}$$

where $r_< = r_1$, $r_> = r_2$ if $r_1 < r_2$ and $r_< = r_2$, $r_> = r_1$ if $r_1 > r_2$. Finally, $(l_1,i,l_2,m-i|l,m)$ are Clebsch-Gordan (CG) coefficients.

The non-relativistic spin and orbital RHF equations then read, see Eqs. (2.2) and (2.3),

$$\hat{\mathsf{f}}_a\,|a\rangle = \varepsilon_a\,|a\rangle\,, \quad \hat{\mathsf{f}}_a\,|a\rangle_1 = \hat{\mathsf{h}}_0^{l_a}\,|a\rangle_1 + \frac{1}{Z}\sum_{b=1}^{\nu}\frac{2l_b+1}{\langle b|b\rangle}\,\langle b|_2\left(2\hat{\mathsf{v}}_c\,|a\rangle_1|b\rangle_2 - \hat{\mathsf{v}}_e\,|b\rangle_1|a\rangle_2\right). \tag{3.3}$$

The one-electron energies ε_a are related to the total energy via the relation

$$\frac{E_{\mathrm{HF}}}{Z^2} = \sum_{a=1}^{\nu}(2l_a+1)\left(\varepsilon_a + \frac{\langle a|\,\hat{\mathsf{h}}_0^{l_a}\,|a\rangle}{\langle a|a\rangle}\right). \tag{3.4}$$

The RHF equations are usually solved by expanding radial functions $\phi_{n_a,l_a}(r)$ into a discrete radial basis set; the problem is thus transformed into a generalized eigenvalue problem:

$$\mathsf{Fc} = \varepsilon\mathsf{Sc}\,.$$

These are the well-known Roothan equations.

3.2.2 Stability Matrix

The spin-adapted stability matrix for closed-shell atomic systems was introduced already by Paldus and Čížek [56, 57] (following the notation used in the cited works):

$$\Lambda^S_{a,b} = \delta_{o_a,o_b}\left(\hat{\mathsf{f}}_{o^a,o^b} - \delta_{o^a,o^b}\varepsilon_a\right) + \frac{1}{Z}\Big\{2(\hat{\mathsf{r}}_{12}^{-1})_{o^ao^b,o_ao_b}[1+(-1)^S] - \\ - (\hat{\mathsf{r}}_{12}^{-1})_{o^ao^b,o_bo_a} - (\hat{\mathsf{r}}_{12}^{-1})_{o^ao_b,o^bo_a}\Big\}. \tag{3.5}$$

Here, the Fock matrix $\hat{\mathsf{f}}_{o^a o^b}$ is defined as, cf. Eq. (3.3),

$$\hat{\mathsf{f}}_{o^a o^b} = (\hat{\mathsf{h}}_0)_{o^a o^b} + \frac{1}{Z} \sum_{c}^{\text{occ.}} \left[2(\hat{\mathsf{r}}_{12}^{-1})_{o^a o_c, o^b o_c} - (\hat{\mathsf{r}}_{12}^{-1})_{o^a o_c, o_c o^b} \right]$$

where the summation in the last equation runs through all occupied orbitals. The stability matrix is expressed here in the basis of monoexcitations labeled by a and b. Each monoexcitation a is determined by the occupied and virtual *orbitals* labeled by o_a and o^a, respectively. These orbitals are eigenstates of the Fock operator and are uniquely defined by the triples of quantum numbers (n_a, l_a, m_a) and (n^a, l^a, m_a), respectively. Finally, $S = 0$ and $S = 1$ correspond to spin conserving (singlet) and spin violating (triplet) stability matrices, respectively.

To investigate the stability of the RHF solution we are to solve the eigenvalue problem (we suppress here the superscript S)

$$\Lambda \, |\lambda\rangle = \lambda \, |\lambda\rangle \ . \tag{3.6}$$

According to the sign of the lowest eigenvalue λ, the RHF solution is stable (if $\lambda > 0$) or unstable (if $\lambda < 0$).

3.2.3 Critical Nuclear Charge

To conclude this theoretical chapter, we would like to explain the term critical nuclear charge. This will be important later for the interpretation of our results.

It has been generally agreed that the critical nuclear charge Z_c is the minimum charge for which an atomic system has at least one bound state (so that the attraction of electrons to the nucleus exactly compensates for the electron-electron repulsion). This physical meaning has been ascribed to the critical nuclear charge by numerous studies from recent years, e.g., [72, 73, 74]. In those, the authors obtained perturbative energy series for the exact solution of the Schrödinger equation, analyzed those series, and found their radius of convergence. The radius of convergence is given by the position of the closest singularity, which is in turn identified with the critical nuclear charge Z_c. Note that the determination of Z_c is a challenging task as one needs to find the last bound state that is on the verge of entering the continuum for $Z = Z_c$.

3.3 Our Systematic Approach

Now we will turn to our contribution. The aim of this work is to systematically investigate all closed-shell atoms and determine the onsets of spin or orbital symmetry breaking. Therefore, we start with the adapation of the spin-SA stability matrix to the orbital symmetry (Chapter 3.3.1). Next, we show how one can implement the perturbative method and in three steps obtain series for the eigenvalues of the stability matrix (Chapter 3.3.2). Finally, we summarize methodological tools for the analysis of the obtained series (Chapter 3.3.3).

3.3.1 Symmetry-Adapted Stability Matrix

In the case of atoms in the non-relativistic approximation, there are in general five mutually commuting operators that commute with the atomic Hamiltonian:

$\hat{\mathsf{S}}^2, \hat{\mathsf{S}}_z, \hat{\mathsf{L}}^2, \hat{\mathsf{L}}_z, \hat{\Pi}$, where $\hat{\mathbf{S}}$, $\hat{\mathbf{L}}$ and $\hat{\Pi}$ stand for the total spin, total angular momentum and parity operators, respectively. The monoexcitations generally conserve S_z and L_z, but not $S(S+1)$, $L(L+1)$ and Π. Thus, the stability matrix may be factorized according to the total spin, total orbital momentum and total parity of the monoexcitations.

The adaptation to spin symmetry has been already done by Paldus and Čížek [56, 57], cf. Eq. (3.5). Further factorization according to the total angular momentum L and parity Π of the monoexcitations is achieved by means of CG coefficients; the spin and orbital SA stability matrix thus reads

$$\begin{aligned}
\Lambda^{S,L,\Pi}_{a,b} &= \sum_{m_a=-l_a}^{l_a} \sum_{m_b=-l_b}^{l_b} (l^a, m_a, l_a, -m_a|L, 0)(l^b, m_b, l_b, -m_b|L, 0)(-1)^{m_a+m_b} \Lambda^{S}_{a,b} = \\
&= \sum_{m_a=-l_a}^{l_a} \sum_{m_b=-l_b}^{l_b} (l^a, m_a, l_a, -m_a|L, 0)(l^b, m_b, l_b, -m_b|L, 0)(-1)^{m_a+m_b} \times \\
&\quad \times \Bigg(\delta_{o_a,o_b} \left(\hat{\mathsf{f}}_{o^a,o^b} - \delta_{o^a,o^b} \varepsilon_a \right) + \\
&\quad + \frac{1}{Z} \left\{ 2[1 + (-1)^S] (\hat{\mathsf{r}}^{-1}_{12})_{o^a o^b, o_a o_b} - (\hat{\mathsf{r}}^{-1}_{12})_{o^a o^b, o_b o_a} - (\hat{\mathsf{r}}^{-1}_{12})_{o^a o_b, o^b o_a} \right\} \Bigg) .
\end{aligned} \tag{3.7}$$

The parity Π of the monoexcitation is defined as

$$(-1)^{\Pi} = (-1)^{l^a + l_a} = (-1)^{l^b + l_b} .$$

Note that with this symmetry adaptation, each monoexcitation a is characterized by quantum numbers (n_a, l_a, n^a, l^a), where n_a, l_a and n^a, l^a are principal and orbital quantum numbers of the occupied and virtual orbitals, respectively.

When using the SA monoexcitations, one of the blocks of the stability matrix preserves all the symmetries of the Hamiltonian. We will term this block as a *pure singlet* stability matrix, to distinguish it from the molecular case, where the singlet stability matrix consists of a mixture of a pure stability matrix and a stability matrix violating other than spin symmetry (usually spatial).

3.3.2 Perturbative Series for the Eigenvalues of the Stability Matrix

We found that for obtaining a global insight into the stability of a given electron configuration in the field of nucleus with respect to variation of the nuclear charge, it is advantageous to search for the solution of Eq. (3.6), in the form of a series in the inverse powers of nuclear charge Z:

$$|\lambda\rangle = \sum_{r=0}^{\infty} |\lambda_r\rangle \, z^r , \quad \lambda = \sum_{r=0}^{\infty} \lambda_r z^r , \quad z = 1/Z . \tag{3.8}$$

This is achieved in three steps. We first find the perturbative solution of the RHF equations. Then we use it to construct the pertubative series for the stability matrix (3.6) and we thus obtain the well-known perturbative expansion of the

generalized eigenvalue problem. Finally, we use this perturbative expansion of the stability matrix (or more precisely of its each block) to find the perturbative series (3.8) for the lowest eigenvalue.

These series are then analyzed as described in the next Chapter 3.3.3. The goal of the analysis is to determine the values of the nuclear charge Z_i for which $\lambda_{S,L,\Pi}(Z = Z_i) = 0$. For $Z > Z_i$ the found SA solution is stable, i.e., the HF is a suitable starting point for further post-HF calculations. Then at $Z = Z_i$ one root vanishes. Finally, for $Z < Z_i$ the found SA solution is unstable and a BS solution of lower energy exists.

Note that our implementation of the perturbative approach to the stability matrix requires introduction of so-called projectors. Given the very technical nature of their use, we refer the reader to the SI of the attached paper [3].

The RHF Equations in the Sturmian Basis

We expand the radial orbitals $\langle r|a\rangle = \phi_{n_a,l_a}(r)$ appearing in the HF equations (3.3) into the scaled Sturmian basis set $|j, l_a, \xi_a = 1/n_a)$, see Chapter 2.2, (here N denotes the number of basis functions)

$$|a\rangle = \sum_{j=l_a+1}^{l_a+N} c_{j,a}|j, l_a, 1/n_a)\,. \tag{3.9}$$

Further, writing the orbital energies as hydrogenic energy and a correction Δ

$$\varepsilon_a = -\frac{1}{2n_a^2} + \Delta_a$$

and projecting the RHF equations (3.3) onto the states $(i, l_a, 1/n_a|$, we transform these equations into a system of non-linear algebraic equations

$$\begin{aligned}\sum_j \Bigg\{ &\delta_{i,j}\frac{j-n_a}{n_a} + \\ &+ \frac{1}{Z}\sum_b (2l_b+1)\frac{\sum_{p,q}[2v_{(i,a)(p,b),(j,a)(q,b)} - v_{(i,a)(p,b),(q,b)(j,a)}]c_{p,b}c_{q,b}}{\sum_{p,q} S_{(p,b),(q,b)}c_{p,b}c_{q,b}}\Bigg\} c_{j,a} = \\ &= \Delta_a \sum_j S_{(i,a),(j,a)}c_{j,a}\,.\end{aligned} \tag{3.10}$$

The matrix elements of the Coulomb interaction between two electrons are, recall Eq. (3.2) for the definition of $\hat{\mathrm{v}}_c$ and $\hat{\mathrm{v}}_e$,

$$\begin{aligned} v_{(i,a)(p,b),(j,a)(q,b)} &= (i, l_a, 1/n_a|_1(p, l_b, 1/n_b|_2\hat{\mathrm{r}}_1\hat{\mathrm{r}}_2\hat{\mathrm{v}}_c|j, l_a, 1/n_a)_1|q, l_b, 1/n_b)_2\,, \\ v_{(i,a)(p,b),(q,b)(j,a)} &= (i, l_a, 1/n_a|_1(p, l_b, 1/n_b|_2\hat{\mathrm{r}}_1\hat{\mathrm{r}}_2\hat{\mathrm{v}}_e|q, l_b, 1/n_b)_1|j, l_a, 1/n_a)_2\,, \end{aligned}$$

and the elements of the overlap matrix are

$$S_{(i,a),(j,a)} = (i, l_a, 1/n_a|\hat{\mathrm{r}}|j, l_a, 1/n_a)\,.$$

Note that we have to distinguish between integrals in the space of ordinary functions, Eq. (2.10), and Sturmian functions, Eq. (2.9). Therefore, the above matrix

elements contain an "extra" operator $\hat{\mathsf{r}}$. The matrix elements are evaluated using a method developed in [50], see also [4].

The total energy is then obtained by substitution of Eq. (3.9) into Eq. (3.4)

$$\frac{E_{\rm HF}}{Z^2} = \sum_a^{\nu} (2l_a+1) \left(\varepsilon_a + \frac{\sum_{p,q} (p,l_a,1/n_a| \, \hat{\mathsf{r}}\hat{\mathsf{h}}_0^{l_a} \, |q,l_a,1/n_a) \, c_{p,a} c_{q,a}}{\sum_{p,q} S_{(p,a),(q,a)} c_{p,a} c_{q,a}} \right) . \tag{3.11}$$

Perturbative Solution of the RHF Equations

Equations (3.10) have the form of a pseudoeigenvalue problem; they are usually solved by the SC method. Here, we solve Eq. (3.10) by expanding the energy Δ_a and the coefficients $c_{i,a}$ into a perturbative series in the inverse powers of the nuclear charge Z (note that the zeroth-order energy term is the hydrogenic energy $-1/(2n^2)$),

$$\Delta_a = \sum_{r=1}^{\infty} z^r \varepsilon_a^{(r)} , \quad c_{i,a} = \sum_{r=0}^{\infty} z^r c_{i,a}^{(r)} , \quad z = 1/Z . \tag{3.12}$$

We first simplify Eq. (3.10) by imposing the normalization condition

$$\langle b|b\rangle = \sum_{p,q} c_{p,b} c_{q,b} S_{(p,b),(q,b)} = 1 . \tag{3.13}$$

Substituting Eq. (3.12) into Eqs. (3.10) and (3.13) we obtain at the r-th order

$$\begin{aligned} n_a^{-1}(i-n_a) c_{i,a}^{(r)} + \sum_j \Bigg\{ & - \sum_{s=0}^{r-1} \varepsilon_a^{(r-s)} S_{(i,a),(j,a)} c_{j,a}^{(s)} + \\ & + \sum_b (2l_b+1) \sum_{p,q} \Big[2v_{(i,a)(p,b),(j,a)(q,b)} - v_{(i,a)(p,b),(q,b)(j,a)} \Big] + \\ & + \sum_{s=0}^{r-1} \sum_{t=0}^{r-1-s} c_{p,b}^{(s)} c_{q,b}^{(t)} c_{j,a}^{(r-1-s-t)} \Bigg\} = 0 \end{aligned} \tag{3.14}$$

and

$$\sum_{p,q} \sum_{s=0}^{r} c_{p,b}^{(s)} c_{q,b}^{(r-s)} S_{(p,b),(q,b)} = \delta_{r,0} , \tag{3.15}$$

respectively. The zeroth-order solution of the last two equations is

$$c_{i,a}^{(0)} = \frac{\delta_{i,n_a}}{\sqrt{n_a}} .$$

At the higher orders we first solve Eq. (3.14) for $i = n_a$ to obtain $\varepsilon_a^{(r)}$. Next, we successively solve Eq. (3.14) to obtain $c_{i,a}^{(r)}$ with i descending from $l_a + N$, cf. Eq. (3.9), to $l_a + 1$ excluding the case $i = n_a$. Finally, we use the normalization requirement, Eq. (3.15), to obtain the last missing coefficient $c_{n_a,a}^{(r)}$.

The total energy is calculated by substituting Eqs. (3.12) and (3.13) into Eq. (3.11)

$$\frac{E_{\rm HF}}{Z^2} = \sum_{r=0}^{\infty} z^r \mathcal{E}^{(r)} , \tag{3.16}$$

$$\mathcal{E}^{(r)} = \sum_{a=1}^{\nu} (2l_a+1) \left[\varepsilon_a^{(r)} + \sum_{j,k,p} (k,l_a,1/n_a|\hat{\mathsf{r}}\hat{\mathsf{h}}_0^{l_a}|j,l_a,1/n_a) c_{k,a}^{(p)} c_{j,a}^{(r-p)} \right] .$$

Perturbative Expansion of the Stability Matrix

We use the above obtained perturbative coefficients and orbital energies to construct the perturbative series for the stability matrix (3.6). We then solve it and find perturbative series for the lowest eigenvalues; see the attached paper and its SI for details [3].

The zeroth-order solution is, see Eq. (3.7) in the limit $Z \to \infty$,

$$\lambda_0 = \frac{1}{2}\left(\frac{1}{n_{\mathrm{HO}}^2} - \frac{1}{n_{\mathrm{LU}}^2}\right), \quad \langle r|\,\lambda_0\rangle = \frac{1}{n_{\mathrm{LU}}^2} R_{n_{\mathrm{LU}},l^{\mathrm{HO}}}(1/n_{\mathrm{LU}}, r)\,.$$

$R_{n,l}(1/n, r)$ are the screened Sturmian functions, Eq. (2.11). Further, n_{HO} denotes the principal quantum number of the occupied orbital with the highest hydrogenic energy and n_{LU} and l^{HO} denote the principal and orbital quantum numbers of the virtual orbital with the lowest hydrogenic energy, respectively. For example, in the case of neon-like systems, there are two occupied orbitals with the highest hydrogenic energy ($2s$ and $2p$) and three virtual orbitals with the lowest hydrogenic energy ($3s$, $3p$, and $3d$). Thus, in general, one has to employ the degenerate perturbation method.

The physical reasoning behind the choice of the zeroth-order solution is the following. As the nuclear charge Z increases, the role of the electron-electron interaction diminishes, cf. Eq. (3.3); in the limit $Z \to \infty$ the one-particle energies ε_a become that of the hydrogen, $\varepsilon_a = -1/(2n_a^2)$. In this limit, the lowest eigenvalue of the stability matrix is then simply the difference between the lowest unoccupied hydrogenic orbital and the highest occupied hydrogenic orbital. See SI of [3] for more details. It turns out, see the next Chapter 3.4 and also [3], that the stability of the given electronic configuration with respect to variation of the nuclear charge can be classified according to the sign of λ_0, see, again, [3] for details.

The calculation of the higher-order terms of the series (3.8) is too technical and can be found in the SI of the attached paper [3].

3.3.3 Methods for the Analysis of Series

Localization of a Singularity

The obtained HF perturbative energies, derived in the last chapter, can be analyzed by the method given in [75]. Let us assume that a function $f(z)$, e.g., the total or orbital HF energy, has a convergent power series at the origin, cf. Eqs. (3.12) and (3.16),

$$f(z) = \sum_{n=0}^{\infty} K_n z^n \tag{3.17}$$

and behaves in the vicinity of the closest singularity to the origin z_0 as

$$f(z) = c_1\left(1 - \frac{z}{z_0}\right)^{\alpha_1} + c_2\left(1 - \frac{z}{z_0}\right)^{\alpha_2} + \ldots + d_0 + d_1\left(1 - \frac{z}{z_0}\right) + d_2\left(1 - \frac{z}{z_0}\right)^2 + \ldots, \tag{3.18}$$

where α_i are assumed to be non-integer and form an ascending sequence. The integer powers in Eq. (3.18) do not influence the large-order behavior of the series (3.17) and will be ignored here. We also assume that the singularity lies on the

real axis. This turns out to be true for the series considered in this paper. For a more general case, see [75].

Taking j terms in Eq. (3.18), using the generalized binomial theorem,

$$\left(1-\frac{z}{z_0}\right)^{\alpha}=\sum_{n=0}^{\infty}\frac{\Gamma(\alpha+1)}{\Gamma(n+1)\Gamma(\alpha-n+1)}\frac{(-1)^n}{z_0^n}z^n\,,$$

and comparing the terms with the same powers of z in Eqs. (3.17) and (3.18), we obtain

$$K_n^{as}=\sum_{k=1}^{j}c_k\frac{\Gamma(\alpha_k+1)}{\Gamma(n+1)\Gamma(\alpha_k-n+1)}\frac{(-1)^n}{z_0^n}\,,$$

Equating now these asymptotic values of K_n to the actual values of K_n, assuming $\alpha_{k+1}=\alpha_k+1$ and considering these equations for n from n_0-j-1 to n_0 this represents a set of $j+2$ equations for $j+2$ unknowns: z_0, α_1 and j coefficients c_k. We solve the set of linear equations for the coefficients c_k and then solve two non-linear equations for z_0 and α_1 by means of the Newton-Raphson method.

Summation of Divergent Series

We need to sum the perturbation series for the lowest eigenvalue λ of the stability matrix, see Eq. (3.8), on the border of or even beyond its radius of convergence.

It is well-known, see, e.g., [76], that even if the limit of partial sums does not converge it can still be unambiguously summed. For the series (3.8), the most suitable methods seem to be the Weniger or Padé sequence transformations. The series (3.8) are, in principle, of two types: either they do not change the sign after the first-order term, or there are blocks of terms with the same sign.

The Weniger sequence transformation W_n^l of the series (3.17) is defined as [77]

$$W_n^l=s_n+\frac{\sum_{j=0}^{l-1}(-1)^j\frac{(l-1)!}{(l-1-j)!j!}\Pi_{i=1}^{l-2}(j+n+i)\frac{s_{j+n}-s_n}{a_{j+n}}}{\sum_{j=0}^{l-1}(-1)^j\frac{(l-1)!}{(l-1-j)!j!}\Pi_{i=1}^{l-2}(j+n+i)\frac{1}{a_{j+n}}}\,,$$

where $a_n=K_nz^n$ and $s_m=\sum_{n=0}^{m}a_n$ are coefficients and partial sums of the series, respectively. Clearly, the value of n is in principle arbitrary. However, not in practice. Since, as mentioned above, the series (3.8) become regular from the second-order term on, we considered n from 2 to 10 to improve the performance of the Weniger transformation.

The general Padé sequence transformation is defined

$$P_n^{N,M}=s_n+z^{n+1}\frac{\sum_{m=0}^{N}A_mz^m}{\sum_{m=0}^{M}B_mz^m}\quad,\quad M=N,N+1\,.$$

As indicated, we considered only the diagonal and first off-diagonal sequences. We calculated the Padé approximants by quotient-difference algorithm [78].

3.4 Results and Discussion

The full summary of results as well as their proper discussion may be found in the original paper [3]. Here, we will only stress the most important aspects of this study.

Table 3.1: Values of the nuclear charge $Z_i(S, L, \Pi)$ for which the first zero root appears among the eigenvalues of the pure singlet ($S = 0, L = 0, \Pi = 0$) and spin triplet ($S = 1, L = 0, \Pi = 0$) stability matrices. The results were obtained using Weniger (w) or Padé (p) sequence transformations. Z_c is the radius of convergence of the perturbative series for total energy of the given atom.

	Z_c	$Z_i(0,0)$	$Z_i(1,0)$
He-like	0.82	$0.8(2)^p$	1.06^p
Be-like	2.87(3)	2.84^w	3.04^w
Ne-like	8.5(1)	8.6^p	$8.5(2)^w$
Mg-like	10.8(3)	$10.9(2)^p$	11.03^p
Ar-like	16.6(3)	16.60^w	16.29^w
Ca-like	–	$18.9(1)^p$	19.0^p
Zn-like	–	28.9^p	29.0^p
Kr-like	–	34.57^w	34.27^w
Sr-like	–	$37.0(1)^w$	$37.2(1)^p$
Cd-like	–	46.9^w	$47.1(2)^p$
Xe-like	–	$52.4(4)^w$	$52.3(1)^w$

We have analyzed all closed-shell systems of the Mendeleev periodic table up to xenon-like systems. For all these systems, we have obtained basis-independent perturbative series for orbital energies and wave functions, calculated the pertinent stability matrices, and found perturbative series for the lowest stability eigenvalues. We have then analyzed these series and determined onsets of symmetry breaking and characterized the types of symmetry breaking.

First, let us note that the perturbative energy series for the HF solutions yield results that are in excellent agreement with the best results available in the literature [79, 80, 81, 82]. These series for orbital (and total) energies were analyzed using the method described in [75]. We obtained critical nuclear charges that correspond to the lowest value of nuclear charge Z_c (for a given electronic configuration) for which a SA solution can still exist, see Tab. 3.1. We observed that, within numerical errors, the radii of convergence of total and all orbital energies are the same. However, this method yielded reasonable results only for systems up to Ar-like systems. Even for these systems, the convergence of the method was not impressive, though, see Table II of SI of [3] for illustration. This suggests that the assumption on the nature of the closest singularity to the expansion point, which is the basis of the method, is not completely correct; for details see the SI of [3].

Next, the perturbative series of the lowest eigenvalue of each block of the SA stability matrix were resummed using the Padé or Weniger sequence transformations (as we need to sum them outside of their region of convergence). We thus obtained onsets of instabilities $Z_i(S, L, \Pi)$, $\lambda_{S,L,\Pi}(Z = Z_i) = 0$ for $S = 0, 1$, $L = 0, 1, 2, 3$ and $\Pi = 0, 1$.

The found onsets of pure singlet instabilities $Z_i(0, 0)$ are listed in Tab. 3.1. We can see that, within numerical error, the onsets of singlet instabilities $Z_i(0, 0)$ and the critical nuclear charges Z_c coincide, see Tab. 3.1. Thus, for the first time, a physical meaning can be ascribed to the pure singlet instabilities: they

correspond to the lowest nuclear charge for which a given system can exist within the HF approximation. The pure singlet instabilities $Z_i(0,0)$ were found to lie in the interval $(Z_\mathrm{n}-2, Z_\mathrm{n}-1)$, where Z_n denotes the nuclear charge for which the given atom is electrically neutral. This means that one can obtain a HF solution for cations, the neutral atom and once negatively charged anions. We conclude that the results obtained in [83, 84, 85] for O^{2-} (and S^{2-}) are artifacts of finite basis sets [62]. Whence these results are of no relevance to the experimental finding of possible resonances in O^{2-} [86], cf. [87]. Further, for helium-like atoms, $Z_c^\mathrm{exact} \simeq 0.911$ [88]; whence $Z_c^\mathrm{HF} = 0.82 < Z_c^\mathrm{exact}$. From this example we see that electronic correlation has a destabilizing effect and Z_c^HF is a lower bound to Z_c^exact. Although we are not aware of any proof that this indeed holds in general, we find it very likely. Thus probably no exact bound state solution of the Schrödinger equation exists for any double and more negative isolated atomic anions.

We found the pure spin instabilities $Z_i(1,0)$ to lie in the interval (Z_n-1, Z_n), see Tab. 3.1, in the case of rare-earth-metal-, He-, Zn-, and Cd-like systems. This means that for once negative anions of these systems, which still can exist as shown above, a spin-BS solution lies below the SA solution. In the cases of H^- and Li^-, the presence of the BS solution manifests itself through the non-convergence of the SC method for RHF equations. In the case of systems isoelectronic with noble gases, see Tab. 3.1, the pure spin instability lies below $Z_i(0,0)$. That is, the systems cease to exist before a spin instability can appear.

We found that pure orbital instabilities $Z_i(0,L,\Pi)$ are less likely than general instabilities $Z_i(1,L,\Pi)$, i.e., $Z_i(0,L,\Pi) < Z_i(1,L,\Pi)$; the results for the latter may be found in Tables II, III and IV in the attached paper [3]. Depending on the type of the lowest monoexcitation, we can distinguish three cases. Recall that n_HO and n_LU denote the principal quantum numbers of the occupied orbital with the highest and the virtual orbital with the lowest hydrogenic energies, respectively. First, if $n_\mathrm{LU} > n_\mathrm{HO}$, $Z_i(S,L,\Pi) < Z_n - 1$ and all existing systems are stable. Second, if $n_\mathrm{LU} = n_\mathrm{HO}$, $Z_i(S,L,\Pi)$ lies in the interval (Z_n-1, Z_n+1) and there are no other roots above Z_c. Third, if $n_\mathrm{LU} < n_\mathrm{HO}$, $Z_i(S,L,\Pi) > Z_n$ and cations with $Z > Z_i(S,L,\Pi)$ are unstable. There is usually another root $Z_i'(S,L,\Pi) < Z_i(S,L,\Pi)$ and depending on its position, the corresponding neutral atom is (un)stable. See Section III of our attached paper [3] for more details.

4. Evaluation of Matrix Elements in Relativistic Calculations

This chapter focuses on the development of a numerically stable algorithm for the evaluation of one- and two-electron matrix elements between relativistic Sturmian functions. We illustrate the use of the proposed method on a series of closed- and open-shell atoms and their properties. This work has been published as [4] as a methodological paper and as Fortran 2009 program PASC.

4.1 Introduction

One of the methodological obstacles in high-precision quantum calculation is the evaluation of needed integrals to satisfactory accuracy. In the case of atoms, one usually takes advantage of their spherical symmetry first and by means of the angular momentum algebra integrates out the spinor-angular degrees of freedom. One is then left with the radial degree of freedom only; evaluation of the radial integrals is usually the biggest problem, though.

There are two popular approaches. One can obtain the needed radial integrals numerically, see, e.g., [89, 90, 91], by confining the atom to an artificial cavity and replacing the continuous radial variable by a set of discrete points, called the radial grid. Alternatively, one can expand the wave function into a basis set. The most popular choice for the latter is a so-called B-spline basis, see, e.g., [92, 93, 94, 95, 96], where one again confines the atom to an artificial cavity. The radial coordinate is divided into segments, and in each segment the radial part of the atomic function is expanded into piecewise polynomials.

Clearly, the numerical and B-spline approaches are very similar. They both require to enclose the atom in an artificial cavity, and thus they both start to lose their appeal when it comes to highly excited states as then the interval where one needs an accurate numerical description of the wave function becomes too large. Also note that when we wish to obtain physical observables, we have to remove all the artificial restrictions, i.e., one has to ensure that the result is independent of a number of parameters, such as the volume of the artificial cavity, the number of finite intervals the cavity is decomposed into, number of the basis functions or the density of the grid used on each of the finite intervals, etc. This could be problematic for second-order quantities, such as the PNC amplitude, see Eq. (1.12), where summation over complete system of atomic states is required.

Finally, there is a third possibility: to expand the radial part of the atomic function into a complete and entirely discrete set, the so-called Sturmian basis set, see, e.g., [10, 50, 51, 97]. Moreover, this basis is orthonormal, albeit with the weight r^{-1} with respect to the ordinary weight, and thus avoids the problem of basis set linear dependence. In addition, there is only one artificial parameter: the number of considered basis functions. Note that the most accurate non-relativistic calculations of positions and widths of highly doubly excited states in helium [98, 99, 100], single and double photoionization of helium [101], and so on, were done with the use of this basis set.

4.2 Matrix Elements in the Sturmian Basis

Direct integration to obtain matrix elements in the Sturmian basis is not possible due to numerical instabilities. Sturmian functions with high quantum numbers contain many nodes, and thus we are forced to add or subtract close numbers. Fortunately, there is an alternative approach that has been already studied for the non-relativistic case in [50]. The key idea is to consider the Sturmian functions not "analytically", i.e., through their explicit functional form, but "algebraically", i.e., as functions satisfying certain recursion relations which then imply recursion relations for the integrals of these functions. Here, we extend the method to the relativistic case, i.e., to non-integer quantum numbers, and introduce further improvements, for details see the attached paper [4].

Note that the original paper [50] (and Chapters 2.2 and 3, too) indexes the Sturmian functions with principal quantum number n. Here we use the number of nodes $k = n - l - 1$ to label the functions instead. While in the non-relativistic case, the use of the principal quantum number n may be more intuitive, the use of the number of nodes k is clearly more suitable in the relativistic regime. The reason is that in the relativistic case, n is a non-integer, whereas k is an integer.

4.2.1 One-Electron Matrix Elements

We encounter generally two types of one-particle radial integrals: overlap-type integrals that contain a power of the radial coordinate r^p and integrals involving the radial momentum $\hat{\mathsf{p}}_r$. In both cases, the trick is to use the $\hat{\mathsf{T}}_3$ and $\hat{\mathsf{T}}_\pm$ operators, see Eqs. (2.6), (2.7) and (2.8), to express the radial coordinate r or the radial momentum $\hat{\mathsf{p}}_r$ and act with them on the screened Sturmian functions (2.11)

$$\begin{aligned} 2r\xi R_{k,l}(\xi,r) &= (2T_3 - T_+ - T_-)\xi R_{k,l}(\xi,r) = \\ &= 2(k+l+1)R_{k,l}(\xi,r) - \sqrt{(k+2l+2)(k+1)}R_{k+1,l}(\xi,r) - \\ &\quad - \sqrt{k(k+2l+1)}R_{k-1,l}(\xi,r)\,, \end{aligned} \tag{4.1}$$

$$\begin{aligned} 2r\hat{\mathsf{p}}_r R_{k,l}(\xi,r) &= (\hat{\mathsf{T}}_+ - \hat{\mathsf{T}}_-)R_{k,l}(\xi,r) = \\ &= \sqrt{(k+2l+2)(k+1)}R_{k+1,l}(\xi,r) - \\ &\quad - \sqrt{k(k+2l+1)}R_{k-1,l}(\xi,r)\,. \end{aligned} \tag{4.2}$$

Recall that the radial momentum is given as, see Eq. (2.5),

$$\hat{\mathsf{p}}_r = -i\left(\frac{\partial}{\partial r} + \frac{1}{r}\right)\,.$$

By means of Eqs. (4.1) and (4.2) we thus reduce the one-particle integrals into the "basic" overlap integrals

$$(k_1,l_1,\xi_1|k_2,l_2,\xi_2) = \int_0^\infty r\tilde{R}_{k_1,l_1}(\xi_1,r)\tilde{R}_{k_2,l_2}(\xi_2,r)\,\mathrm{d}r. \tag{4.3}$$

Here, $\tilde{R}_{k,l}(r)$ denote unnormalized radial functions. They are related to the normalized functions $R_{k,l}(r)$ via relation

$$\tilde{R}_{k,l}(r) = \sqrt{\frac{(k+2l+1)!}{k!}} R_{k,l}(r). \tag{4.4}$$

By using the unnormalized functions, the irrational factors, see Eqs. (4.1) and (4.2), are conveniently eliminated.

The method for a numerically stable evaluation of these integals is described in the attached paper [4], see also [50]. Here, we will focus on the evaluation of the two-electron integrals, see below, as they are clearly more complicated.

4.2.2 Two-Electron Matrix Elements

Calculation of the matrix elements of the Coulomb and exchange interaction lies in the evaluation of the integrals

$$\int \mathrm{d}^3\mathbf{r}_1 \int \mathrm{d}^3\mathbf{r}_2 R_{k_1,l_1}(\xi_1, r_1) Y_{l_1,m_1}(\mathbf{n}_1) R_{k_2,l_2}(\xi_2, r_2) Y_{l_2,m_2}(\mathbf{n}_2) r_{12}^{-1} \times \\ \times R_{k_3,l_3}(\xi_3, r_1) Y_{l_3,m_3}(\mathbf{n}_1) R_{k_4,l_4}(\xi_4, r_2) Y_{l_4,m_4}(\mathbf{n}_2)\,.$$

To start with, one separates the radial and angular degrees of freedom. This is achieved by means of the multipole expansion of the Coulomb potential:

$$r_{12}^{-1} = \frac{1}{r_>} \sum_{l=0}^{\infty} \left(\frac{r_<}{r_>}\right)^l \frac{4\pi}{2l+1} \sum_{m=-l}^{l} Y_{l,m}(\mathbf{n}_1) Y_{l,m}^*(\mathbf{n}_2)$$

where $r_< = r_1$, $r_> = r_2$ if $r_1 < r_2$ and $r_< = r_2$, $r_> = r_1$ if $r_1 > r_2$.

The spinor-angular part of the two-electron interaction is easily evaluated (see Section 5 of [4]) and we are left with the radial part only. This consists of the evaluation of a double integral over four functions:

$$\mathcal{R}(\{k_1,l_1,\xi_1\},\{k_2,l_2,\xi_2\},\{k_3,l_3,\xi_3\},\{k_4,l_4,\xi_4\},l) = \tag{4.5}$$

$$= \int_0^\infty \mathrm{d}r_1 R_{k_1,l_1}(\xi_1,r_1) R_{k_3,l_3}(\xi_3,r_1) r_1^{l+2} \int_{r_1}^\infty \mathrm{d}r_2 R_{k_2,l_2}(\xi_2,r_2) R_{k_4,l_4}(\xi_4,r_2) r_2^{-l+1} + \\ + \int_0^\infty \mathrm{d}r_1 R_{k_1,l_1}(\xi_1,r_1) R_{k_3,l_3}(\xi_3,r_1) r_1^{-l+1} \int_0^{r_1} \mathrm{d}r_2 R_{k_2,l_2}(\xi_2,r_2) R_{k_4,l_4}(\xi_4,r_2) r_2^{l+2}\,.$$

The algorithm for its numerically stable evaluation can be described in three steps.

1. **Linearization of the Product of Two Sturmians**

   The product of two Sturmian functions can be expressed as a linear combination of a single Sturmian function:

   $$r^p R_{k_1,l_1}(\xi_1,r) R_{k_2,l_2}(\xi_2,r) = \sum_{k=0}^{k_1+k_2+p} (k_1,l_1,\xi_1,k_2,l_2,\xi_2|k)_p R_{k,l}(\xi,r) \tag{4.6}$$

   with $l = l_1 + l_2$ and $\xi = \xi_1 + \xi_2$. Note that in our case of two-electron matrix elements we have $p = 1$. The above coefficients $(k_1,l_1,\xi_1,k_2,l_2,\xi_2|k)_p$ are obtained from Eq. (4.1) as follows, see [50].

First, we multiply Eq. (4.6) from by $rR_{k',l}(\xi,r)$, integrate over r, and use the orthonormality of the radial functions, Eq. (2.9); we obtain

$$(k_1,l_1,\xi_1,k_2,l_2,\xi_2|k')_p = \int_0^\infty r^{p+1} R_{k',l}(\xi,r) R_{k_1,l_1}(\xi_1,r) R_{k_2,l_2}(\xi_2,r)\,\mathrm{d}r\,. \tag{4.7}$$

Then we again take Eq. (4.6), multiply it this time by $2r$, and let $2r$ act on the lhs on $R_{k_1,l_1}(\xi_1,r)$ and on the rhs on $R_{k,l}(\xi,r)$ according to Eq. (4.1). We arrive at Eq. (51) of [50] with $n = k+l+1$:

$$r^p R_{k_2,l_2}(\xi_2,r)\frac{1}{\xi_1}\Big[2(k_1+l_1+1)R_{k_1,l_1}(\xi_1,r) -$$

$$-\sqrt{(k_1+2l_1+2)(k_1+1)}R_{k_1+1,l_1}(\xi_1,r) - \sqrt{k_1(k_1+2l_1+1)}R_{k_1-1,l_1}(\xi_1,r)\Big] =$$

$$= \sum_{k=0}^{k_1+k_2+p} (k_1,l_1,\xi_1,k_2,l_2,\xi_2|k)_p \frac{1}{\xi}\Big[2(k+l+1)R_{k,l}(\xi,r) -$$

$$-\sqrt{(k+2l+2)(k+1)}R_{k+1,l}(\xi,r) - \sqrt{k(k+2l+1)}R_{k-1,l}(\xi,r)\Big]\,.$$

We then multiply this equation by $rR_{k',l}(\xi,r)$, integrate over r, use the orthonormality of the functions, Eq. (2.9), and consider Eq. (4.7); we obtain Eq. (52) of [50]:

$$2(k_1+l_1+1)(k_1,l_1,\xi_1,k_2,l_2,\xi_2|k') -$$

$$-\sqrt{(k_1+2l_1+2)(k_1+1)}(k_1+1,l_1,\xi_1,k_2,l_2,\xi_2|k') -$$

$$-\sqrt{k_1(k_1+2l_1+1)}(k_1-1,l_1,\xi_1,k_2,l_2,\xi_2|k') =$$

$$= \sum_{k=0}^{k_1+k_2+p} (k_1,l_1,\xi_1,k_2,l_2,\xi_2|k)_p \frac{\xi_1}{\xi}\Big[2(k+l+1)\delta_{k',k} -$$

$$-\sqrt{(k+2l+2)(k+1)}\delta_{k',k+1} - \sqrt{k(k+2l+1)}\delta_{k',k-1}\Big]\,.$$

We keep only the non-zero terms on the rhs, shift the values of k_1 by one, $k_1 \to k_1 - 1$, and finally arrive at the following recurrence relation for the coefficients $(k_1,l_1,\xi_1,k_2,l_2,\xi_2|k)_p$, see Eq. (53) of [50],

$$(k_1,l_1,\xi_1,k_2,l_2,\xi_2|k)_p\sqrt{k_1(k_1+2l_1+1)} =$$

$$= 2\left[k_1+l_1-\frac{\xi_1}{\xi}(k_1+l_1+1)\right](k_1-1,l_1,\xi_1,k_2,l_2,\xi_2|k)_p$$

$$-\sqrt{(k_1+2l_1)(k_1-1)}(k_1-2,l_1,\xi_1,k_2,l_2,\xi_2|k)_p +$$

$$+\frac{\xi_1}{\xi}\sqrt{k(k+2l+1)}(k_1-1,l_1,\xi_1,k_2,l_2,\xi_2|k-1)_p +$$

$$+\frac{\xi_1}{\xi}\sqrt{(k+1)(k+2l+2)}(k_1-1,l_1,\xi_1,k_2,l_2,\xi_2|k+1)_p.$$

This expression is used to lower k_1 to 0. However, it turns out that this equation becomes numerically unstable for large numbers of nodes (of the order of forty) when $k_2 > k_1$. Thus, in order to achieve high numerical stability, this equation is used for $k_1 \geq k_2$. For $k_2 > k_1$ we use the same equation, but with the roles of 1 and 2 swapped, see Eq. (61) in the attached paper [4].

The value of the initial coefficients $(0, l_1, \xi_1, 0, l_2, \xi_2|k)_p$ is obtained by inserting the expression for the lowest screened Sturmian function (for a given l)

$$R_{0,l}(\xi, r) = \frac{2\xi}{\sqrt{(2l+1)!}}(2\xi r)^l e^{-\xi r}$$

into Eq. (4.6). We thus obtain

$$(0, l_1, \xi_1, 0, l_2, \xi_2|0)_0 = \frac{2\xi_1^{l_1+1}\xi_2^{l_2+1}}{(\xi_1+\xi_2)^{l_1+l_2+1}}\sqrt{\frac{(2l_1+2l_2+1)!}{(2l_1+1)!(2l_2+1)!}}$$

and

$$(0, l_1, \xi_1, 0, l_2, \xi_2|k)_0 = 0\,,\ k > 0\,.$$

The case of a nonzero p is obtained from Eqs. (4.6) and (4.1). For example

$$(0, l_1, \xi_1, 0, l_2, \xi_2|0)_1 = 2(l_1+l_2+1)\frac{\xi_1^{l_1+1}\xi_2^{l_2+1}}{(\xi_1+\xi_2)^{l_1+l_2+2}}\sqrt{\frac{(2l_1+2l_2+1)!}{(2l_1+1)!(2l_2+1)!}},$$

$$(0, l_1, \xi_1, 0, l_2, \xi_2|1)_1 = -\sqrt{2(l_1+l_2+1)}\frac{\xi_1^{l_1+1}\xi_2^{l_2+1}}{(\xi_1+\xi_2)^{l_1+l_2+2}}\sqrt{\frac{(2l_1+2l_2+1)!}{(2l_1+1)!(2l_2+1)!}}$$

and

$$(0, l_1, \xi_1, 0, l_2, \xi_2|k)_1 = 0,\ k > 1\,.$$

Thus, we reduce the double integral over four functions, Eq. (4.5), to integrals over two functions:

$$\mathcal{R}(\{k_1, l_1, \xi_1\}, \{k_2, l_2, \xi_2\}, \{k_3, l_3, \xi_3\}, \{k_4, l_4, \xi_4\}, l) = \tag{4.8}$$

$$= \sum_{u,v} c_u c_v \sqrt{\frac{u!}{(u+2(l_1+l_3)+1)!}}\sqrt{\frac{v!}{(v+2(l_2+l_4)+1)!}}\times$$

$$\times\left[P_{u,v}^{l_1+l_3,l_2+l_4,l}(\xi_1+\xi_3, \xi_2+\xi_4) + P_{v,u}^{l_2+l_4,l_1+l_3,l}(\xi_2+\xi_4, \xi_1+\xi_3)\right]$$

where

$$P_{K_1,K_2}^{L_1,L_2,l}(\xi_1, \xi_2) = \int_0^\infty \tilde{R}_{K_1,L_1}(\xi_1, r_1) r_1^{l+1} \int_{r_1}^\infty \tilde{R}_{K_2,L_2}(\xi_2, r_2) r_2^{-l}\,\mathrm{d}r_2\,\mathrm{d}r_1 \tag{4.9}$$

and

$$P_{K_2,K_1}^{L_2,L_1,l}(\xi_2, \xi_1) = \int_0^\infty \tilde{R}_{K_1,L_1}(\xi_1, r_1) r_1^{-l} \int_0^{r_1} \tilde{R}_{K_2,L_2}(\xi_2, r_2) r_2^{l+1}\,\mathrm{d}r_2\,\mathrm{d}r_1\,. \tag{4.10}$$

Recall that $\tilde{R}_{k,l}(\xi, r)$ are unnormalized functions defined in Eq. (4.4). c_u and c_v stand for the above coefficients $c_k = (k_1, l_1, \xi_1, k_2, l_2, \xi_2|k)_1$.

2. **Difference Equations in One Variable**

The second step consists of deriving difference equations for the integrals $P^{L_1,L_2,l}_{K_1,K_2}(\xi_1,\xi_2)$ and $P^{L_2,L_1,l}_{K_2,K_1}(\xi_2,\xi_1)$, Eqs. (4.9) and (4.10), respectively, and reducing them to some "basic" integrals (usually $P^{L_2,L_1,l}_{0,0}(\xi_2,\xi_1)$) that can be easily evaluated.

For illustration, we will show how one can reduce the values of K_1 and K_2 (while keeping L_1, L_2 and l constant), see [4] and also [50]. First, we substitute the unnormalized functions (4.4) into Eq. (4.2) and obtain, cf. Eq. (64) of [50]:

$$2r\left(\frac{\mathrm{d}}{\mathrm{d}r}+\frac{1}{r}\right)\tilde{R}_{k,l}(\xi,r)=(k+1)\tilde{R}_{k+1,l}(\xi,r)-(k+2l+1)\tilde{R}_{k-1,l}(\xi,r)\,. \quad (4.11)$$

Next, we consider the "analytic" equation (63) of [50] (which is obtained by integration by parts)

$$\int_{r_1}^{\infty} r_2\left(\frac{\mathrm{d}}{\mathrm{d}r_2}+\frac{1}{r_2}\right)\left[r_2^{-l}\tilde{R}_{K_2,L_2}(\xi_2,r_2)\right]\mathrm{d}r_2=-r_1^{-l+1}\tilde{R}_{K_2,L_2}(\xi_2,r_1)\,. \quad (4.12)$$

First, by means of fundamental commutation relations, we exchange the positions of r_2^{-l} and the term in the round brackets on the lhs of (4.12). Next, we substitute Eq. (4.11) into the lhs of the above equation (4.12). Then we multiply it by $2\tilde{R}_{K_1,L_1}(\xi_1,r_1)r_1^{l+1}$ and integrate over r_1 from zero to infinity. We thus obtain (see Eq. (69) of [4] and also Eq. (67) of [50])

$$(K_2+1)P^{L_1,L_2,l}_{K_1,K_2+1}(\xi_1,\xi_2)-2lP^{L_1,L_2,l}_{K_1,K_2}(\xi_1,\xi_2)-(K_2+2L_2+1)P^{L_1,L_2,l}_{K_1,K_2-1}(\xi_1,\xi_2)= \quad (4.13)$$
$$=-2(K_1,L_1,\xi_1|r|K_2,L_2,\xi_2)\,.$$

The overlap integrals on the rhs are

$$(K_1,L_1,\xi_1|r|K_2,L_2,\xi_2)=\int_0^{\infty} r^2\tilde{R}_{K_1,L_1}(\xi_1,r)\tilde{R}_{K_2,L_2}(\xi_2,r)\,\mathrm{d}r\,, \quad (4.14)$$

cf. those given by Eq. (4.3). The equation (4.13) is used to lower K_2 to 0.

To obtain an expression for lowering K_1 to 0, we consider a modification of the "analytic" equation (4.12), see Eq. (71) of [50], (again obtained by integration by parts)

$$\int_0^{\infty}\mathrm{d}r_1\,r_1\left(\frac{\mathrm{d}}{\mathrm{d}r_1}+\frac{1}{r_1}\right)\left[r_1^{l+1}\tilde{R}_{K_1,L_1}(\xi_1,r_1)\right]\int_{r_1}^{\infty}\mathrm{d}r_2\,\tilde{R}_{K_2,L_2}(\xi_2,r_2)r_2^{-l}=$$
$$=\int_0^{\infty}\mathrm{d}r_1\,r_1^2\tilde{R}_{K_1,L_1}(\xi_1,r_1)\tilde{R}_{K_2,L_2}(\xi_2,r_1)\,.$$

As in the case of K_2, we first move r_1^{l+1} on the lhs to the left, then we substitute Eq. (4.11) into the lhs of the above modified "analytic" equation, and finally we find, see Eq. (70) of [4] and also Eq. (72) of [50],

$$(K_1+1)P^{L_1,L_2,l}_{K_1+1,K_2}(\xi_1,\xi_2)+2(l+1)P^{L_1,L_2,l}_{K_1,K_2}(\xi_1,\xi_2)- \quad (4.15)$$
$$-(K_1+2L_1+1)P^{L_1,L_2,l}_{K_1-1,K_2}(\xi_1,\xi_2)=2(K_1,L_1,\xi_1|r|K_2,L_2,\xi_2)\,.$$

Thus, by means of Eqs. (4.13) and (4.15), we reduce the above integrals $P^{L_1,L_2,l}_{K_1,K_2}(\xi_1,\xi_2)$, and $P^{L_2,L_1,l}_{K_2,K_1}(\xi_2,\xi_1)$, Eqs. (4.9) and (4.10), to the integrals over nodeless functions $P^{L_1,L_2,l}_{0,0}(\xi_1,\xi_2)$ and $P^{L_2,L_1,l}_{0,0}(\xi_2,\xi_1)$, respectively. We can express these nodeless integrals for general non-integer values of orbital quantum numbers L_1 and L_2 in terms of the hypergeometric function F, see Eq. (72) in [4]:

$$P^{L_1,L_2,l}_{0,0}(\xi_1,\xi_2) = \frac{2^{L_1+L_2+2}\xi_1^{L_1+1}\xi_2^{-L_1-2}\Gamma(L_1+L_2+3)}{l+L_1+2}\times$$

$$\times F\left(L_1+l+2, L_1+L_2+3, L_1+l+3, -\frac{\xi_1}{\xi_2}\right);$$

see Appendix A of [4] where we show how to obtain the hypergeometric function for this particular case. See the attached paper [4] also for a more detailed discussion of this algorithm.

3. **Asymptotic Form**

Finally, to ensure that the method is stable even for very large quantum numbers, we find the asymptotic form of the one-variable difference equations. See Section 5.3 of the attached paper [4].

Consider the exchange integrals, for example. In this case, we can always reduce the evaluation of the integrals to the integrals (4.9) and (4.10) with $\xi = \xi_1 = \xi_2$ and $L = L_1 = L_2$. Note further that for $K_1 \neq K_2$, the rhs of (4.13) and (4.15) are zero, i.e., it suffices to solve the pertinent homogeneous equations.

Both linearly independent solutions of homogeneous Eqs. (4.13) and (4.15) can be obtained as a solution of the equation

$$(K+1)[a_{K+1,p,L} - a_{K-1,p,L}] - 2La_{K-1,p,L} + 2pa_{K,p,L} = 0\,. \tag{4.16}$$

The two linearly independent solutions of the homogeneous Eq. (4.13) are obtained by setting $P^{L_1,L_2,l}_{K_1,K_2}(\xi_1,\xi_2) = a_{K_2,-l,L_2}$ and $P^{L_1,L_2,l}_{K_1,K_2}(\xi_1,\xi_2) = (-1)^{K_2}a_{K_2,l,L_2}$. Likewise, the two linearly independent solutions of homogeneous Eq. (4.15) are obtained by setting $P^{L_1,L_2,l}_{K_1,K_2}(\xi_1,\xi_2) = a_{K_1,l+1,L_1}$ and $P^{L_1,L_2,l}_{K_1,K_2}(\xi_1,\xi_2) = (-1)^{K_1}a_{K_1,-l-1,L_1}$. Following the general method outlined in [76], we search for an asymptotic solution of Eq. (4.16) in the form

$$a_{K,p,L} = \sum_{q=0}^{Q} A_q \frac{\Gamma(K)}{\Gamma(K+q-L+p)}\,. \tag{4.17}$$

In the actual calculation we take $Q \simeq 25$. Substituting this into Eq. (4.16) we obtain after some algebraic manipulation a recursive relation for the coefficients A_q

$$A_{q+1}(-2)(q+1) + A_q(q-L+p)(3q-3-3L+p) -$$

$$-A_{q-1}(q-L+p)(q-L+p-1)(q-L+p-2) = 0\,.$$

One starts this recurrence with $q = 0$ setting $A_{-1} = 0$; A_0 is an overall multiplicative constant undetermined from these relations, but all A_q/A_0

for $q > 0$ are determined uniquely. We first set $A_0 = 1$ and determine overall multiplicative constant later, see [4].

For $|K_1 - K_2| > 0$, a general solution of Eqs. (4.13) and (4.15) for the case $L_1 = L_2 = L$ and $\xi_1 = \xi_2 = \xi$ can be written in the form

$$P^{L,L,l}_{K_1,K_2}(\xi,\xi) = \Big[c_{1,1}a_{K_1,l+1,L} + c_{1,2}a_{K_1,-l-1}(-1)^{K_1}\Big]a_{K_2,-l,L} +$$

$$+\Big[c_{2,1}a_{K_1,l+1,L} + c_{2,2}a_{K_1,-l-1,L}(-1)^{K_1}\Big]a_{K_2,l,L}(-1)^{K_2}\,,$$

$$|K_1 - K_2| > 0\,, \quad K_{1,2} \geq K_0$$

where $K_0 \simeq 10$ is the smallest number for which the asymptotic solution (4.17) holds to desired accuracy; further,

$$P^{L,L,l}_{K_1,K_2}(\xi,\xi) = c_{1,1}a_{K_1,l+1} + c_{1,2}a_{K_1,-l-1}(-1)^{K_1} \quad K_1 \geq K_0 > K_2$$

and

$$P^{L,L,l}_{K_1,K_2}(\xi,\xi) = c_{1,1}a_{K_2,-l} + c_{2,1}a_{K_2,l}(-1)^{K_2} \quad K_2 \geq K_0 > K_1\,.$$

The coefficients c are fitted to the actual values of the integrals obtained by running equations (4.13) and (4.15) up to $K_{1,2} \simeq 10$, see the attached paper [4] for details.

4.3 Illustration on the DHF Model

In this chapter, we will show how the above proposed algorithm can be used in practice. We will illustrate it on a series of calculations of closed- and open-shell atoms and their properties in the relativistic DHF approximation. The numerical results and their discussion may be found in the next Chapter 4.4.

4.3.1 Dirac-Hartree-Fock Model

The most general HF model was introduced in Chapter 2.1. The HF model for atoms in the non-relativistic approximation was studied in Chapter 3. Here, we will focus on the relativistic DHF model for atoms.

In the restricted DHF model we put N electrons into N spin-orbitals labeled by a. These spin-orbitals are successively put in accordance with the Bohr Aufbau principle into ν shells labeled by A. Each shell is characterized by the total (orbital plus spin) angular momentum j_A, relativistic parity κ_A and principal quantum number n_A, the last number distinguishing different shells of the same spinor-angular symmetry. Each shell comprises $2j_A + 1$ states of different projections m of the total angular momentum on one of the coordinate axes.

The relativistic energy of N electrons in N spin-orbitals a in the DHF approximation is, recall Eq. (2.1) (and note that here we scaled the electronic coordinates $\mathbf{r}^{(i)} \to \mathbf{r}^{(i)}/Z$),

$$\frac{E_{\mathrm{DHF}}}{Z^2} = \sum_{a=1}^{N} \langle a|\,\hat{\mathsf{z}}\,|a\rangle + \frac{1}{2Z}\sum_{a=1}^{N}\sum_{b=1}^{N} \langle a|_1\,\langle b|_2\,\hat{\mathsf{v}}\,(1-\mathcal{P}_{12})\,|a\rangle_1\,|b\rangle_2$$

and the DHF equations are, see Eqs. (2.2) and (2.3),

$$\hat{\mathsf{f}}\,|a\rangle = \varepsilon_a\,|a\rangle\ , \qquad \hat{\mathsf{f}} = \hat{\mathsf{z}} + \frac{1}{Z}\sum_{b=1}^{N}\langle b|_2\,\hat{\mathsf{v}}\,(1-\mathcal{P}_{12})\,|b\rangle_2\ . \tag{4.18}$$

The one-electron $\hat{\mathsf{z}}$ and two-electron $\hat{\mathsf{v}}$ operators now take the form (in atomic units)

$$\hat{\mathsf{z}} = \frac{1}{Z\alpha}\gamma_0\boldsymbol{\gamma}\cdot\hat{\mathbf{p}} + \frac{\gamma_0-1}{(Z\alpha)^2} - \frac{1}{r}\,, \tag{4.19}$$

$$\hat{\mathsf{v}} = \hat{\mathsf{r}}_{12}^{-1}\,. \tag{4.20}$$

Note that in the one-particle operator $\hat{\mathsf{z}}$ we subtract the electron rest mass, $1/(Z\alpha)^2$. Here, γ_i are the Dirac matrices in the standard (Dirac) representation and, recall, $\alpha = 1/137.0359991$ is the fine-structure constant [1].

4.3.2 Integrals of Motion

As is well-known, see, e.g., [89], there are three operators commuting with the Dirac Hamiltonian for a particle in a spherically symmetric field: the square, $\hat{\mathsf{J}}^2$, and the third component, $\hat{\mathsf{J}}_z$, of the total angular momentum given by the sum of orbital and spin angular momentum,

$$\hat{\mathbf{J}} = \hat{\mathbf{L}} + \frac{1}{2}\boldsymbol{\Sigma}\,, \tag{4.21}$$

and the relativistic parity operator $\hat{\mathsf{K}}$,

$$\hat{\mathsf{K}} = \gamma_0\left(\boldsymbol{\Sigma}\cdot\hat{\mathbf{L}} + 1\right)\,. \tag{4.22}$$

As noted in [102], in the case of a purely Coulomb field, $\hat{\mathsf{v}} = 0$ in Eq. (4.20) and hence $\hat{\mathsf{f}} = \hat{\mathsf{z}}$, another integral of motion appears for the second-order Dirac Hamiltonian, see our attached paper [4] for more details,

$$\hat{\mathsf{G}} = \gamma_0\left(\hat{\mathsf{K}} + i(Z\alpha)\boldsymbol{\gamma}\cdot\mathbf{n}\right)\,. \tag{4.23}$$

Simple calculation shows that

$$\hat{\mathsf{K}}^2 = \hat{\mathsf{J}}^2 + \frac{1}{4}\,, \quad \hat{\mathsf{G}}^2 = \hat{\mathsf{K}}^2 - (Z\alpha)^2\,.$$

Whence the eigenvalues of the operators $\hat{\mathsf{K}}$ and $\hat{\mathsf{G}}$ read

$$K = \kappa|K|\,, \quad \kappa = \pm 1\,, \quad |K| = j + 1/2 \tag{4.24}$$

and

$$G = g\kappa|G|\,, \quad g = \pm 1\,, \quad |G| = \sqrt{K^2 - (Z\alpha)^2}\,, \tag{4.25}$$

respectively. Note that the sign of G is defined relative to the sign of K.

All the four operators $\hat{\mathsf{G}}, \hat{\mathsf{K}}, \hat{\mathsf{J}}^2$ and $\hat{\mathsf{J}}_z$ commute one with another; whence they possess common eigenfunctions

$$\hat{\mathsf{G}}|g,\kappa,j,m\rangle = g\kappa|G||g,\kappa,j,m\rangle\,, \tag{4.26}$$

$$\hat{\mathsf{K}}|g,\kappa,j,m\rangle = \kappa|K||g,\kappa,j,m\rangle\,, \tag{4.27}$$

$$\hat{\mathsf{J}}^2|g,\kappa,j,m\rangle = j(j+1)|g,\kappa,j,m\rangle\,, \tag{4.28}$$

$$\hat{\mathsf{J}}_z|g,\kappa,j,m\rangle = m|g,\kappa,j,m\rangle\,. \tag{4.29}$$

The explicit form of the bispinors $|g,\kappa,j,m\rangle$ reads

$$\langle\mathbf{n}|\,g,\kappa,j,m\rangle = \begin{pmatrix} c_1^g\langle\mathbf{n}|j,m\rangle^\kappa \\ c_2^g\langle\mathbf{n}|j,m\rangle^{-\kappa} \end{pmatrix}\,, \tag{4.30}$$

where the symbol $\langle\mathbf{n}|j,m\rangle^\kappa$ denotes spherical spinors

$$\langle\mathbf{n}|\,j,m\rangle^\kappa = \sum_{S_z=-\frac{1}{2}}^{\frac{1}{2}} \left(j-\frac{\kappa}{2}, m-S_z, \frac{1}{2}, S_z|j,m\right) Y_{j-\frac{\kappa}{2},m-S_z}(\mathbf{n}) \left|\frac{1}{2}, S_z\right\rangle\,.$$

A condition for the coefficients c in the expansion (4.30) follows from Eqs. (4.22), (4.23), (4.26), and (4.27) and together with the normalization condition allows us to uniquely determine these coefficients c, see the attached paper [4].

4.3.3 Form of the Spin-Orbitals

A common tehchnique in relativistic calculations is to decompose the electronic wave function into its upper and lower components and then impose matching conditions on them (usually known as the Grant conditions). Here, however, we propose a different approach (in which, note, the Grant matching conditions are automatically satisfied). See the details in Section 2.3 of [4] for our motivation.

Notice that the Fock operator (4.18) with (4.19) and (4.20) mixes states $\langle r|\,n,l_g\rangle\,\langle\mathbf{n}|\,g,\kappa,j,m\rangle$ with different signs of g and different principal quantum numbers n. Thus, a general eigenstate of this Fock operator can be searched for in the form

$$\langle\mathbf{r}|\,a\rangle = \langle\mathbf{r}|\,n_A,\kappa_A,j_A,m\rangle = \tag{4.31}$$

$$= \langle r|\,n_A,|G|-\delta_{\kappa_A,+}\rangle\,\langle\mathbf{n}|\,+,\kappa_A,j_A,m\rangle + \langle r|\,n_A,|G|-\delta_{\kappa_A,-}\rangle\,\langle\mathbf{n}|\,-,\kappa_A,j_A,m\rangle\,.$$

The bispinors $\langle\mathbf{n}|\,g,\kappa_A,j_A,m\rangle$ are given by Eq. (4.30), see also Eqs. (26) and (27) in [4]. The radial parts of the orbitals are expanded into the screened Sturmian functions, Eqs. (2.6) and (2.11), (here, again, N denotes the number of basis functions)

$$\langle r|\,n_A,|G|-1\rangle = \sum_{k=0}^{N} c^+_{A,k} R_{k,|G|-1}(\xi_A,r)\,, \tag{4.32}$$

$$\langle r|\,n_A,|G|\rangle = \sum_{k=0}^{N-1} c^-_{A,k} R_{k,|G|}(\xi_A,r)\,. \tag{4.33}$$

The screening constant ξ_A is set to $\xi_A = 1/n_A$, n_A is the non-relativistic principal quantum number of the pertinent shell.

4.3.4 Roothaan Form of the DHF Equations

Substituting now expansions (4.31), (4.32) and (4.33) into the DHF equation (4.18) and projecting this equation onto the considered basis vectors, we obtain the Roothaan form of the DHF equations

$$\sum_k \begin{pmatrix} f_{ik}^{++} & f_{ik}^{+-} \\ f_{ik}^{-+} & f_{ik}^{--} \end{pmatrix} \begin{pmatrix} c_{A,k}^{\delta_{\kappa_A,+}-\delta_{\kappa_A,-}} \\ c_{A,k}^{\delta_{\kappa_A,-}-\delta_{\kappa_A,+}} \end{pmatrix} =$$

$$= \varepsilon_a \sum_k \begin{pmatrix} S_{ik}^{++} & S_{ik}^{+-} \\ S_{ik}^{-+} & S_{ik}^{--} \end{pmatrix} \begin{pmatrix} c_{A,k}^{\delta_{\kappa_A,+}-\delta_{\kappa_A,-}} \\ c_{A,k}^{\delta_{\kappa_A,-}-\delta_{\kappa_A,+}} \end{pmatrix},$$

where

$$f_{ik}^{g,\overline{g}} = z_{ik}^{g,\overline{g}} + \frac{1}{Z} v_{ik}^{g,\overline{g}}\,.$$

The operators $\hat{\mathsf{z}}$ and $\hat{\mathsf{v}}$ are given by Eqs. (4.19) and (4.20), respectively. The pertinent matrix elements are

$$z_{ik}^{g,\overline{g}} = \int_0^\infty \mathrm{d}r r^2 R_{i,l_g}(\xi,r) \left\langle g,\kappa,j,m\right| \hat{\mathsf{z}} \left|\overline{g},\kappa,j,m\right\rangle R_{k,l_{\overline{g}}}(\xi,r)\,, \tag{4.34}$$

$$S_{ik}^{g,\overline{g}} = \left\langle g,\kappa,j,m|\overline{g},\kappa,j,m\right\rangle \int_0^\infty \mathrm{d}r r^2 R_{i,l_g}(\xi,r) R_{k,l_{\overline{g}}}(\xi,r)\,, \tag{4.35}$$

and

$$\begin{aligned} v_{ik}^{g,\overline{g}} = \sum_{\{n_B,j_B,\kappa_B\}} \sum_{p,g'} \sum_{q,\overline{g}'} & c_{B,p}^{\delta_{\kappa_B,g'}-\delta_{\kappa_B,-g'}} c_{B,q}^{\delta_{\kappa_B,\overline{g}'}-\delta_{\kappa_B,-\overline{g}'}} \\ & \sum_{l=0}^{\infty} \mathcal{A}^C(j_A,\kappa_A,g,\overline{g},j_B,\kappa_B,g',\overline{g}',l)\times \\ & \times\mathcal{R}(\{i,l_g,\xi_A\},\{p,l_{g'},\xi_B\},\{k,l_{\overline{g}},\xi_A\},\{q,l_{\overline{g}'},\xi_B\},l) \\ & -\mathcal{A}^E(j_A,\kappa_A,g,\overline{g},j_B,\kappa_B,g',\overline{g}',l)\times \\ & \times\mathcal{R}(\{i,l_g,\xi_A\},\{p,l_{g'},\xi_B\},\{q,l_{\overline{g}'},\xi_B\},\{k,l_{\overline{g}},\xi_A\},l)\,. \end{aligned} \tag{4.36}$$

The explicit expressions for the spinor-angular part of the Coulomb $\mathcal{A}^C$ and exchange $\mathcal{A}^E$ integrals may be found in Section 4 of [4]. The radial part $\mathcal{R}$ is given by Eq. (4.8). Evaluation of these matrix elements (4.34), (4.35) and (4.36) is discussed in Chapter 4.2.2 and in more detail in [4].

As usual, these equations are solved iteratively. In each step, we obtain $2N-1$ values for energy, see Eqs. (4.32) and (4.33). Of those, one half belongs to negative-energy states (known as the "Dirac sea") and the other half to positive-energy states that correspond to the energies of the atomic shells.

4.3.5 PNC Amplitude in Cesium

The DHF model for closed shells, as described in the previous chapters, can be also directly used for open-shell atoms with one valence electron. The one-particle valence electron Hamiltonian is taken in the form of the Fock operator, Eq. (4.18) with (4.19) and (4.20), where we use the field of $Z-1$ core electrons obtained by solving restricted DHF equations for the pertinent closed-shell cation, for instance

for Cs^+. This, the so-called frozen-core approximation, is advantageous for later consideration of electron correlation, see, e.g., [8].

The PNC amplitude was derived earlier in Chapter 1.4 in natural units, Eq. (1.12):

$$i\mathrm{Im}\mathcal{E}_{\mathrm{PNC}} = \langle 7s| \left[\hat{\mathsf{H}}_{\mathrm{PNC}} \frac{1}{\hat{\mathsf{H}}_{\mathrm{at}} - E_{7s}} \hat{\mathsf{d}}_z + \hat{\mathsf{d}}_z \frac{1}{\hat{\mathsf{H}}_{\mathrm{at}} - E_{6s}} \hat{\mathsf{H}}_{\mathrm{PNC}} \right] |6s\rangle \ .$$

Changing to atomic units, see Eqs. (92)–(99) in Section 6 of [4], considering the nucleus to be a spherically homogeneous sphere with radius r_{N}, cf. Eq. (1.3), inserting the value for the charge radius of ^{133}Cs nucleus $r_{\mathrm{N}} = 4.804\,\mathrm{fm}$ [103], and substituting these expressions into the above equation, we obtain

$$\mathrm{Im}\mathcal{E}_{\mathrm{PNC}} = i\frac{e}{m_e\alpha}\left(-\frac{Q_W}{N}\right) 10^{-11}\overline{\mathcal{E}}_{\mathrm{PNC}}\,, \tag{4.37}$$

where

$$\overline{\mathcal{E}}_{\mathrm{PNC}} = i\frac{(0.5446)^2}{\sqrt{8}} N\alpha \sum_{\mathrm{n}} \times \tag{4.38}$$

$$\times \langle 7s| \left\{ \frac{\rho\gamma_5 \left|np_{1/2}\right\rangle \left\langle np_{1/2}\right| r n_3}{\varepsilon_{np_{1/2}} - \varepsilon_{7s}} + \frac{r n_3 \left|np_{1/2}\right\rangle \left\langle np_{1/2}\right| \rho\gamma_5}{\varepsilon_{np_{1/2}} - \varepsilon_{6s}} \right\} |6s\rangle \ .$$

In Eq. (4.37), we also separated the usual units, $ie/(m_e\alpha)\,(-Q_W/N)\,10^{-11}$, used for reporting theoretical results for the PNC amplitude. Recall that Q_W is the weak nuclear charge, N number of neutrons ($N = 78$ for ^{133}Cs nucleus), α the fine-structure constant, e the elementary (electron) charge, and m_e the electron rest mass.

We can take advantage of an important identity

$$[\hat{\mathsf{r}}, \hat{\mathsf{f}}] = \frac{i}{Z\alpha}\gamma_0\boldsymbol{\gamma}$$

and further rewrite Eq. (4.38) as

$$\overline{\mathcal{E}}_{\mathrm{PNC}} = \frac{(0.5446)^2}{\sqrt{8}} \frac{N}{Z} \times \tag{4.39}$$

$$\times \sum_{\mathrm{n}} \frac{\langle 7s| \left[\rho\gamma_5 \left|np_{1/2}\right\rangle \left\langle np_{1/2}\right| \gamma_0\gamma_3 - \gamma_0\gamma_3 \left|np_{1/2}\right\rangle \left\langle np_{1/2}\right| \rho\gamma_5\right] |6s\rangle}{(\varepsilon_{7s} - \varepsilon_{np_{1/2}})(\varepsilon_{6s} - \varepsilon_{np_{1/2}})} \,.$$

These two expressions (4.38) and (4.39) allow us to control the numerical accuracy of the obtained results.

We then expand the atomic states in Eqs. (4.38) or (4.39) into the basis set Eq. (4.31) with $j = 1/2$ and $m = 1/2$, see Section 6 of [4] for details.

4.4 Results and Discussion

The full list of results and their discussion may be found in our paper [4]; here, we will focus only on the most important ones. Also, in [4] one may find a discussion

of the computational aspect of this work as well as a note on the use of the related Fortran program PASC.

The most important contribution of this work is the development of a numerically stable algorithm for the evaluation of one- and two-electron integrals between relativistic (and also non-relativistic) Sturmian functions. Hopefully, this will allow for a wider use of this basis set in high-precision atomic structure calculations. The relative numerical error (double vs. quadruple precision) of the obtain matrix elements is 10^{-9}–10^{-15}, see Table B.2 of [4] for illustration. See also Table B.1 of [4]; it illustrates that our method yields results in excellent agreement with the GRASP2K method [90] (GRASP2K uses numerical integration). Notice that for heavier systems, especially xenon, we obtain even slightly better results than [90]. In addition, our program is not limited to 20 relativistic shells, as is the case of GRASP2K.

Apart from its methodological significance, this work, using the frozen-core DHF model for one-electron open shells, also represents the first step towards the most precise calculation of the so-called PNC amplitude in cesium, see Eq. (1.12). First, orbital energies for cesium $6s$, $7s$ and several $p_{1/2}$ states obtained using our method are compared to those produced by other codes, see Tab. 4.1. One can see that the orbital energies more or less agree. However, once we test the quality of the wave functions near the nucleus (by calculating the hyperfine integrals, see Tab. 4.2) as well as at large distances from the nucleus (by calculating the reduced dipole matrix elements, see Tab. 4.3), we see that our results differ from those published by other authors. Moreover, we obtain an even bigger disagreement for the PNC amplitude, see Tab. 4.4.

Table 4.1: Excited one-particle energies of Cs in the frozen-core DHF approximation (in atomic units). For comparison with other results we use the same nomenclature as in [95]; FD stands for finite difference code, DKB for dual kinetic basis set code [96] and ND for Notre Dame code [92]. See also Table B.3 in [4].

	$6s$	$7s$	$6p_{1/2}$
this work	−0.1273734422(1)	−0.0551888581(1)	−0.085615749
FD	−0.127368	−0.05518735	−0.08561589
DKB	−0.1273674	−0.05518714	−0.08561576
ND	−0.1273682	−0.0551875	−0.08561616
Ref. [13]	−0.127368	−0.0551863	−0.0856135

Table 4.2: Hyperfine integrals for cesium, see Eq. (122) of [4], (in atomic units). As in Tab. 4.1, FD stands for finite difference code, DKB for dual kinetic basis set code [96] and ND for Notre Dame code [92].

	$6s$ $(\times 10^{-1})$	$7s$ $(\times 10^{-2})$	$6p_{1/2}$ $(\times 10^{-2})$
this work	1.14301	3.1410	−1.25543
FD	1.114751	3.063077	−1.252026
DKB	1.114741	3.063069	−1.252018
ND	1.121812	3.084164	−1.218362

Table 4.3: Reduced dipole matrix elements $(n's|D|np_{1/2})$ for cesium (in atomic units); $(n's|D|np_{1/2}) = (n's|z|np_{1/2})\sqrt{2}/(1/2, 1/2, 1, 0|1/2)$. See [4] for more details.

		$6p_{1/2}$	$7p_{1/2}$	$8p_{1/2}$
this work	$6s$	5.0367970	0.30564910	0.0956989
Ref. [13]		5.2777	0.3717	
this work	$7s$	4.2458375	10.789637	0.857288
Ref. [13]		4.4131	11.009	

Table 4.4: PNC amplitude in cesium, see Eqs. (4.38) and (4.39), in the frozen-core DHF approximation. As in Tab. 4.1, FD stands for finite difference code, DKB for dual kinetic basis set code [96] and ND for Notre Dame code [92].

	$\overline{\mathcal{E}}_{\rm PNC}$
this work	0.8097
FD	0.74
DKB	0.7395
ND	0.8546

5. Symmetry-Adapted Coupled Clusters

In the previous Chapter 4, we showed how one can use the Sturmian functions for relativistic (and non-relativistic) calculations and illustrated the proposed method for the evaluation of one- and two-electron matix elements on a series of calculations on the DHF level. In this chapter, we will add the missing methodological piece that separates us from attaining the experimental accuracy: the electron correlation.

Our aim is to obtain ionization energies of all I.A elements that are comparable with the pertinent experimental values. The ionization energy of an atom (e.g., Cs) is given as the difference between the total energy of the pertinent +1 cation (e.g., Cs^+) and the total energy of the electroneutral atom (e.g., Cs). To obtain the energy of the closed-shell cation, we run DHF calculation followed by the CC method to add the missing electron correlation. To calculate the energy of a one-electron open shell, we run a DHF calculation of the pertinent closed-shell cation first and then use the CI-CC method to include the extra electron and the electron correlation. See also Chapter 4.3.

In this chapter, we show how one can take advantage of the spherical symmetry of atoms and simplify the CC and CI methods. This part forms the basis of our next paper and will be submitted once all calculations finish.

5.1 Introduction

The probably most difficult and still unresolved problem in electronic structure calculations is the inclusion of electron correlation. By this term we understand the influence of the motion of one electron on the motion of another electron. This interaction is quantified via so-called correlation energy.

Traditionally, the correlation energy is defined as the difference between the exact energy (which we usually do not know) and the HF limit (i.e., HF energy independent of basis type and size)

$$\Delta E = E_{\text{exact}} - E_{\text{HF}} \,.$$

However, we should note that this definition could be somewhat misleading as the electron correlation is already partially included in the HF approximation. Within the HF model, the two-electron interaction is expressed via a classical Coulomb term and an exchange term, see Chapter 2.1. The latter describes the correlation between two electrons with parallel spins and prevents two parallel-spin electrons from being found at the same point in space.

The usual approach is to perform a HF (or DHF) calculation first and then continue with one of the post-HF methods to include this missing electron correlation. In atomic and molecular physics, one usually opts for the CI method, perturbative Moller-Plesset methods, explicitly correlated wave functions, or the CC method. Here, we will focus mainly on the last.

The CC method, also nicknamed the golden standard of quantum chemistry, was originally introduced in 1960 by Coester and Kümmel [104] in the field of

nuclear physics. Its use for electronic structure calculations was first proposed by Jiří Čížek in his PhD thesis, later published as [105], and followed by a series of works of Čížek and Paldus, e.g., [105, 106, 107], and later by many others, see the references, e.g., in the review [49].

The key idea of the CC method (see Chapter 5.3 for a more detailed introduction) is the so-called exponential ansatz:

$$|\Psi\rangle = e^{\hat{\mathsf{T}}} |\Phi\rangle \ .$$

We assume that the true wave function $|\Psi\rangle$ can be obtained from a reference state $|\Phi\rangle$ (for example a HF solution) via inclusion of all excitations. Unlike the CI method, where we consider only a linear combination of single, double, etc. excited states, in the CC approach the relation is via an exponential of the excitation operator $\hat{\mathsf{T}}$.

In practice, this means that we have to solve a system of non-linear and coupled equations to obtain the coefficients for the individual contribution of each excitation (so-called cluster amplitudes) and only then we can calculate the correlation energy. Many works have focused on possible simplification of such a complicated system of equations. For example, one could take into account the symmetry of the studied problem.

In quantum chemistry one nearly exclusively deals with spin-independent non-relativistic Hamiltonian. Therefore, considerable attention has been devoted to the adaptation of the CC method to spin symmetry [108, 109]. When considering relativistic theory of isolated atoms, however, the Hamiltonian is not spin-independent, but is spherically symmetric. Adaptation of the CC method to this symmetry has not been done so far, to the best of our knowledge, and is thus subject of this part of this thesis. For adaptation of the non-relativistic theory to spin and spherical symmetry see [110, 111].

The nontrivial aspect of the symmetry adaptation is that one wants the wave function to be adapted to the spherical symmetry and at the same time to be antisymmetric with respect to the interchange of any two electrons. Of the two basic approaches to symmetry adaptation, the "algebraic" due to Racah, see, e.g., [71] and references therein, and the"geometric" due to Löwdin, see, e.g., [112, 113] and references therein, we follow the former one. However, in contrast to Racah, who first considers states adapted to the spherical symmetry and only then takes care, by means of coefficients of fractional parantage, of permutation symmetry, we found that for computer implementation is somewhat easier first to conform to the permutation symmetry and only then take care of spherical symmetry. The only new feature this procedure brings is that for symmetry adaptation one has to keep the information whether for a given electron configuration the electrons occupy the same radial orbitals.

5.2 Atomic Hamiltonian in the Second Quantization Formalism

Before turning to the CC method, let us introduce the Hamiltonian for our system in the second quantization formalism. Throughout this Chapter, we will use the same notation as in [114] except for the upside down reverse of biexcitation cluster

amplitudes; our t_{ab}^{rs} equals t_{rs}^{ab} of [114]. As is common, $a, b, \ldots$ and $r, s, \ldots$ refer to occupied and virtual spin-orbitals, respectively. The greek letters $\mu, \nu, \ldots$ denote generic HF spin-orbitals.

The atomic N-electron no-pair Hamiltonian in the formalism of the second quantization takes the form (using Einstein summation convention and dimensionless atomic units with electronic coordinates scaled $\mathbf{r}^{(i)} \to \mathbf{r}^{(i)}/Z$)

$$\hat{\mathsf{H}} = E_{\mathrm{HF}} + :\hat{\mathsf{H}}:, \quad :\hat{\mathsf{H}} := \varepsilon_\mu :\hat{\mathsf{e}}_\mu^\mu: + \frac{1}{4} v_{\kappa\lambda}^{\mu\nu} :\hat{\mathsf{e}}_{\mu\nu}^{\kappa\lambda}:, \tag{5.1}$$

where the one- and two-electron excitation operators read

$$\hat{\mathsf{e}}_\nu^\mu = \hat{\mathsf{X}}_\mu^\dagger \hat{\mathsf{X}}_\nu, \quad \hat{\mathsf{e}}_{\mu\nu}^{\kappa\lambda} = \hat{\mathsf{X}}_\kappa^\dagger \hat{\mathsf{X}}_\lambda^\dagger \hat{\mathsf{X}}_\nu \hat{\mathsf{X}}_\mu . \tag{5.2}$$

Here, $\hat{\mathsf{X}}_\mu^\dagger$ and $\hat{\mathsf{X}}_\mu$ designate the electron creation and annihilation operators in a generic HF spin-orbital μ, respectively. These operators obey anticommutation relations

$$\{\hat{\mathsf{X}}_\mu, \hat{\mathsf{X}}_\nu^\dagger\} = \delta_{\mu,\nu}, \quad \{\hat{\mathsf{X}}_\mu, \hat{\mathsf{X}}_\nu\} = 0, \quad \{\hat{\mathsf{X}}_\mu^\dagger, \hat{\mathsf{X}}_\nu^\dagger\} = 0 . \tag{5.3}$$

The colon symbol in Eq. (5.1) stands for normal ordering; meaning that the upper and lower indices in excitation operator are not allowed to be contracted. Further, E_{HF} is the atom's total binding energy in the HF approximation, ε_μ designate generic HF one-particle energies in atomic units and the antisymmetrized two-electron matrix elements read

$$v_{\kappa\lambda}^{\mu\nu} = \frac{1}{Z} \langle\kappa|_1 \langle\lambda|_2 \hat{\mathsf{r}}_{12}^{-1} \left(|\mu\rangle_1 |\nu\rangle_2 - |\nu\rangle_1 |\mu\rangle_2\right) . \tag{5.4}$$

These matrix elements are antisymmetric with respect to the interchange of any pair of indices, i.e.,

$$v_{\kappa\lambda}^{\mu\nu} = -v_{\lambda\kappa}^{\mu\nu} = -v_{\kappa\lambda}^{\nu\mu} = v_{\lambda\kappa}^{\nu\mu} . \tag{5.5}$$

To be obtain the correlation energy ΔE, we need to solve the Schrödinger equation with the Hamiltonian (5.1),

$$:\hat{\mathsf{H}}: |\Psi\rangle = \Delta E \ |\Psi\rangle . \tag{5.6}$$

The total energy is then simply a sum of the HF and correlation energy

$$E = E_{\mathrm{HF}} + \Delta E .$$

5.3 Coupled Cluster Method For Closed Shells

A pedagogical introduction to the CC method based on diagrams may be found, e.g., in [115, 116]. Here, we will follow an algebraic one from [114].

As already mentioned in Chapter 5.1, the key idea of the CC method is to use the exponential ansatz

$$|\Psi\rangle = e^{\hat{\mathsf{T}}} |\Phi\rangle \tag{5.7}$$

where, recall, $|\Psi\rangle$ is the exact wave function, $|\Phi\rangle$ reference state wave function and $\hat{\mathsf{T}}$ is the cluster operator. This ansatz converts Schrödinger equation (5.6) for eigenvalues of the Hamiltonian (5.1) into an equation for eigenvalues of the

transformed Hamiltonian $\hat{\bar{\mathsf{H}}}$ (we multiplied Eq. (5.6) with $\exp\{-\hat{\mathsf{T}}\}$ from the left),

$$\hat{\bar{\mathsf{H}}}\,|\Phi\rangle = \Delta E\,|\Phi\rangle\ , \quad \hat{\bar{\mathsf{H}}} = e^{-\hat{\mathsf{T}}} : \hat{\mathsf{H}} : e^{\hat{\mathsf{T}}}\,. \tag{5.8}$$

For closed-shell atoms we can set

$$|\Phi\rangle = |0\rangle\ ,$$

where $|0\rangle$ is Fermi vacuum defined by the relations (recalling that r and a stand for virtual and occupied spin-orbitals, respectively)

$$\hat{\mathsf{X}}_r\,|0\rangle = 0\,, \quad \hat{\mathsf{X}}_a^\dagger\,|0\rangle = 0\,. \tag{5.9}$$

5.3.1 CCD Method in the Standard Spin-Orbital Form

As a first approximation, we can restrict the expansion of the cluster operator $\hat{\mathsf{T}}$

$$\hat{\mathsf{T}} = \hat{\mathsf{T}}_1 + \hat{\mathsf{T}}_2 + \hat{\mathsf{T}}_3 + \hat{\mathsf{T}}_4 + \cdots$$

to only biexcited clusters

$$\hat{\mathsf{T}} \simeq \hat{\mathsf{T}}_2 \tag{5.10}$$

as those contribute to the correlation energy the most. This is known as the CC doubles (CCD) approximation. Sometimes, monoexcited clusters are considered as well; this leads to the CC singles and doubles (CCSD) approximation, see, e.g., [114]. However, in the case of a HF reference state, the singles do not influence the results significantly. Triple (T) and quadruple (Q) excitations are usually included only perturbatively, if at all. Note, though, that S, T and Q begin to contribute at the same order of the perturbative method and they influence the correlation energy via interaction with the biexcitations. In our work, we consider the STQ only perturbatively (not discussed here).

To obtain the CCD equations, we use Čížek's expansion [105, 106, 107, 117] for the clusters

$$\hat{\mathsf{T}}_2 = \frac{1}{4} t_{ab}^{rs} \hat{\mathsf{e}}_{ab}^{rs} \tag{5.11}$$

where t_{ab}^{rs} are cluster amplitudes that we want to find and $\hat{\mathsf{e}}_{ab}^{rs}$ is the excitation operator as in Eq. (5.2). It follows from this equation that the cluster amplitudes t_{ab}^{rs} are completely antisymmetric with respect to the interchange of any two indices, cf. Eq. (5.5),

$$t_{ab}^{rs} = -t_{ba}^{rs} = -t_{ab}^{sr} = t_{ba}^{sr}\,. \tag{5.12}$$

It follows from the last equation that no pair of electrons can occupy the same occupied or virtual spin-orbital. This is the Pauli exclusion principle.

The projection of Eq. (5.8) onto the Fermi vacuum state, Eq. (5.9), yields an expression for the correlation energy

$$\Delta E = \langle 0|\,\hat{\bar{\mathsf{H}}}\,|0\rangle$$

and projection onto biexcited states leads to coupled equations for the cluster amplitudes t_{ab}^{rs}

$$0 = \langle 0|\,\hat{\mathsf{e}}_{rs}^{ab}\hat{\bar{\mathsf{H}}}\,|0\rangle\ . \tag{5.13}$$

To obtain the explicit form of the CCD equations, we use the well-known Baker-Campbell-Hausdorff (BCH) formula

$$\mathrm{e}^{-\hat{\mathsf{B}}}\hat{\mathsf{A}}\mathrm{e}^{\hat{\mathsf{B}}} = \hat{\mathsf{A}} + \left[\hat{\mathsf{A}},\hat{\mathsf{B}}\right] + \frac{1}{2}\left[\left[\hat{\mathsf{A}},\hat{\mathsf{B}}\right],\hat{\mathsf{B}}\right] + \frac{1}{3!}\left[\left[\left[\hat{\mathsf{A}},\hat{\mathsf{B}}\right],\hat{\mathsf{B}}\right],\hat{\mathsf{B}}\right] + \cdots \tag{5.14}$$

to expand the exponentials in the definition of the transformed Hamiltonian, Eq. (5.8) with the CCD approximation (5.10). Thus, by virtue of Eqs. (5.3) and (5.9), the correlation energy in terms of the cluster amplitudes is

$$\Delta E = \langle 0|\left[:\hat{\mathsf{H}}:,\hat{\mathsf{T}}_2\right]|0\rangle = \frac{1}{4}v_{rs}^{ab}t_{ab}^{rs}\,. \tag{5.15}$$

The coupled equations for the amplitudes t_{ab}^{rs}, Eq. (5.13), can be simplified to

$$0 = \langle 0|\,\hat{\mathsf{e}}_{rs}^{ab}\left(:\hat{\mathsf{H}}: + :\hat{\mathsf{H}}:\hat{\mathsf{T}}_2 - \hat{\mathsf{T}}_2:\hat{\mathsf{H}}:\hat{\mathsf{T}}_2 + \frac{1}{2}:\hat{\mathsf{H}}:\hat{\mathsf{T}}_2^2\right)|0\rangle\ .$$

One can easily verify that within the CCD approximation no higher commutators contribute than the double commutator that leads to the last two terms in the brackets. Using the expressions (5.1) and (5.11) for the Hamiltonian and cluster operators, respectively, the anticommutation relations (5.3) and the definition of the Fermi vacuum state, Eq. (5.9), we obtain the spin-orbital form of the coupled CC equations for the cluster amplitudes (e_{rs}^{ab} denotes the equation for the $(ab)\rightarrow(rs)$ biexcitation)

$$e_{rs}^{ab} = 0\,,\quad e_{rs}^{ab} = v_{rs}^{ab} + \frac{1}{2^2}t_{cd}^{uv}\mathcal{L}_{rs,cd}^{ab,uv} + \frac{1}{2^5}t_{cd}^{uv}t_{ef}^{xy}\mathcal{Q}_{rs,cd,ef}^{ab,uv,xy}\,. \tag{5.16}$$

The linear term is

$$\mathcal{L}_{rs,cd}^{ab,uv} = \langle 0|\,\hat{\mathsf{e}}_{rs}^{ab}:\hat{\mathsf{H}}:\hat{\mathsf{e}}_{cd}^{uv}\,|0\rangle = \tag{5.17}$$

$$= (\varepsilon_r+\varepsilon_s-\varepsilon_a-\varepsilon_b)\Delta_{rs}^{uv}\Delta_{cd}^{ab} + v_{cd}^{ab}\Delta_{rs}^{uv} + v_{rs}^{uv}\Delta_{cd}^{ab} + \mathcal{A}_{rs}^{ab}\mathcal{A}_{cd}^{uv}v_{rc}^{au}\delta_v^s\delta_b^d$$

and the quadratic term is

$$\mathcal{Q}_{rs,cd,ef}^{ab,uv,xy} = \langle 0|\,\hat{\mathsf{e}}_{rs}^{ab}\left[-2\hat{\mathsf{e}}_{cd}^{uv}:\hat{\mathsf{H}}:+:\hat{\mathsf{H}}:\hat{\mathsf{e}}_{cd}^{uv}\right]\hat{\mathsf{e}}_{ef}^{xy}\,|0\rangle = \tag{5.18}$$

$$\mathcal{A}_{cd}^{uv}\mathcal{A}_{ef}^{xy}\Delta_{rs}^{vx}\Delta_{de}^{ab}v_{cf}^{uy} + 2\mathcal{A}^{uv}\mathcal{A}^{xy}\Delta_{rs}^{ux}\Delta_{cd}^{ab}v_{ef}^{yv} - 2\mathcal{A}_{cd}\mathcal{A}_{ef}\Delta_{rs}^{xy}\Delta_{ed}^{ab}v_{cf}^{uv} + 2\Delta_{rs}^{xy}\Delta_{cd}^{ab}v_{ef}^{uv}\,.$$

Here

$$\Delta_{uv}^{rs} = \delta_u^r\delta_v^s - \delta_v^r\delta_u^s$$

and $\mathcal{A}$ denotes antisymmetrizer with respect to pertinent indices, for instance the last equation can also be written

$$\Delta_{uv}^{rs} = \mathcal{A}^{rs}\delta_u^r\delta_v^s\,.$$

Of course, one could further simplify the antisymmetrizers and the deltas and obtain equations as in [114]. However, for further manipulation and then for the actual programming of the CC methods, it is advantageous to keep this form.

5.3.2 Adaptation to the Permutation Symmetry

There is an additional simplification that can be traced back to Pauli exclusion principle, that is, to the antisymmetry of the matrix elements (5.5) and amplitudes (5.12). Equations (5.16) hold for unordered pairs of upper and lower indices, r, s and a, b, respectively. For given pairs of upper and lower indices, one can form four orthogonal linear combinations of unordered amplitudes that differ by the (anti)symmetry with respect to the exchange of upper and lower indices

$$\begin{pmatrix} \left(t_{\overline{ab}}^{\overline{rs}}\right)^{++} \\ \left(t_{\overline{ab}}^{\overline{rs}}\right)^{+-} \\ \left(t_{\overline{ab}}^{\overline{rs}}\right)^{-+} \\ \left(t_{\overline{ab}}^{\overline{rs}}\right)^{--} \end{pmatrix} = \frac{1}{2} \begin{pmatrix} 1 & 1 & 1 & 1 \\ 1 & 1 & -1 & -1 \\ 1 & -1 & 1 & -1 \\ 1 & -1 & -1 & 1 \end{pmatrix} \begin{pmatrix} t_{ab}^{rs} \\ t_{ab}^{sr} \\ t_{ba}^{rs} \\ t_{ba}^{sr} \end{pmatrix} .$$

This transformation is orthogonal, so the inverse transformation reads

$$\begin{pmatrix} t_{ab}^{rs} \\ t_{ab}^{sr} \\ t_{ba}^{rs} \\ t_{ba}^{sr} \end{pmatrix} = \frac{1}{2} \begin{pmatrix} 1 & 1 & 1 & 1 \\ 1 & 1 & -1 & -1 \\ 1 & -1 & 1 & -1 \\ 1 & -1 & -1 & 1 \end{pmatrix} \begin{pmatrix} \left(t_{\overline{ab}}^{\overline{rs}}\right)^{++} \\ \left(t_{\overline{ab}}^{\overline{rs}}\right)^{+-} \\ \left(t_{\overline{ab}}^{\overline{rs}}\right)^{-+} \\ \left(t_{\overline{ab}}^{\overline{rs}}\right)^{--} \end{pmatrix} .$$

Now, if we substitute the last equation into Eq. (5.15) and Eqs. (5.16) – (5.18), we find that, due to the antisymmetry of the matrix elements (5.5), only the combination $\left(t_{\overline{ab}}^{\overline{rs}}\right)^{--}$ contributes to the correlation energy and this combination decouples from the other three combinations. Thus, the last equation can be simplified to

$$t_{ab}^{rs} = \frac{1}{2} \mathcal{A}_{ab}^{rs} T_{\overline{ab}}^{\overline{rs}} , \quad T_{\overline{ab}}^{\overline{rs}} = \left(t_{\overline{ab}}^{\overline{rs}}\right)^{--} . \tag{5.19}$$

Further, we order not only the amplitudes, but also Eqs. (5.16) themselves,

$$E_{\overline{rs}}^{\overline{ab}} = \frac{1}{2} \mathcal{A}_{rs}^{ab} e_{rs}^{ab} = 2 v_{rs}^{ab} + T_{\overline{cd}}^{\overline{uv}} \mathcal{L}_{rs,cd}^{ab,uv} + \frac{1}{2^2} T_{\overline{cd}}^{\overline{uv}} T_{\overline{ef}}^{\overline{xy}} \mathcal{Q}_{rs,cd,ef}^{ab,uv,xy} = 0 , \tag{5.20}$$

where we substituted Eq. (5.19) and used the fact that the expressions (5.16), (5.17) and (5.18) are automatically antisymmetric with respect to the interchange of the pertinent indices and each additional antisymmetrization in each pair of indices produces a factor of 2. Finally, substituting Eq. (5.19) into Eq. (5.15), we obtain the correlation energy in terms of the ordered amplitudes

$$\Delta E = \frac{1}{2} v_{rs}^{ab} T_{\overline{ab}}^{\overline{rs}} .$$

5.3.3 Adaptation to the Spherical Symmetry

As already discussed earlier, see Chapter 4.3.3, atoms are spherically symmetric. Mathematically, this means that the Hamiltonian (5.1) commutes with the total angular momentum operator of the electron field

$$\hat{\mathbf{J}} = \mathbf{J}_{\mu}^{\nu} \hat{\mathbf{e}}_{\nu}^{\mu} ,$$

where $\mathbf{J}_\mu^\nu$ are the matrix elements of one-electron total angular momentum operator, cf. Eq. (4.21); explicitly

$$\mathbf{J}_\mu^\nu = \langle\mu|\,\hat{\mathbf{L}} + \frac{\mathbf{\Sigma}}{2}\,|\nu\rangle\ .$$

Recall that the first and second operators inside the inner product stand for the one-electron orbital angular momentum and spin operators, respectively. Furthermore, the Hamiltonian (5.1) commutes with the parity operator of the electron field, Eq. (4.22). Whence, the Hamiltonian (5.1) does not mix the two-electron states of different total angular momentum and parity.

Further, the restricted DHF method for atoms yields the spin-orbitals in the form, see Chapter 4.3.3,

$$|a\rangle = |n_a, \kappa_a, j_a, m_a\rangle = |A, m_a\rangle\ ,$$

where, recall, n, κ, j and m designate the spin-orbital principal quantum number, parity, total angular momentum and its projection onto one of the coordinate axes, respectively, see Eqs. (4.26) – (4.29).

Considering the following linear combination of matrix elements (5.4)

$$\sum_{m_a=-j_a}^{j_a}\sum_{m_r=-j_r}^{j_r}(j_a, m_a, j_b, m-m_a|j)(j_r, m_r, j_s, m'-m_r|j')v_{rs}^{ab} =$$

$$= v_{AB}^{RS}(j)\delta_{m,m'}\delta_{j',j}$$

we find that the result (the rhs of the last equation) is non-zero only if the resulting angular momenta j, j', and their projections m, m', of holes and particles are the same. If this is the case, the result is independent of the total magnetic quantum number m. Further, for one-electron states the reflection of coordinate axes around origin produces the factor $(-1)^{j-\kappa/2}$. Whence the matrix elements v_{rs}^{ab} and $v_{AB}^{RS}(j)$ vanish unless the combined parities of holes and particles are the same

$$(-1)^{j_a+j_b-(\kappa_a+\kappa_b)/2} = (-1)^{j_r+j_s-(\kappa_r+\kappa_s)/2}\,.$$

Owing to the reality and orthonormality of the CG coefficients, the matrix elements (5.4) can be expressed in terms of SA elements as

$$v_{rs}^{ab} = \sum_{j=\max(|j_a-j_b|,|j_r-j_s|)}^{\min(j_a+j_b,j_r+j_s)}(j_a, m_a, j_b, m-m_a|j)(j_r, m_r, j_s, m-m_r|j)v_{AB}^{RS}(j)\,. \quad (5.21)$$

Finally, substituting Eq. (5.21) into Eq. (5.5) we obtain by virtue of the symmetry of the CG coefficients

$$v_{AB}^{RS}(j) = (-1)^{j-j_a-j_b-1}v_{BA}^{RS}(j) = (-1)^{j-j_r-j_s-1}v_{AB}^{SR}(j)\,.$$

This in particular yields

$$v_{AA}^{RS}(j) = (-1)^{j-2j_a-1}v_{AA}^{RS}(j) = (-1)^j v_{AA}^{RS}(j)\,, \quad (5.22)$$

where in the last equation we took the advantage of the fact that since j_a is a half-integer, $2j_a+1$ is even. We thus see that the matrix elements $v_{AA}^{RS}(j)$ vanish for odd j.

Similarly, we can make orthogonal transformation between the unordered amplitudes t_{ab}^{rs} and amplitudes $t_{AB}^{RS}(j_+, j_-, J)$ describing the biexcited states of definite total angular momenta J

$$t_{ab}^{rs} = \sum_{j_+,j_-,J} (j_a, m_a, j_b, m_b|j_-)(j_r, m_r, j_s, m_s|j_+)(j_+, m_r + m_s, j_-, -m_a - m_b|J)\times \\ \times(-1)^{j_- - m_a - m_b} t_{AB}^{RS}(j_+, j_-, J) \tag{5.23}$$

When adding the angular momenta of particles and holes, the magnetic quantum numbers of the holes have to be taken with the opposite sign and the pertinent CG coefficient has to be multiplied by the appropriate phase factor, see e.g. [108, 109, 110, 111, 118].

Now, due to the spherical symmetry, the amplitudes $t_{AB}^{RS}(j_+, j_-, J)$ with $J > 0$ decouple and do not influence the ground state energy. Therefore in the last equation, Eq. (5.23), we keep only the first term in the expansion on the rhs, namely,

$$t_{ab}^{rs} = \sum_{j=\max(|j_a - j_b|, |j_r - j_s|)}^{\min(j_a+j_b, j_r+j_s)} (j_a, m_a, j_b, m_b|j)(j_r, m_r, j_s, m_s|j)\delta_{m_a+m_b}^{m_r+m_s} t_{AB}^{RS}(j)\,, \tag{5.24}$$

$$t_{AB}^{RS}(j) = \frac{t_{AB}^{RS}(j, j, 0)}{\sqrt{2j+1}}\,.$$

When considering the above transformation between the *ordered* amplitudes, we have to distinguish whether the radial orbitals are the same or not. Thus Eq. (5.24) is modified as follows:

$$T_{\overline{ab}}^{\overline{rs}} = \sum_{j=\max(|j_a - j_b|, |j_r - j_s|)}^{\min(j_a+j_b, j_r+j_s)} D_{j_a, m_a, j_b, m_b, \delta_{AB}}^{j_r, m_r, j_s, m_s, \delta_{RS}}(j) T_{\overline{AB}}^{\overline{RS}}(j)\,, \tag{5.25}$$

where

$$D_{j_a, m_a, j_b, m_b, \delta_{AB}}^{j_r, m_r, j_s, m_s, \delta_{RS}}(j) = V_{j_a, j_b, \delta_{AB}}^{j_r, j_s, \delta_{RS}}(j) \Big[\delta_{AB}(1 - (-1)^{j - j_a - j_b})\Theta(m_b - m_a) + 1 - \delta_{AB}\Big] \times \\ \times \Big[\delta_{RS}(1 - (-1)^{j - j_r - j_s})\Theta(m_s - m_r) + 1 - \delta_{RS}\Big] \times \\ \times(j_a, m_a, j_b, m_b|j)(j_r, m_r, j_s, m_s|j)\delta_{m_a+m_b}^{m_r+m_s}\,, \tag{5.26}$$

where $\Theta(x)$ is Heaviside function, $\Theta(x) = 1$ for $x > 0$ and zero otherwise. Further, $V_{j_a, j_b, \delta_{AB}}^{j_r, j_s, \delta_{RS}}(j)$ is determined from the normalization condition

$$\sum_{m_a, m_b, m_r, m_s} \Big[D_{j_a, m_a, j_b, m_b, \delta_{AB}}^{j_r, m_r, j_s, m_s, \delta_{RS}}(j)\Big]^2 = 1\,. \tag{5.27}$$

If the radial orbitals A and B, and R and S are different, then the coefficients D are the same as those in Eq. (5.24). However, if, say the orbitals A and B, are the same, then, first, the requirement of the ordering enforces the restriction $m_a < m_b$. Second, we sum over the permutation of the spin-orbitals a and b to exclude the values of j that are symmetric with respect of the interchange of the spin-orbitals a and b, as then the Pauli exclusion principle is not satisfied.

Note that these two changes do not spoil the orthogonality of the transformation (5.24). For instance, if the radial orbitals A and B are the same, then $j_a = j_b = j$. The orthogonality relations for CG coefficients then read

$$\sum_{m=-j}^{j} (j, -m, j, m|J)(j, -m, j, m|J') = \delta_{J,J'} \, .$$

Now, for half-integral j this can be rewritten as

$$\sum_{m=-j}^{-1/2} (j, -m, j, m|J)(j, -m, j, m|J') \left[1 + (-1)^{J+J'-4j}\right] = \delta_{J,J'} \, ,$$

where the term in the square bracket is clearly independent of m. Since j is half-integral, the term in the square-bracket vanishes if the sum $J + J'$ is odd. If the sum $J + J'$ is even, then

$$\sum_{m=-j}^{-1/2} (j, -m, j, m|J)(j, -m, j, m|J') = \frac{\delta_{J,J'}}{2} \, .$$

Thus, the orthogonality is preserved and one has to take care of the normalization only.

Substituting now the transformation (5.25) into Eqs. (5.20) we obtain CCD equations for the ordered SA amplitudes $T^{\overline{RS}}_{\overline{AB}}(j)$. Their explicit form is given in Appendix A.1.

5.4 Configuration Interaction Method for Open Shells

In the CI approach, we express the exact wave function $|\Psi\rangle$ as a linear combination of possible excited states of the reference state $|\Phi\rangle$

$$|\Psi\rangle = \hat{\mathsf{R}} \, |\Phi\rangle$$

and instead of Eq. (5.6), we solve

$$: \hat{\mathsf{H}} : \hat{\mathsf{R}} \, |\Phi\rangle = \Delta E \hat{\mathsf{R}} \, |\Phi\rangle \tag{5.28}$$

$\hat{\mathsf{R}}$ is a general excitation operator similar to $\hat{\mathsf{T}}$. Note that in the case of open shells, the numbers of annihilation and creation operators differ, see for example Eqs. (5.30) below. The so-called full CI (FCI) method, in which we include all possible excitations, should in principle yield the exact result. However, in practice, we have to truncate the expansion; the FCI is feasible only for small systems.

In our case of one-electron open-shell systems, we consider only the first three terms of the expansion:

$$|\Psi\rangle \simeq |1\rangle + |3\rangle + |5\rangle \, , \tag{5.29}$$

where the one-, three- and five-particle states are

$$|1\rangle = c^u \hat{\mathsf{e}}^u \, |0\rangle \, , \quad |3\rangle = \frac{1}{2} c^{uv}_d \hat{\mathsf{e}}^{uv}_d \, |0\rangle \, , \quad |5\rangle = \frac{1}{3!2} c^{uvw}_{de} \hat{\mathsf{e}}^{uvw}_{de} \, |0\rangle \, , \tag{5.30}$$

respectively. Note that this expansion is exact for Li-like systems. The above states represent the extra valence electron (the one-particle term) and its combination with a monoexcitation (the three-particle term) or a biexcitation (the five-particle term). As before, $|0\rangle$ is our reference closed-shell state defined by Eqs. (5.9) and $\hat{\mathsf{e}}^u$, $\hat{\mathsf{e}}^{uv}_d$ and $\hat{\mathsf{e}}^{uvw}_{de}$ are excitation operators analogous to (5.2), and coeffcients c we want to find. The coefficients c are completely antisymmetric in the pertinent indices:

$$\begin{aligned} &c^{uv}_d = -c^{vu}_d \,, \\ &c^{uvw}_{de} = -c^{uvw}_{ed} = c^{vwu}_{de} = c^{wuv}_{de} = -c^{uwv}_{de} = -c^{vuw}_{de} = -c^{wvu}_{de} \,. \end{aligned}$$

Projecting now Eq. (5.28) with (5.29) and (5.30), successively on the states $\langle 0|\,\hat{\mathsf{e}}_q$, $\langle 0|\,\hat{\mathsf{e}}^a_{qr}$ and $\langle 0|\,\hat{\mathsf{e}}^{ab}_{qrs}$ we obtain by means of the anticommutators, Eqs. (5.3), definition of the Fermi vacuum, Eqs. (5.9), and the expansion of the exact wave function, Eq. (5.30),

$$\begin{pmatrix} \mathcal{H}^u_q & \mathcal{H}^{uv}_{qd} & \mathcal{H}^{uvw}_{qcd} \\ \mathcal{H}^{au}_{qr} & \mathcal{H}^{auv}_{qrd} & \mathcal{H}^{auvw}_{qrcd} \\ \mathcal{H}^{abu}_{qrs} & \mathcal{H}^{abuv}_{qrsd} & \mathcal{H}^{abuvw}_{qrscd} \end{pmatrix} \begin{pmatrix} 1 & 0 & 0 \\ 0 & \frac{1}{2!} & 0 \\ 0 & 0 & \frac{1}{3!2!} \end{pmatrix} \begin{pmatrix} c^u \\ c^{uv}_d \\ c^{uvw}_{cd} \end{pmatrix} = \Delta E \begin{pmatrix} c^q \\ c^{qr}_a \\ c^{qrs}_{ab} \end{pmatrix} . \quad (5.31)$$

The individual contributions are given by

$$\begin{aligned} \mathcal{H}^u_q &= \langle 0|\,\hat{\mathsf{e}}_q : \hat{\mathsf{H}} : \hat{\mathsf{e}}^u\,|0\rangle = \varepsilon_q \delta^u_q \,, \\ \mathcal{H}^{uv}_{qd} &= \langle 0|\,\hat{\mathsf{e}}_q : \hat{\mathsf{H}} : \hat{\mathsf{e}}^{uv}_d\,|0\rangle = v^{uv}_{qd} \,, \\ \mathcal{H}^{uvw}_{qcd} &= \langle 0|\,\hat{\mathsf{e}}_q : \hat{\mathsf{H}} : \hat{\mathsf{e}}^{uvw}_{cd}\,|0\rangle = \mathcal{A}^{wuv}\left\{\delta^w_q v^{uv}_{cd}\right\} , \\ \mathcal{H}^{auv}_{qrd} &= \langle 0|\,\hat{\mathsf{e}}^a_{qr} : \hat{\mathsf{H}} : \hat{\mathsf{e}}^{uv}_d\,|0\rangle = (\varepsilon_q + \varepsilon_r - \varepsilon_a)\delta^a_d \Delta^{uv}_{qr} + v^{uv}_{qr}\delta^a_d + \mathcal{A}^{uv}_{qr}\left\{v^{ua}_{dq}\delta^v_r\right\} , \\ \mathcal{H}^{auvw}_{qrcd} &= \langle 0|\,\hat{\mathsf{e}}^a_{qr} : \hat{\mathsf{H}} : \hat{\mathsf{e}}^{uvw}_{cd}\,|0\rangle = \mathcal{A}^{wuv}\left\{v^{wa}_{cd}\Delta^{uv}_{qr}\right\} + \mathcal{A}_{qr}\mathcal{A}^{wuv}_{cd}\left\{\delta^a_c\delta^w_q v^{uv}_{dr}\right\} , \\ \mathcal{H}^{abuvw}_{qrscd} &= \langle 0|\,\hat{\mathsf{e}}^{ab}_{qrs} : \hat{\mathsf{H}} : \hat{\mathsf{e}}^{uvw}_{cd}\,|0\rangle = (\varepsilon_q + \varepsilon_r + \varepsilon_s - \varepsilon_a - \varepsilon_b)\Delta^{uvw}_{qrs}\Delta^{ab}_{cd} + v^{ab}_{cd}\Delta^{uvw}_{qrs} + \\ &\quad + \mathcal{A}^{uvw}_{qrs}\left\{\delta^w_q \Delta^{ab}_{cd} v^{uv}_{rs}\right\} + \mathcal{A}^{ab}_{qrs}\mathcal{A}^{uvw}_{cd}\left\{\Delta^{uv}_{rs}\delta^a_c v^{wb}_{dq}\right\} . \end{aligned}$$

The symbol $\mathcal{A}^{qrs}$ creates all even permutations of indices involved. The remaining matrix elements are obtained from the hermicity of the Hamilton operator,

$$\mathcal{H}^{au}_{qr} = \mathcal{H}^{rq}_{ua} \,, \quad \mathcal{H}^{abu}_{qrs} = \mathcal{H}^{srq}_{uba} \,, \quad \mathcal{H}^{abuv}_{qrsd} = \mathcal{H}^{dsrq}_{vuba} \,.$$

5.4.1 Adaptation to the Permutation Symmetry

Following the same reasoning as in the case of the CC in Chapter 5.3.2, we can change from unordered to ordered amplitudes

$$\begin{pmatrix} c^u \\ c^{uv}_d \\ c^{uvw}_{cd} \end{pmatrix} = \begin{pmatrix} 1 & 0 & 0 \\ 0 & \frac{\mathcal{A}^{uv}}{\sqrt{2!}} & 0 \\ 0 & 0 & \frac{\mathcal{P}^{uvw}_{cd}}{\sqrt{3!2!}} \end{pmatrix} \begin{pmatrix} C^u \\ C^{\overline{uv}}_{\overline{d}} \\ C^{\overline{uvw}}_{\overline{cd}} \end{pmatrix} .$$

The symbol $\mathcal{P}^{uvw}$ denotes all (odd and even) permutations of the three indices.

Multiplying Eq. (5.31) by the operator

$$\begin{pmatrix} 1 & 0 & 0 \\ 0 & \frac{\mathcal{A}_{qr}}{\sqrt{2!}} & 0 \\ 0 & 0 & \frac{\mathcal{P}^{ab}_{qrs}}{\sqrt{3!2!}} \end{pmatrix}$$

from the left, Eq. (5.31) is transformed to

$$\begin{pmatrix} 1 & 0 & 0 \\ 0 & \sqrt{2!} & 0 \\ 0 & 0 & \sqrt{3!2!} \end{pmatrix} \begin{pmatrix} \mathcal{H}_q^u & \mathcal{H}_{qd}^{uv} & \mathcal{H}_{qcd}^{uvw} \\ \mathcal{H}_{qr}^{au} & \mathcal{H}_{qrd}^{auv} & \mathcal{H}_{qrcd}^{auvw} \\ \mathcal{H}_{qrs}^{abu} & \mathcal{H}_{qrsd}^{abuv} & \mathcal{H}_{qrscd}^{abuvw} \end{pmatrix} \times \tag{5.32}$$

$$\times \begin{pmatrix} 1 & 0 & 0 \\ 0 & \frac{1}{\sqrt{2!}} & 0 \\ 0 & 0 & \frac{1}{\sqrt{3!2!}} \end{pmatrix} \begin{pmatrix} C^u \\ C_{\overline{d}}^{\overline{uv}} \\ C_{\overline{cd}}^{\overline{uvw}} \end{pmatrix} = \Delta E \begin{pmatrix} C^q \\ C_{\overline{a}}^{\overline{qr}} \\ C_{\overline{ab}}^{\overline{qrs}} \end{pmatrix} .$$

5.4.2 Adaptation to the Spherical Symmetry

We now introduce the orthogonal transformations from the spin-orbital coefficients to the coefficients describing the states of definite square of the total angular momenta J and projection to the one of the axes M. The reasoning behing this step is similar to the CC case from Chapter 5.3.3. These transformations read for one-particle

$$c^Q(J) = c^q \delta_{j_q,J} \delta_{m_q,M} ,$$

three-particle

$$c_A^{QR,J_+}(J) = \sum_{m_q,m_a} (j_q, m_q, j_r, M + m_a - m_q | J_+)(J_+, M + m_a, j_a, -m_a | J) \times$$

$$\times (-1)^{j_a - m_a} c_a^{qr} ,$$

and five-particle states

$$c_{AB,J_-}^{QRS,J_{rs},J_+}(J) = \sum_{m_r,m_q,m_s,m_a,m_b} (j_r, m_r, j_s, m_s | J_{rs})(j_q, m_q, J_{rs}, m_r + m_s | J_+) \times$$

$$\times (j_a, m_a, j_b, m_b | J_-)(J_+, m_q + m_r + m_s, J_-, -m_a - m_b) | J) \times$$
$$\times (-1)^{J_- - m_a - m_b} \delta_{M+m_a+m_b}^{m_q+m_r+m_s} c_{ab}^{qrs} .$$

The inverse tranformations for the three-particle and five-particle states are

$$c_a^{qr} = \sum_{J_+,J} (j_q, m_q, j_r, M + m_a - m_q | J_+)(J_+, M + m_a, j_a, -m_a | J)(-1)^{j_a - m_a} c_A^{QR,J_+}(J) \tag{5.33}$$

and

$$c_{ab}^{qrs} = \sum_{J_{rs},J_+,J_-,J} (j_r, m_r, j_s, m_s | J_{rs})(j_q, m_q, J_{rs}, m_r + m_s | J_+) \times \tag{5.34}$$

$$\times (j_a, m_a, j_b, m_b | J_-)(J_+, m_q + m_r + m_s, J_-, -m_a - m_b) | J) \times$$
$$\times (-1)^{J_- - m_a - m_b} \delta_{M+m_a+m_b}^{m_q+m_r+m_s} c_{AB,J_-}^{QRS,J_{rs},J_+}(J) ,$$

respectively.

In the case of ordered amplitudes, the transformations from Eqs. (5.33) and (5.34) are modified as follows, cf. Eqs. (5.25), (5.26) and (5.27),

$$C_a^{\overline{qr}} = \sum_{J_+,J} D_{j_a,m_a}^{j_q,m_q,j_r,m_r,\delta_{QR}}(J_+, J) C_A^{\overline{QR},J_+}(J)$$

with

$$D^{j_q,m_q,j_r,m_r,\delta_{QR}}_{j_a,m_a}(J_+,J) = V^{j_q,j_r,\delta_{QR}}_{j_a}(J_+,J)\times$$

$$\times(j_q,m_q,j_r,M+m_a-m_q|J_+)(J_+,M+m_a,j_a,-m_a|J)(-1)^{j_a-m_a}\times$$

$$\times\left\{1-\delta_{QR}+\delta_{QR}\Theta(m_r-m_q)[1-(-1)^{J_+-j_r-j_q}]\right\}$$

and

$$C^{\overline{qrs}}_{\overline{ab}} = \sum_{J_{rs},J_+,J_-,J} D^{j_q,m_q,j_r,m_r,j_s,m_s,\delta_{QR},\delta_{RS}}_{j_a,m_a,j_b,m_b,\delta_{AB}}(J_{rs},J_+,J_-,J)C^{\overline{QRS},J_{rs},J_+}_{\overline{AB},J_-}(J)\,,$$

with

$$D^{j_q,m_q,j_r,m_r,j_s,m_s,\delta_{QR},\delta_{RS}}_{j_a,m_a,j_b,m_b,\delta_{AB}}(J_{rs},J_+,J_-,J) = V^{j_q,j_r,j_s,\delta_{QR},\delta_{RS}}_{j_a,j_b,\delta_{AB}}(J_{rs},J_+,J_-,J)\times \quad (5.35)$$

$$\times(J_+,m_q+m_r+m_s,J_-,-m_a-m_b|J)(-1)^{J_--m_a-m_b}\delta^{m_q+m_r+m_s}_{M+m_a+m_b}\times$$

$$\times(j_a,m_a,j_b,m_b|J_-)\left\{1-\delta_{AB}+\delta_{AB}\Theta(m_b-m_a)\left[1-(-1)^{J_--j_a-j_b}\right]\right\}\times$$

$$\times\Bigg\{(1-\delta_{QR})(j_r,m_r,j_s,m_s|J_{rs})(j_q,m_q,J_{rs},m_r+m_s|J_+)\times$$

$$\times\left\{1-\delta_{RS}+\delta_{RS}\Theta(m_s-m_r)\left[1-(-1)^{J_{rs}-j_r-j_s}\right]\right\}+$$

$$+\delta_{QR}\delta_{RS}\Theta(m_s-m_r)\Theta(m_r-m_q)\times$$

$$\times\left[\delta_{J_{rs},j_r+j_s}\frac{1+(-1)^{j_r+j_s}}{2}+\delta_{J_{rs},j_r+j_s-1}\frac{1-(-1)^{j_r+j_s}}{2}\right]\times$$

$$\times\sum_{i=1}^{6}\mathrm{sgn}(\mathcal{P}_i)(j_{\mathcal{P}_i(r)},m_{\mathcal{P}_i(r)},j_{\mathcal{P}_i(s)},m_{\mathcal{P}_i(s)}|J_{rs})\times$$

$$\times(j_{\mathcal{P}_i(q)},m_{\mathcal{P}_i(q)},J_{rs},m_{\mathcal{P}_i(r)}+m_{\mathcal{P}_i(s)}|J_+)\Bigg\}\,,$$

respectively.

Substituting now the last two equations into Eq. (5.32) we obtain equations for ordered SA coefficients C. Their explicit form is given in Appendix A.2.

The equation (5.35) requires some explanation. In general we have to distinguish three cases concerning three virtual radial orbitals, denoted by Q, R, S: 1) all of them are different, 2) the two of them are the same and the third is different, 3) all of them are the same. The second case can be always arranged in such a way that the same orbitals are labeled by R and S. In the third case the value of J_{rs} is irrelevant, as all the possible symmetry adapted states with different values of J_{rs} are linearly dependent. For definitness we choose the highest possible value of J_{rs}.

5.5 A Combined CI-CC Method for Open Shells

Now that we have introduced the CC and CI methods, we will turn to their combination for open-shell systems. This approach is usually known as the EOM-CC method (although one might find this name somewhat misleading) and a summary may be found, e.g., in [119].

In the previous chapter, we consider the HF (or DHF) solution as our reference state for the CI method, see Eqs. (5.29) and (5.30). We could consider the CC wave function, Eq. (5.7), as our reference state, though:

$$|\Psi\rangle = \hat{\mathsf{R}}\,|\Phi\rangle = \hat{\mathsf{R}}\mathrm{e}^{\hat{\mathsf{T}}}\,|0\rangle \ .$$

Since both $\hat{\mathsf{R}}$ and $\hat{\mathsf{T}}$ are excitation operators, they necessarily commute; the Schrödinger equation (5.6) thus may be rewritten, considering Eq. (5.8), as

$$\hat{\overline{\mathsf{H}}}\hat{\mathsf{R}}\,|0\rangle = \Delta E\hat{\mathsf{R}}\,|0\rangle \ ,$$

i.e., into an eigenvalue problem with the effective Hamiltonian (5.8), cf. Eq. (5.28). This CI-CC approach is, in principle, exact as none of the introduced transformations changes the eigenvalues of the full Hamiltonian. However, in practice we have to truncate the expansions of the excitation operators $\hat{\mathsf{R}}$ and $\hat{\mathsf{T}}$ at some level, and thereby compromise the exactness of the method.

In [119], the authors nicely summarize the superiority of the CI-CC approach over the pure (truncated) CI method. "One rather subtle point concerning the similarity transformation is that the wave operator is nonlinear and therefore includes configurations that lie outside the space defined by the truncation of the $\hat{\mathsf{T}}$ operator. As a result, the eigenvalues of $\hat{\overline{\mathsf{H}}}$ within the space of singly and doubly substituted determinants are not the same as those of $\hat{\mathsf{H}}$, i.e., the configuration interaction singles and doubles (CISD) roots. The nonlinear transformation acts to 'fold in' effects of higher excitations, thereby allowing superior results to be obtained in the same determinantal subspace."

In our study, we focus on one-electron open-shell systems. This means that the CI expansion is of the form (5.30) and truncated after the third term. The CC method is restricted to only CCD as described in Chapter 5.3.1.

Now there are two options how to proceed. One could again use the BCH formula (5.14) to expand the exponentials, and then use the expressions (5.1), (5.11) and (5.30) for the Hamiltonian, cluster operators and one-, three- and five-particle states, respectively, the anticommutation relations (5.3) and the definition of the Fermi vacuum state, Eq. (5.9), to obtain the spin-orbital form of the CI-CC equations.

Alternatively, we can consider the relation between this CI-CC problem and the CI problem described in the previous chapter. The CI-CC coefficients c to be determined can be expressed using the cluster amplitudes t_{ab}^{rs} and some other coefficients f.The explicit form of Eq. (5.7) in the basis (5.30) reads

$$\begin{pmatrix} c^{q} \\ c_{a}^{qr} \\ c_{ab}^{qrs} \end{pmatrix} = e^{\hat{\mathsf{T}}} \begin{pmatrix} f^{p} \\ f_{g}^{pt} \\ f_{gh}^{ptz} \end{pmatrix} \ ,$$

where

$$e^{\pm\hat{\mathsf{T}}} = \begin{pmatrix} \delta_q^p & 0 & 0 \\ 0 & \Delta_{qr}^{pt}\delta_g^a & 0 \\ \pm t_{qrs}^{abp} & 0 & \Delta_{qrs}^{ptz}\Delta_{gh}^{ab} \end{pmatrix}, \tag{5.36}$$

$$t_{qrs}^{abp} = \langle 0|\, \hat{\mathsf{e}}_{qrs}^{ab}\hat{\mathsf{T}}_2\hat{\mathsf{e}}^p\,|0\rangle = \frac{1}{4}t_{ef}^{xy}\Delta_{qrs}^{xyp}\Delta_{ef}^{ab}\,.$$

Thus, the transformed Hamiltonian, $\hat{\overline{\mathsf{H}}} = \exp\{-\hat{\mathsf{T}}\} : \hat{\mathsf{H}} : \exp\{\hat{\mathsf{T}}\}$, Eq. (5.8), is obtain simply by multiplying the matrices in Eqs. (5.31) and (5.36):

$$\begin{pmatrix} \overline{\mathcal{H}}_{11} & \overline{\mathcal{H}}_{13} & \overline{\mathcal{H}}_{15} \\ \overline{\mathcal{H}}_{31} & \overline{\mathcal{H}}_{33} & \overline{\mathcal{H}}_{35} \\ \overline{\mathcal{H}}_{51} & \overline{\mathcal{H}}_{53} & \overline{\mathcal{H}}_{55} \end{pmatrix} \tag{5.37}$$

where

$$\begin{aligned}
\overline{\mathcal{H}}_{11} &= \mathcal{H}_q^u + \mathcal{H}_{qgh}^{xyz}t_{xyz}^{ghu} \\
\overline{\mathcal{H}}_{31} &= \mathcal{H}_{qr}^{au} + \mathcal{H}_{qrgh}^{axyz}t_{xyz}^{ghu} \\
\overline{\mathcal{H}}_{51} &= \mathcal{H}_{qrs}^{abu} - t_{qrs}^{abp}\mathcal{H}_{pgh}^{xyz}t_{xyz}^{ghu} - t_{qrs}^{abp}\mathcal{H}_p^u + \mathcal{H}_{qrsgh}^{abxyz}t_{xyz}^{ghu} \\
\overline{\mathcal{H}}_{53} &= \mathcal{H}_{qrsd}^{abuv} - t_{qrs}^{abp}\mathcal{H}_{pd}^{uv} \\
\overline{\mathcal{H}}_{55} &= \mathcal{H}_{qrscd}^{abuvw} - t_{qrs}^{abp}\mathcal{H}_{pcd}^{uvw}
\end{aligned}$$

and the other elements are the same as in (5.31).

Note that one can formulate in a similar manner also the CCD approach discussed in Chapter 5.3 for closed shells. In that case, one considers a basis given by the reference state $|0\rangle$, four-particle state (a biexcitation) $\hat{\mathsf{e}}_{ab}^{rs}\,|0\rangle$, eight-particle state (a quadruple excitation) $\hat{\mathsf{e}}_{abcd}^{rsuv}\,|0\rangle$ etc.

5.5.1 Adaptation to the Permutation and Spherical Symmetry

Once again, we change first to the ordered and second to the SA amplitudes and CI coefficients; we thus have

$$\begin{pmatrix} C^q \\ C_{\overline{a}}^{\overline{qr}} \\ C_{\overline{ab}}^{\overline{qrs}} \end{pmatrix} = \begin{pmatrix} 1 & 0 & 0 \\ 0 & \sqrt{2!} & 0 \\ 0 & 0 & \sqrt{3!2!} \end{pmatrix} \begin{pmatrix} \delta_q^p & 0 & 0 \\ 0 & \Delta_{qr}^{pt}\delta_g^a & 0 \\ T_{qrs}^{abp} & 0 & \Delta_{qrs}^{ptz}\Delta_{gh}^{ab} \end{pmatrix} \times$$

$$\times \begin{pmatrix} 1 & 0 & 0 \\ 0 & \frac{1}{\sqrt{2!}} & 0 \\ 0 & 0 & \frac{1}{\sqrt{3!2!}} \end{pmatrix} \begin{pmatrix} F^p \\ F_{\overline{g}}^{\overline{pt}} \\ F_{\overline{gh}}^{\overline{ptz}} \end{pmatrix}$$

with

$$T_{qrs}^{abp} = \frac{1}{2}T_{\overline{ef}}^{\overline{xy}}\Delta_{qrs}^{xyp}\Delta_{ef}^{ab}\,,$$

and

$$\begin{pmatrix} C^Q \\ C_A^{\overline{QR},J_{qr}} \\ C_{\overline{AB},J_{ab}}^{\overline{QRS},J_{rs},J_{qrs}} \end{pmatrix} = \begin{pmatrix} 1 & 0 & 0 \\ 0 & \sqrt{2!} & 0 \\ 0 & 0 & \sqrt{3!2!} \end{pmatrix} \times$$

$$\times \begin{pmatrix} \delta^P_Q & 0 & 0 \\ 0 & \delta^P_Q \delta^R_T \delta^A_G \delta^{J_{qr}}_{J_{pt}} & 0 \\ T^{ABP,J_{ab}}_{QRS,J_{rs},J_{qrs}} & 0 & \delta^Q_P \delta^R_T \delta^S_Z \delta^G_A \delta^H_B \delta^{J_{rs}}_{J_{tz}} \delta^{J_{qrs}}_{J_{ptz}} \delta^{J_{ab}}_{J_{gh}} \end{pmatrix} \times$$

$$\times \begin{pmatrix} 1 & 0 & 0 \\ 0 & \frac{1}{\sqrt{2!}} & 0 \\ 0 & 0 & \frac{1}{\sqrt{3!2!}} \end{pmatrix} \begin{pmatrix} F^P \\ F^{\overline{PT},J_{pt}}_G \\ F^{\overline{PTZ},J_{tz},J_{ptz}}_{\overline{GH},J_{gh}} \end{pmatrix},$$

respectively. Here,

$$T^{ABP}_{QRS} = \frac{1}{2} \sum_{i,q,J'} \mathrm{sgn}(\mathcal{P}_p)\mathrm{sgn}(\mathcal{P}_q) G^{j_x,j_y,\delta_{XY},j_a,j_b,\delta_{AB},q}_{j_e,j_f,\delta_{EF},j_q,j_r,j_s,\delta_{QR},\delta_{RS},i}(J', J_{rs}, J_{qrs}, J_{ab}, J) \times$$

$$\times T^{\overline{XY}}_{\overline{EF}}(J') \delta^X_{\mathcal{P}_i(Q)} \delta^Y_{\mathcal{P}_i(R)} \delta^P_{\mathcal{P}_i(S)} \delta^{\mathcal{P}_q(A)}_E \delta^{\mathcal{P}_q(B)}_F ,$$

where

$$G^{j_x,j_y,\delta_{XY},j_a,j_b,\delta_{AB},q}_{j_e,j_f,\delta_{EF},j_q,j_r,j_s,\delta_{QR},\delta_{RS},i}(J', J_{rs}, J_{qrs}, J_{ab}, J) = \sum_{\mathrm{all}\, m's} D^{j_x,m_x,j_y,m_y\delta_{XY}}_{j_e,m_e,j_f,m_f,\delta_{EF}}(J') \times$$

$$\times D^{j_q,m_q,j_r,m_r,j_s,m_s,\delta_{QR},\delta_{RS}}_{j_a,m_a,j_b,m_b,\delta_{AB}}(J_{rs}, J_{qrs}, J_{ab}, J) \delta^{m_x}_{m_{\mathcal{P}_i(q)}} \delta^{m_y}_{m_{\mathcal{P}_i(r)}} \delta^{m_p}_{m_{\mathcal{P}_i(s)}} \delta^{m_{\mathcal{P}_q(a)}}_{m_e} \delta^{m_{\mathcal{P}_q(b)}}_{m_f} .$$

The permutations are defined as, for instance,

$$\begin{aligned} &\mathcal{P}_1(a) = a\,, \quad \mathcal{P}_1(b) = b\,, \quad \mathrm{sgn}(\mathcal{P}_1) = 1\,, \\ &\mathcal{P}_2(a) = b\,, \quad \mathcal{P}_2(b) = a\,, \quad \mathrm{sgn}(\mathcal{P}_2) = -1 \end{aligned}$$

and so on.

5.6 Practical Implementation

5.6.1 Implementation of Symmetry Adaptation

The adaptation to the spherical and permutation symmetry is implemented as follows. First, we generate a list of all possible spinor-angular states (for a given electronic configuration); for example a list of all possible biexcited (i.e., four-particle) states. Next, during the generation of the actual configurations that are then used in the calculation (e.g., biexcitations for the CC method), we mark on the above list those spinor-angular states that will be indeed needed in the calculation. Note that this is only a small fraction of the list of all possible states. Finally, we precalculate the SA factors for the selected spinor-angular states. Later in the calculation of matrix elements for the CC or CI methods, we only load them from memory.

Consider the lithium atom in the non-relativistic approximation for example. It consists of three electrons and is the simplest many-electron open-shell system. The pertinent closed-shell cation is Li^+, i.e., a two-electron helium-like system. On the technical side, let us consider only S and P states and a basis of 3 Sturmian functions per spin-orbital; our basis is thus: $\{1s_{1/2}, 2s_{1/2}, 3s_{1/2}, 2p_{1/2}, 3p_{1/2}, 4p_{1/2}, 2p_{3/2}, 3p_{3/2}, 4p_{3/2}\}$. Recall that for $ns_{1/2}$ states $j = 1/2$, $|K| = 1$, $\kappa = +1$, for $np_{1/2}$ states $j = 1/2$, $|K| = 1$, $\kappa = -1$, for $np_{3/2}$ states $j = 1/2$,

$|K| = 2$, $\kappa = +1$, see Eqs. (4.26)–(4.28). In the CCD calculation, the occupied SA orbitals are $A = B = 1s_{1/2}$ and the virtual SA orbitals R, S are all those remaining ones from the above list, cf. Chapter 5.3.3. There are in general 12 possible configurations for the spinor-angular factors, see Tab. 5.1. However, the 15 possible biexcitations $(\overline{AB}) \to (\overline{RS})$ lead to only 4 types of spinor-angular factors, see Tab. 5.1. Thus, only these four factors are evaluated and then used in the CCD calculation. Notice also that there are no pairs of same orbitals QRS (i.e., $\delta_{X,Y} = 1$) for the configurations 10 – 12 with $J = 1$; this is due to Eq. (5.22).

Table 5.1: List of possible spinor-angular configurations for biexcitations (four-particle states) for He-like systems when S and P states are considered. Note that for He-like systems $j_A = j_B = 1/2$ and thus are not listed in the table. J is the combined total momentum of holes and particles. δ_{XY} denotes whether the spin-orbitals X and Y are the same (1) or not (0). "present" designates whether the given configuration is indeed present in the calculation.

	j_R	j_S	J	δ_{AB}	δ_{RS}	present
1	1/2	1/2	0	0	0	×
2	1/2	1/2	0	0	1	×
3	1/2	1/2	0	1	0	yes
4	1/2	1/2	0	1	1	yes
5	3/2	3/2	0	0	0	×
6	3/2	3/2	0	0	1	×
7	3/2	3/2	0	1	0	yes
8	3/2	3/2	0	1	1	yes
9	1/2	1/2	1	0	0	×
10	1/2	3/2	1	0	0	×
11	3/2	1/2	1	0	0	×
12	3/2	3/2	1	0	0	×

5.6.2 Computational Details

The described post-HF methods were added as an extension to the PASC program published earlier [4]. The program is again written in Fortran 2009 and uses LAPACK for linear algebra operations and OpenMP for parallelization.

The program consists of two parts. First, it contains procedures for both relativistic and non-relativistic HF calculation of closed shells and one-electron open shells using the Sturmian basis set. This part was published earlier [4] and we refer the reader to Ref. [4] for computational details related to these procedures.

Second, it contains post-HF methods described in this paper. Here, the program starts with precalculation of two-electron integrals v_{ij}^{kl} and of factors for adaptation to spherical symmetry. Next it calculates expressions for CC or CI and then solves the CC equations or the CI or CI-CC eigenvalue problem, respectively.

The most time-consuming part is the summation over orbital coefficients in the evaluation of two-electron integrals v_{ij}^{kl}. The problem is that there are very many possible combinations of four orbitals i, j, k, l even when the symmetry of the integrals is taken into account. This part is parallelized and requires the highest number of processors of the whole program; however, it still remains the time bottleneck of the calculation.

In terms of memory, the most problematic are the final matrices to be diagonalized in the CI or CI-CC methods. The reason is simply that there are many three-particle states and even many more five-particle states that need to be included in the calculation to obtain satisfactory results. Note, though, that in the case of CI-CC, it suffices to consider the 2x2 block matrix; it already partially includes the five-particle states and yet it spares us the evaluation of the interaction between two five-particle states which is the most demanding part memory-wise.

5.7 Results and Discussion

The final program contains three optimized post-HF methods: the CCD method for closed shells, the CI method with one-, three- and five-particle states for one-electron open shells, and the combined CI-CC method for one-electron open shells. They all include adaptation to the permutation and spherical symmetry. During the development of the program, we also considered the CI and CC methods in the standard spin-orbital form without any adaptation to the symmetries, with adaptation to the permutation symmetry only and with adaptation to the spherical symmetry only, and verified for small systems that all the approaches yield the same results.

See Tabs. 5.2 and 5.3 for illustration of the significance of the symmetry adaptation and its reduction of the number of configurations. There, we consider the simplest closed-shell system – He-like – and the simplest one-electron open-shell system – Li-like – for illustration. It is important to realize that in the program there are, in fact, nested loops, and thus the reduction factors listed in the tables should be raised to the power of two for linear terms, three for quadratic terms, etc. The factors rapidly increase with the inclusion of higher states, as one can already deduce from the three lowest states presented in the two tables. With increasing basis size, the factors also slightly increase, but they seem to converge to values close (i.e. of the same order) to those listed in the tables.

Further, we can clearly see that the huge number of possible configurations is due to the five-particle states. Unfortunately, we cannot neglect them; their contribution is too large as, for example, the CI method shows. Within the CI-CC approach, it suffices, though, to consider only the 2x2 block matrix instead of the whole 3x3 block matrix, see Eq. (5.37), to obtain accurate enough results. We thus avoid the evaluation of the largest term $\overline{\mathcal{H}}_{55}$. In addition, we only sum over the five-particle states and we are thus left for the final diagonalization with a square matrix which size is given by the sum of the number of one- and three-particle states only. Note also that even the first block $\overline{\mathcal{H}}_{11}$ by itself yields a good estimate on the correlation energy.

We aim to use this methodology to obtain ionization energies of all I.A sys-

tems and eventually compare them with the experimental values. We start, though, with non-relativistic calculations. For lithium, which is a very light element with $Z = 3$, the non-relativistic regime should already yield a very good estimate. Explicitly correlated functionals give $E_{\mathrm{Li}} = -7.4780603239101$ [120] and $E_{\mathrm{Li}^+} = -7.27991341266914$ [121], which then yields ionization energy $E_{\mathrm{ion}} \simeq 0.198147$. The experimental value is $E_{\mathrm{ion}}^{\mathrm{exp}} \simeq 0.19\ 814\ 199\ 04$ [122]. Our current results for lithium, where we used a completely basis independent result $E_{\mathrm{HF}} = -7.236415201452$ and then 20 functions for the $s_{1/2}$-states, 20 functions for the $p_{1/2}$- and $p_{3/2}$-states, 20 functions for the $d_{3/2}$- and $d_{5/2}$-states, 15 functions for the $f_{5/2}$- and $f_{7/2}$-states, gives $E_{\mathrm{Li}} = -7.477471$ and $E_{\mathrm{Li}^+} = -7.279363$ and hence $E_{\mathrm{ion}} \simeq 0.19811$. Notice that the error of the calculations of Li and Li^+ energies partially cancels in the calculation of ionization energy. So far, we have thus obtained a 4-digit agreement and we are now heading towards the 5th digit. Calculation of heavier I.A atoms is also in progress.

Table 5.2: Number of configurations for CCD of He-like systems and illustration of the significance of adaptation to the permutation and spherical symmetry. "all" means all spin-orbitals, "PSA" permutation symmetry-adaptation, "SA" permutation and spherical symmetry-adaptation, S, P, D denotes states that are considered. For this case, 20 basis functions per state were considered.

	S	S, P	S, P, D
all	1 444	15 524	55 204
PSA	361	3 881	13 801
SA	190	610	1 030
factor SA/PSA	2	6	13
factor SA/all	8	25	54

Table 5.3: As Tab. 5.2, but for CI of Li-like systems. 1p, 3p and 5p stand for one-, three- and five-particle states, respectively. For this case, 20 basis functions per state were considered.

		S	S, P	S, P, D
1p	all	19	39	39
	PSA	19	39	39
	SA	19	19	19
	factor SA/PSA	1	2	2
	factor SA/all	1	2	2
3p	all	1 064	13 544	51 584
	PSA	532	6 772	25 792
	SA	361	1 561	3 141
	factor SA/PSA	1.5	4	8
	factor SA/all	3	9	16
5p	all	39 710	1 914 550	15 891 990
	PSA	3 249	158 769	1 321 509
	SA	2 280	25 080	116 440
	factor SA/PSA	1.4	6	11
	factor SA/all	17	76	136

Conclusion

The main results reported in this thesis are:

- We first study the singular behavior of the HF equations. We employ a high-order perturbative method to obtain RHF solutions. Next we use these series to construct stability matrices, which we adapt to spin and orbital symmetry, and to obtain perturbative series for the lowest eigenvalues. The series are then analyzed and onsets of pure singlet, pure spin, pure orbital, and general instabilities are determined. From their positions, we deduce that as long as the shells are filled according to hydrogenic energies, electronic correlation is likely to destabilize the system. However, once this ceases to hold, for instance the 4s orbital is filled before the 3d orbital, electronic correlation has a tendency to stabilize the system.

- Next, we focus on the development of a numerically stable algorithm for the evaluation of integrals between relativistic Sturmian functions. We show how one can obtain one- and two-electron matrix elements with relative error of 10^{-9} – 10^{-15}. We illustrate the method on the calculation of the ground and excited energies, the electric dipole moments, hyperfine integrals and PNC amplitude of Cs in the frozen-core approximation. Except for the energies, our results significantly differ from those previously reported.

- Third, we focus on the electron correlation. We consider the CC method for closed-shell systems and a combined CI-CC method for one-electron open-shell systems. We propose adaptation to permutation symmetry and to the spherical symmetry of atoms; this significantly reduces the number of configurations. We illustrate the proposed approach on the calculation of ionization energies of the I.A elements. So far, we obtained for the lithium atom a 4-digit agreement with the experiment. We are currently progressing towards better agreement with the experiment as well as towards heavier I.A atoms: Na, K, Rb, Cs. Once this project is completed, we believe that we will be able to systematically provide the best theoretical results that may be used for a variety of experiments.

One can continue in these research topics further, for example:

(i) Continuation of the study of singular behavior of the HF equations:

- Apply the proposed perturbative approach and consequent series analysis to more complex systems (e.g., diatomics and extendend systems).

- Study symmetry breaking in open-shell systems.

- Focus on finding a deterministic method for the localization of BS solutions. An idea has been already outlined in [52].

(ii) Use of the algorithm for integrals between relativistic Sturmian functions:

- Apply the devised algorithm to calculation of resonances in helium and other atoms. We have already started this project.

- Use the basis set for the description of the interaction of atoms with strong EM fields, e.g., using the Floquet theory [123].

(iii) Continuation of the inclusion of electron correlation and evaluation of the atomic PNC amplitude:

- Apply additional similarity transformation to eliminate the contribution of three-particle states and thus transform the problem to an effective one-electron Hamiltonian.
- Optimize the screening constants by means of golden-section search algorithm (and thus reduce the required basis size).
- Estimate perturbatively the neglected terms ($\hat{\mathsf{T}}_1$ and $\hat{\mathsf{T}}_3$ clusters for closed shells, transformed five-, Eq. (5.37), and seven-particle states for open shells).
- Transform the relativistic Hamiltonian to a positive definite operator to have the possibility to extrapolate toward infinite basis limit.
- Calculate PNC amplitude (and other properties) for Cs with the CC wave function and improve the convergence of the EW contribution to the PNC amplitude.
- Focus on two-, three-, and more-electron open-shell systems, specifically on Yb, Tl, Pb, and Bi, on which the PNC amplitude has been measured.

References

[1] P. J. Mohr, D. B. Newell, and B. N. Taylor. CODATA recommended values of the fundamental physical constants: 2014. *Reviews of Modern Physics*, 88:035009, 2016.

[2] J. Čížek. Origins of coupled cluster technique for atoms and molecules. *Theoretica Chimica Acta*, 80:91–94, 1991.

[3] T. Uhlířová and J. Zamastil. Stability of the closed-shell atomic configurations with respect to variations in nuclear charge. *Physical Review A*, 101:062504, 2020.

[4] T. Uhlířová, J. Zamastil, and J. Benda. Calculation of atomic integrals between relativistic functions by means of algebraic methods. *Computer Physics Communications*, 280:108490, 2022.

[5] D. Castelvecchi. Next-generation LHC: CERN lays out plans for 21-billion supercollider. *Nature*, 565:410, 2019.

[6] G. Isidori, Y. Nir, and G. Perez. Flavor Physics Constraints for Physics Beyond the Standard Model. *Annual Review of Nuclear and Particle Science*, 60:355–380, 2010.

[7] B. M. Roberts, V. A. Dzuba, and V. V. Flambaum. Parity and Time-Reversal Violation in Atomic Systems. *Annual Review of Nuclear and Particle Science*, 65:63–86, 2015.

[8] J. S. M. Ginges and V. V. Flambaum. Violations of fundamental symmetries in atoms and tests of unification theories of elementary particles. *Physics Reports*, 397:63–154, 2004.

[9] M. S. Safronova, D. Budker, D. DeMille, D. F. J. Kimball, A. Derevianko, and C. W. Clark. Search for new physics with atoms and molecules. *Reviews of Modern Physics*, 90:025008, 2018.

[10] J. Zamastil and J. Benda. *Quantum Mechanics and Electrodynamics*. Springer, 2017.

[11] T. D. Lee and C. N. Yang. Question of Parity Conservation in Weak Interactions. *Physical Review*, 104:254, 1956.

[12] C. S. Wu, E. Ambler, R. W. Hayward, D. D. Hoppes, and R. P. Hudson. Experimental Test of Parity Conservation in Beta Decay. *Physical Review*, 105:1413, 1957.

[13] S. G. Porsev, K. Beloy, and A. Derevianko. Precision determination of weak charge of 133cs from atomic parity violation. *Physical Review D*, 82:036008, 2010.

[14] S. L. Gilbert and C. E. Wieman. Atomic-beam measurement of parity Nonconservation in Cesium. *Physical Review A*, 34(2):792, 1986.

[15] C. S. Wood, S. C. Bennett, D. Cho, B. P. Masterson, J. L. Roberts, C. E. Tanner, and C. E. Wieman. Measurement of Parity Nonconservation and an Anapole Moment in Cesium. *Science*, 275:1759, 1997.

[16] M. Tanabashi et al. (Particle Data Group). Review of Particle Physics. *Physical Review D*, 98:030001, 2018.

[17] https://resonaances.blogspot.com/2022/04/how-large-is-w-boson anomaly.html. How large is the W mass anomaly, 2022.

[18] J. Guéna, D. Chauvat, Ph. Jacquier, E. Jahier, M. Lintz, S. Sanguinetti, A. Wasan, M. A. Bouchiat, A. V. Papoyan, and D. Sarkisyan. New Manifestation of Atomic Parity Violation in Cesium: A Chiral Optical Gain Induced by Linearly Polarized 6S-7S Excitation. *Physical Review Letters*, 90:143001, 2003.

[19] P. S. Drell and E. D. Commins. Parity nonconservation in atomic thallium. *Physical Review A*, 32:2196, 1985.

[20] K. Tsigutkin, D. Dounas-Frazer, A. Family, J. E. Stalnaker, V. V. Yashchuk, and D. Budker. Observation of a Large Atomic Parity Violation Effect in Ytterbium. *Physical Review Letters*, 103:071601, 2009.

[21] D. Antypas, A. M. Fabricant, J. E. Stalnaker, K. Tsigutkin, V. V. Flambaum, and D. Budker. Isotopic variation of parity violation in atomic ytterbium. *Nature Physics*, 15:120–123, 2019.

[22] P. A. Vetter, D. M. Meekhof, P. K. Majumder, S. K. Lamoreaux, and E. N. Fortson. Precise Test of Electroweak Theory from a New Measurement of Parity Nonconservation in Atomic Thallium. *Physical Review Letters*, 74:2658, 1995.

[23] N. H. Edwards, S. J. Phipp, P. E. G. Baird, and S. Nakayama. Precise Measurement of Parity Nonconserving Optical Rotation in Atomic Thallium. *Physical Review Letters*, 74:2654, 1995.

[24] D. M. Meekhof, P. Vetter, P. K. Majumder, S. K. Lamoreaux, and E. N. Fortson. High-precision measurement of parity nonconserving optical rotation in atomic lead. *Physical Review Letters*, 71:3442, 1993.

[25] D. M. Meekhof, P. A. Vetter, P. K. Majumder, S. K. Lamoreaux, and E. N. Fortson. Optical-rotation technique used for a high-precision measurement of parity nonconservation in atomic lead. *Physical Review A*, 52:1895, 1995.

[26] S. J. Phipp, N. H. Edwards, P. E. G. Baird, and S. Nakayama. A measurement of parity non-conserving optical rotation in atomic lead. *Journal of Physics B: Atomic, Molecular and Optical Physics*, 29:1861, 1996.

[27] M. J. D. Macpherson, K. P. Zetie, R. B. Warrington, D. N. Stacey, and J. P. Hoare. Precise measurement of parity nonconserving optical rotation at 876 nm in atomic bismuth. *Physical Review Letters*, 67:2784, 1991.

[28] V. A. Dzuba and V. V. Flambaum. Off-diagonal hyperfine interaction and parity nonconservation in cesium. *Physical Review A*, 62:052101, 2000.

[29] S. C. Bennett and C. E. Wieman. Measurement of the 6S-7S Transition Polarizability in Atomic Cesium and an Improved Test of the Standard Model. *Physical Review Letters*, 82, 1999.

[30] D. Cho, C. S. Wood, S. C. Bennett, J. L. Roberts, and C. E. Wieman. Precision measurement of the ratio of scalar to tensor transition polarizabilities for the cesium 6S-7S transition. *Physical Review A*, 55:1007, 1997.

[31] G. Toh, A. Damitz, N. Glotzbach, J. Quirk, I. C. Stevenson, J. Choi, M. S. Safronova, and D. S. Elliott. Electric dipole matrix elements for the $6p^2P_J \rightarrow 7s^2S_{1/2}$ transition in atomic cesium. *Physical Review A*, 99:032504, 2019.

[32] G. Toh, A. Damitz, C. E. Tanner, W. R. Johnson, and D. S. Elliott. Determination of the Scalar and Vector Polarizabilities of the Cesium $6s^2S_{1/2} \rightarrow 7s^2S_{1/2}$ Transition and Implications for Atomic Parity Nonconservation. *Physical Review Letters*, 123:073002, 2019.

[33] V. A. Dzuba, V. V. Flambaum, and O. P. Sushkov. Summation of the high orders of perturbation theory for the parity nonconserving E1-amplitude of the 6s–7s transition in the cesium atom. *Physics Letters A*, 141:147–153, 1989.

[34] S. A. Blundell, W. R. Johnson, and J. Sapirstein. High-accuracy calculation of the 6S-7S parity-nonconserving transition in atomic cesium and implications for the standard model. *Physical Review Letters*, 65:1411, 1990.

[35] S. A. Blundell, J. Sapirstein, and W. R. Johnson. High-accuracy calculation of parity nonconservation in cesium and implications for particle physics. *Physical Review D*, 45:1602, 1992.

[36] M. G. Kozlov, S. G. Porsev, and I. I. Tupitsyn. High-Accuracy Calculation of 6S-7S Parity-Nonconserving Amplitude in Cs. *Physical Review Letters*, 86:3260, 2001.

[37] V. A. Dzuba, V. V. Flambaum, and J. S. M. Ginges. High-precision calculation of parity nonconservation in cesium and test of the standard model. *Physical Review D*, 66:076013, 2002.

[38] V. A. Dzuba, J. C. Berengut, V. V. Flambaum, and B. M. Roberts. Revisiting Parity Nonconservation in Cesium. *Physical Review Letters*, 109:203003, 2012.

[39] V. A. Dzuba and V. V. Flambaum. Calculation of parity non-conservation in neutral ytterbium. *Physical Review A*, 83:042514, 2011.

[40] V. A. Dzuba and V. V. Flambaum. Calculation of nuclear-spin-dependent parity nonconservation in *s-d* transitions of Ba^+, Yb^+, and Ra^+ ions. *Physical Review A*, 83:052513, 2011.

[41] V. A. Dzuba, V. V. Flambaum, P. G. Silvestrov, and O. P. Sushkov. Calculation of parity non-conservation in thallium. *Journal of Physics B: Atomic and Molecular Physics*, 20:3297, 1987.

[42] M. G. Kozlov, S. G. Porsev, and W. R. Johnson. Parity nonconservation in thallium. *Physical Review A*, 64:052107, 2001.

[43] V. A. Dzuba, V. V. Flambaum, P. G. Silvestrov, and O. P. Sushkov. Relativistic Many-Body Calculations of Parity Nonconservation in Lead and Bismuth Atoms. *Europhysics Letters*, 7:413, 1988.

[44] S. A. Blundell, W. R. Johnson, Z. W. Liu, and J. Sapirstein. Relativistic all-order calculations of energies and matrix elements for Li and Be+. *Physical Review A*, 20:2233, 1989.

[45] S. A. Blundell, W. R. Johnson, Z. W. Liu, and J. Sapirstein. Relativistic all-order equations for helium. *Physical Review A*, 39:3768, 1989.

[46] S. A. Blundell, W. R. Johnson, and J. Sapirstein. Relativistic all-order calculations of energies and matrix elements in cesium. *Physical Review A*, 43:3407, 1991.

[47] M. S. Safronova, A. Derevianko, and W. R. Johnson. Relativistic many-body calculations of energy levels, hyperfine constants, and transition rates for sodiumlike ions, Z=11–16. *Physical Review A*, 58:1016, 1998.

[48] L. F. Pasteka, E. Eliav, A. Borschevsky, U. Kaldor, and P. Schwerdtfeger. Relativistic Coupled Cluster Calculations with Variational Quantum Electrodynamics Resolve the Discrepancy between Experiment and Theory Concerning the Electron Affinity and Ionization Potential of Gold. *Physical Review Letters*, 118:023002, 2017.

[49] R. J. Bartlett and M. Musial. Coupled-cluster theory in quantum chemistry. *Reviews of Modern Physics*, 79:291, 2007.

[50] J. Zamastil, F. Vinette., and M. Šimánek. Calculation of atomic integrals using commutation relations. *Physical Review A*, 75:022506, 2007.

[51] B. G. Adams, J. Čížek, and J. Paldus. Lie Algebraic Methods and Their Applications to Simple Quantum Systems. *Advances in Quantum Chemistry*, 19:1–85, 1988.

[52] T. Uhlířová. Singular Behavior of the Hartree-Fock equations. Master's thesis, 2018.

[53] S. Keller, K. Boguslawski, T. Janowski, M. Reiher, and P. Pulay. Selection of active spaces for multiconfigurational wavefunctions. *Journal of Chemical Physics*, 142:244104, 2015.

[54] D. J. Thouless. Stability Conditions and Nuclear Rotations in the Hartree-Fock Theory. *Nuclear Physics*, 21:225–232, 1960.

[55] D. J. Thouless. *The Quantum Mechanics of Many-body Systems*. Academic Press, 1961.

[56] J. Čížek and J. Paldus. Stability Conditions for the Solutions of the Hartree-Fock Equations for Atomic and Molecular Systems. Application to the Pi-Electron Model of Cyclic Polyenes. *Journal of Chemical Physics*, 47(10):3976–3985, 1967.

[57] J. Paldus and J. Čížek. Stability Conditions for the Solutions of the Hartree-Fock Equations for Atomic and Molecular Systems. II. Simple Open-Shell Case. *Journal of Chemical Physics*, 52(6):2919–2936, 1969.

[58] J. Čížek and J. Paldus. Stability Conditions for the Solutions of the Hartree-Fock Equations for Atomic and Molecular Systems. III. Rules for the Singlet Stability of Hartree-Fock Solutions of Pi-Electronic Systems. *Journal of Chemical Physics*, 53(2):821, 1970.

[59] J. Paldus and J. Čížek. Stability Conditions for the Solutions of the Hartree-Fock Equations for Atomic and Molecular Systems. IV. A Study of Doublet Stability for Odd Linear Polyenic Radicals. *Journal of Chemical Physics*, 54:2293, 1971.

[60] J. Čížek and J. Paldus. Stability Conditions for the Solutions of the Hartree-Fock Equations for Atomic and Molecular Systems. V. The Nonanalytic Behavior of the Broken-Symmetry Solutions at the Branching Point. *Physical Review A*, 3(2):525, 1971.

[61] J. Paldus and J. Čížek. Stability Conditions for the Solutions of the Hartree-Fock Equations for Atomic and Molecular Systems. VI. Singlet-Type Instabilities and Charge-Density-Wave Hartree-Fock Solutions for Cyclic Polyenes. *Physical Review A*, 2(6):2268, 1970.

[62] J. Paldus and J. Čížek. Hartree-Fock stability and symmetry breaking: oxygen doubly negative ion. *Canadian Journal of Chemistry*, 63(7):1803–1811, 1985.

[63] H. Fukutome. Unrestricted Hartree-Fock Theory and Its Applications to Molecules and Chemical Reactions. *International Journal fo Quantum Chemistry*, 20:955–1065, 1981.

[64] J. L. Stuber. *Broken symmetry Hartree-Fock solutions and the many-electron correlation problem*. PhD thesis, University of Waterloo, 2002.

[65] J. L. Stuber and J. Paldus. Symmetry breaking in the independent paricle model. In E. J. Brändas and E. S. Kryachko, editors, *Fundamental World of Quantum Chemistry, A Tribute Volume to the Memory of Per-Olov Löwdin*, volume 1, pages 67–139. Kluwer Academic Publishers, Dordrecht, The Netherlands, 2003.

[66] P. Pulay and T. P. Hamilton. UHF natural orbital for defining and starting MC-SCF calculations. *Journal of Chemical Physics*, 88(8):4926, 1988.

[67] J. M. Bofill and P. Pulay. The unrestricted natural orbital - complete active space (UNO-CAS) method: An inexpensive alternative to the complete active space - self-consistent field (CAS-SCF) method. *Journal of Chemical Physics*, 90(7):3637, 1989.

[68] X. Li and J. Paldus. Computation of molecular vibrational frequencies using anomalous harmoniclike potentials. *Journal of Chemical Physics*, 131:044121, 2009.

[69] X. Li and J. Paldus. Real or artifactual symmetry breaking in the BNB radical: A multireference coupled cluster viewpoint. *Journal of Chemical Physics*, 126:224304, 2007.

[70] Z. Tóth and P. Pulay. Finding symmetry breaking Hartree-Fock solutions: The case of triplet instability. *Journal of Chemical Physics*, 145:164102, 2016.

[71] I. Lindgren and J. Morrison. *Atomic Many-Body Theory*. Springer, 1986.

[72] J. Zamastil, J. Čížek, L. Skála, and M. Šimánek. Convergence of the 1/Z expansion for the energy levels of two-electron atoms. *Physical Review A*, 81:032118, 2010.

[73] N. L. Guevara and A. V. Turbiner. Heliumlike and lithiumlike ionic sequences: Critical charges. *Physical Review A*, 84:064501, 2011.

[74] C. S. Estienne, M. Busuttil, A. Moini, and G. W. F. Drake. Critical Nuclear Charge for Two-Electron Atoms. *Physical Review Letters*, 112:173001, 2014.

[75] J. Zamastil and F. Vinette. Determination of singularities of a function from its perturbation expansion. *Journal of Physics A: Mathematical and General*, 38:4009–4025, 2005.

[76] C. M. Bender and S. A. Orszag. *Advanced Mathematical Methods for Scientists and Engineers*. McGraw-Hill, 1978.

[77] E. J. Weniger. Nonlinear sequence transformations for the acceleration of convergence and the summation of divergent series. *Computer Physics Reports*, 10:189, 1989.

[78] P. Henrici. *Applied and Computational Complex Analysis*. Wiley, 1974.

[79] T. Koga, S. Watanabe, K. Kanayama, R. Yasuda, and A. J. Thakkar. Improved Roothaan–Hartree–Fock wave functions for atoms and ions with N≤54. *The Journal of Chemical Physics*, 103:3000, 1995.

[80] C. F. Bunge, J. A. Barrientos, A. V. Bunge, and J. A. Cogordan. Hartree-Fock and Roothaan-Hartree-Fock energies for the ground states of He through Xe. *Physical Review A*, 46:3691, 1992.

[81] C. F. Bunge, J. A. Barrientos, and A. V. Bunge. Roothan-Hartree-Fock Ground State Atomic Wave Functions, Atomic Data and Nuclear Data Tables 53,113-162, 1993.

[82] E. Clementi and C. Roetti. Roothaan-Hartree-Fock atomic wavefunctions: Basis functions and their coefficients for ground and certain excited states of neutral and ionized atoms, Z≤54. *Atomic Data and Nuclear Data Tables*, 14:177, 1974.

[83] E. Clementi and A. D. McLean. Atomic Negative Ions. *Physical Review*, 133:A419, 1964.

[84] S. Huzinaga and A. Hart-Davis. Stability of the Restricted Hartree-Fock-Roothaan Method. *Physical Review A*, 8:1734, 1973.

[85] G. Delgado-Barrio and R. F. Prat. Deformed Hartree-Fock solutions for atoms. III. Convergent iterative process and results for O–. *Physical Review A*, 12:2288, 1975.

[86] B. Peart, R. A. Forrest, and K. Dolder. A search for structure in cross sections for detachment from C- and O- ions by electron impact. *Journal of Physics B: Atomic and Molecular Physics*, 12:2735, 1979.

[87] S. J. Buckman and C.W. Clark. Atomic negative-ion resonances. *Reviews of Modern Physics*, 66:539, 1994.

[88] J. D. Baker, D. E. Freund, R. N. Hill, and J. D. Morgan III. Radius of convergence and analytic behavior of the 1/Z expansion. *Physical Review A*, 41:1247, 1990.

[89] C. F. Fischer, M. Godefroid, T. Brage, P. Jonsson, and G. Gaigalas. Advanced multiconfiguration methods for complex atoms: I. Energies and wave functions. *Journal of Physics B: Atomic, Molecular and Optical Physics*, 49:182004, 2016.

[90] P. Jönsson, G. Gaigalas, J. Bieron, C. F. Fischer, and I. P. Grant. New version: GRASP2K relativistic atomic structure package. *Computer Physics Communications*, 184:9, 2013.

[91] I. P. Grant. *Relativistic Quantum Theory of Atoms and Molecules, Theory and Computations*. Springer, 2007.

[92] W. R. Johnson, S. A. Blundell, and J. Sapirstein. Finite basis sets for the Dirac equation constructed from B-splines. *Physical Review A*, 37:307, 1988.

[93] W. R. Johnson. *Atomic Structure Theory*. Springer, 2007.

[94] S. Fritzsche. A fresh computational approach to atomic structures, processes and cascades. *A fresh computational approach to atomic structures, processes and cascades*, 240:1–14, 2019.

[95] K. Beloy and A. Derevianko. Application of the dual-kinetic-balance sets in the relativistic many-body problem of atomic structure. *Computer Physics Communications*, 179:310–319, 2008.

[96] V. M. Shabaev, I. I. Tupitsyn, V. A. Yerokhin, G. Plunien, and G. Soff. Dual Kinetic Balance Approach to Basis-Set Expansions for the Dirac Equation. *Physical Review Letters*, 93:130405, 2004.

[97] B. G. Adams. *Algebraic Approach to Simple Quantum Systems with Applications to Perturbation Theory.* Springer Verlag, 1994.

[98] J. Eiglsperger, B. Piraux, and J. Madronero. Spectral representation of the three-body Coulomb problem: Perspectives for highly doubly excited states of helium. *Physical Review A*, 80:02251, 2009.

[99] J. Eiglsperger, B. Piraux, and J. Madronero. Spectral representation of the three-body Coulomb problem. I. Nonautoionizing doubly excited states of high angular momentum in helium. *Physical Review A*, 81:042527, 2010.

[100] J. Eiglsperger, M. Schönwetter, B. Piraux, and J. Madroñero. Spectral data for doubly excited states of helium with non-zero total angular momentum. *Atomic Data and Nuclear Data Tables*, 98:120–148, 2012.

[101] E. Foumouo, G. Lagmago Kamta, G. Edah, and B. Piraux. Theory of multiphoton single and double ionization of two-electron atomic systems driven by short-wavelength electric fields: An ab initio treatment. *Physical Review A*, 74:063409, 2006.

[102] L. C. Biedenharn. Remarks on the Relativistic Kepler Problem. *Physical Review*, 126:845, 1962.

[103] G. Fricke, C. Bernhardt, K. Heilig, L. A. Schaller, L. Schellenberg, E. B. Shera, and C. W. Dejager. Nuclear Ground State Charge Radii from Electromagnetic Interactions. *Atomic Data and Nuclear Data Tables*, 60:177–285, 1995.

[104] F. Coester and H. Kümmel. Short-range correlations in nuclear wave functions. *Nuclear Physics*, 17:477–485, 1960.

[105] J. Čížek. On the Correlation Problem in Atomic and Molecular Systems. Calculation of Wavefunction Components in Ursell-Type Expansion Using Quantum-Field Theoretical Methods. *Journal of Chemical Physics*, 45:4256, 1966.

[106] J. Čížek. On the Use of the Cluster Expansion and the Technique of Diagrams in Calculations of Correlation Effects in Atoms and Molecules. *Advances in Chemical Physics*, 17:35, 1969.

[107] J. Paldus, J. Čížek, and I. Shavitt. Correlation Problems in Atomic and Molecular Systems. IV. Extended Coupled-Pair Many-Electron Theory and Its Application to the BH3 Molecule. *Physical Review A*, 5:50, 1972.

[108] J. Paldus. Correlation problems in atomic and molecular systems. V. Spin-adapted coupled cluster many-electron theory. *The Journal of Chemical Physics*, 67:303, 1977.

[109] J. Paldus and B. G. Adams. Orthogonally-spin-adapted coupled-cluster theory for closed-shell systems including triexcited clusters. *Physical Review A*, 20:1, 1979.

[110] B. G. Adams and J. Paldus. Symmetry-adapted coupled-pair approach to the many-electron correlation problem. I. LS-adapted theory for closed-shell atoms. *Physical Review A*, 24:2302, 1981.

[111] B. G. Adams, K. Jankowski, and J. Paldus. Symmetry-adapted coupled-pair approach to the many-electron correlation problem. II. Application to the Be atom. *Physical Review A*, 24:2316, 1981.

[112] P. O. Löwdin. Angular Momentum Wavefunctions Constructed by Projector Operators. *Reviews of Modern Physics*, 36:966, 1964.

[113] A. V. Bunge, C. F. Bunge, R. Jauregui, and G. Cisneros. Spin eigenfunctions for many-electron calculations. *Computers & Chemistry*, 13:239–254, 1989.

[114] J. Paldus. Plenum Press, nato asi series edition, 1993.

[115] J. Paldus. Nijmegen lectures.

[116] I. Hubač and P. Čársky. In *Organic Chemistry and Theory. Topics in Current Chemistry.* Springer, 1978.

[117] J. Čížek and J. Paldus. Correlation Problems in Atomic and Molecular Systems III. Rederivation of the Coupled-Pair Many-Electron Theory Using the Traditional Quantum Chemical Methods. *International Journal of Quantum Chemistry*, 5:359, 1971.

[118] J. Paldus and B. Jeziorski. Clifford algebra and unitary group formulations of the many-electron problem. *Theoretica Chimica Acta*, 78:81–103, 1988.

[119] J. F. Stanton and R. J. Bartlett. The equation of motion coupled-cluster method. A systematic biorthogonal approach to molecular excitation energies, transition probabilities, and excited state properties. *The Journal of Chemical Physics*, 98:7029, 1993.

[120] M. Puchalski, D. Kedziera, and K. Pachucki. Ground state of Li and Be+ using explicitly correlated functions. *Physical Review A*, 80:032521, 2009.

[121] A. J. Thakkar and T. Koga. Ground-state energies for the helium isoelectronic series. *Physical Review A*, 50:854, 1994.

[122] B. A. Bushaw, W. Nörtershäuser, G. W. F. Drake, and H. J. Kluge. Ionization energy of 6,7Li determined by triple-resonance laser spectroscopy. *Physical Review A*, 75:052503, 2007.

[123] N. Moiseyev. Quantum theory of resonances: calculating energies, widths and cross-sections by complex scaling. *Physics Reports*, 302:212–293, 1998.

List of Figures

List of Tables

Appendix A

A.1 Symmetry-Adapted Form of CC Equations

Forming the SA equations for the cluster amplitudes, we obtain

$$E^{\overline{AB}}_{\overline{RS}}(J) = \sum_{m_a,m_b,m_r,m_s} D^{j_a,m_a,j_b,m_b,\delta_{AB}}_{j_r,m_r,j_s,m_s,\delta_{RS}}(J) E^{\overline{ab}}_{\overline{rs}} =$$

$$\sum_{J'} \Big\{ 2v^{AB}_{RS}(J')[A_0]^{j_a,j_b,\delta_{AB}}_{j_r,j_s,\delta_{RS}}(J,J') + T^{\overline{UV}}_{\overline{CD}}(J')\mathcal{L}^{AB,UV}_{RS,CD}(J,J') +$$

$$+\frac{1}{2^2}\sum_{J''} T^{\overline{UV}}_{\overline{CD}}(J')T^{\overline{XY}}_{\overline{EF}}(J'')\mathcal{Q}^{AB,UV,XY}_{RS,CD,EF}(J,J',J'')\Big\} = 0\,,$$

where the absolute term is

$$[A_0]^{j_a,j_b,\delta_{AB}}_{j_r,j_s,\delta_{RS}}(J,J') = \sum_{\text{all } m's} D^{j_a,m_a,j_b,m_b,\delta_{AB}}_{j_r,m_r,j_s,m_s,\delta_{RS}}(J)\times$$
$$\times\,(j_r,m_r,j_s,m_s|J')(j_a,m_a,j_b,m_b|J')\delta^{m_r+m_s}_{m_a+m_b}\,,$$

the linear term is

$$\mathcal{L}^{AB,UV}_{RS,CD}(J,J') = (\varepsilon_r+\varepsilon_s-\varepsilon_a-\varepsilon_b)\delta^U_R\delta^V_S\delta^A_C\delta^B_D\delta_{J,J'} +$$
$$+\sum_{J''}\Big\{[A_{11}]^{j_a,j_b,\delta_{AB},j_u,j_v,\delta_{UV}}_{j_r,j_s,\delta_{RS},j_c,j_d,\delta_{CD}}(J,J',J'')v^{AB}_{CD}(J'')\delta^U_R\delta^V_S +$$
$$+[A_{12}]^{j_a,j_b,\delta_{AB},j_u,j_v,\delta_{UV}}_{j_r,j_s,\delta_{RS},j_c,j_d,\delta_{CD}}(J,J',J'')v^{UV}_{RS}(J'')\delta^A_C\delta^B_D +$$
$$+\sum_{p_1,p_2,q_1,q_2}\prod_{i=1}^{2}\mathrm{sgn}(\mathcal{P}_{p_i})\mathrm{sgn}(\mathcal{P}_{q_i})[A_{13}]^{j_a,j_b,\delta_{AB},q_1,j_u,j_v,\delta_{UV},q_2}_{j_r,j_s,\delta_{RS},p_1,j_c,j_d,\delta_{CD},p_2}(J,J',J'')\times$$
$$\times\, v^{\mathcal{P}_{q_1}(A),\mathcal{P}_{q_2}(U)}_{\mathcal{P}_{p_1}(R),\mathcal{P}_{p_2}(C)}(J'')\delta^{\mathcal{P}_{p_1}(S)}_{\mathcal{P}_{q_2}(V)}\delta^{\mathcal{P}_{p_2}(D)}_{\mathcal{P}_{q_1}(B)}\Big\}$$

and the quadratic term is

$$\mathcal{Q}^{AB,UV,XY}_{RS,CD,EF}(J,J',J'') = \sum_{J'''}\Big\{\sum_{p_1,p_2,p_3,q_1,q_2,q_3}\prod_{i=1}^{3}\mathrm{sgn}(\mathcal{P}_{p_i})\mathrm{sgn}(\mathcal{P}_{q_i})\times$$
$$\times\,[A_{21}]^{j_a,j_b,\delta_{AB},q_1,j_u,j_v,\delta_{UV},q_2,j_x,j_y,\delta_{XY},q_3}_{j_r,j_s,\delta_{RS},p_1,j_c,j_d,\delta_{CD},p_2,j_e,j_f,\delta_{EF},p_3}(J,J',J'',J''')\times$$
$$\times\,\delta^{\mathcal{P}_{q_2}(V)}_{\mathcal{P}_{p_1}(R)}\delta^{\mathcal{P}_{q_3}(X)}_{\mathcal{P}_{p_1}(S)}\delta^{\mathcal{P}_{q_1}(A)}_{\mathcal{P}_{p_2}(D)}\delta^{\mathcal{P}_{q_1}(B)}_{\mathcal{P}_{p_3}(E)}v^{\mathcal{P}_{q_2}(U),\mathcal{P}_{q_3}(Y)}_{\mathcal{P}_{p_2}(C),\mathcal{P}_{p_3}(F)}(J''')$$
$$+2\sum_{p_1,q_1,q_2,q_3}\prod_{i=1}^{3}\mathrm{sgn}(\mathcal{P}_{p_1})\mathrm{sgn}(\mathcal{P}_{q_i})\times$$
$$\times\,[A_{22}]^{j_a,j_b,\delta_{AB},q_1,j_u,j_v,\delta_{UV},q_2,j_x,j_y,\delta_{XY},q_3}_{j_r,j_s,\delta_{RS},p_1,j_c,j_d,\delta_{CD},j_e,j_f,\delta_{EF}}(J,J',J'',J''')\times$$
$$\times\,\delta^{\mathcal{P}_{q_2}(U)}_{\mathcal{P}_{p_1}(R)}\delta^{\mathcal{P}_{q_3}(X)}_{\mathcal{P}_{p_1}(S)}\delta^{\mathcal{P}_{q_1}(A)}_{C}\delta^{\mathcal{P}_{q_1}(B)}_{D}v^{\mathcal{P}_{q_3}(Y),\mathcal{P}_{q_2}(V)}_{E,F}(J''')$$
$$-2\sum_{p_1,p_2,p_3,q_1}\prod_{i=1}^{3}\mathrm{sgn}(\mathcal{P}_{p_i})\mathrm{sgn}(\mathcal{P}_{q_1})\times$$
$$\times\,[A_{23}]^{j_a,j_b,\delta_{AB},q_1,j_u,j_v,\delta_{UV},j_x,j_y,\delta_{XY}}_{j_r,j_s,\delta_{RS},p_1,j_c,j_d,\delta_{CD},p_2,j_e,j_f,\delta_{EF},p_3}(J,J',J'',J''')\times$$

$$\times \delta^{X}_{\mathcal{P}_{p_1}(R)}\delta^{Y}_{\mathcal{P}_{p_1}(S)}\delta^{\mathcal{P}_{q_1}(A)}_{\mathcal{P}_{p_3}(E)}\delta^{\mathcal{P}_{q_1}(B)}_{\mathcal{P}_{p_2}(D)}v^{U,V}_{\mathcal{P}_{p_2}(C),\mathcal{P}_{p_3}(F)}(J''')$$
$$+ 2\sum_{p_1,q_1}\mathrm{sgn}(\mathcal{P}_{p_1})\mathrm{sgn}(\mathcal{P}_{q_1})[A_{24}]^{j_a,j_b,\delta_{AB},q_1,j_u,j_v,\delta_{UV},j_x,j_y,\delta_{XY}}_{j_r,j_s,\delta_{RS},p_1,j_c,j_d,\delta_{CD},j_e,j_f,\delta_{EF}}(J,J',J'',J'''){\times}$$
$$\times \delta^{X}_{\mathcal{P}_{p_1}(R)}\delta^{Y}_{\mathcal{P}_{p_1}(S)}\delta^{\mathcal{P}_{q_1}(A)}_{C}\delta^{\mathcal{P}_{q_1}(B)}_{D}v^{U,V}_{E,F}(J''')\Bigg\}.$$

The functions A arising from the spinor-angular integrations are for the linear terms

$$[A_{11}]^{j_a,j_b,\delta_{AB},j_u,j_v,\delta_{UV}}_{j_r,j_s,\delta_{RS},j_c,j_d,\delta_{CD}}(J,J',J'') = \sum_{\mathrm{all}\,m's} D^{j_a,m_a,j_b,m_b,\delta_{AB}}_{j_r,m_r,j_s,m_s,\delta_{RS}}(J)D^{j_u,m_u,j_v,m_v,\delta_{UV}}_{j_c,m_c,j_d,m_d,\delta_{CD}}(J'){\times}$$
$$\times (j_a,m_a,j_b,m_b|J'')(j_c,m_d,j_c,m_d|J'')\delta^{m_a+m_b}_{m_c+m_d}\delta^{m_u}_{m_r}\delta^{m_v}_{m_s},$$

$$[A_{12}]^{j_a,j_b,\delta_{AB},j_u,j_v,\delta_{UV}}_{j_r,j_s,\delta_{RS},j_c,j_d,\delta_{CD}}(J,J',J'') = \sum_{\mathrm{all}\,m's} D^{j_a,m_a,j_b,m_b,\delta_{AB}}_{j_r,m_r,j_s,m_s,\delta_{RS}}(J)D^{j_u,m_u,j_v,m_v,\delta_{UV}}_{j_c,m_c,j_d,m_d,\delta_{CD}}(J'){\times}$$
$$\times (j_r,m_r,j_s,m_s|J'')(j_u,m_u,j_v,m_v|J'')\delta^{m_u+m_v}_{m_r+m_s}\delta^{m_a}_{m_c}\delta^{m_b}_{m_d},$$

$$[A_{13}]^{j_a,j_b,\delta_{AB},q_1,j_u,j_v,\delta_{UV},q_2}_{j_r,j_s,\delta_{RS},p_1,j_c,j_d,\delta_{CD},p_2}(J,J',J'') =$$
$$= \sum_{\mathrm{all}\,m's} D^{j_a,m_a,j_b,m_b,\delta_{AB}}_{j_r,m_r,j_s,m_s,\delta_{RS}}(J)D^{j_u,m_u,j_v,m_v,\delta_{UV}}_{j_c,m_c,j_d,m_d,\delta_{CD}}(J'){\times}$$
$$\times (j_{\mathcal{P}_{p_1}(r)},m_{\mathcal{P}_{p_1}(r)},j_{\mathcal{P}_{p_2}(c)},m_{\mathcal{P}_{p_2}(c)}|J''){\times}$$
$$\times (j_{\mathcal{P}_{q_1}(a)},m_{\mathcal{P}_{q_1}(a)},j_{\mathcal{P}_{q_2}(u)},m_{\mathcal{P}_{q_2}(u)}|J''){\times}$$
$$\times \delta^{m_{\mathcal{P}_{q_1}(a)}+m_{\mathcal{P}_{q_2}(u)}}_{m_{\mathcal{P}_{p_1}(r)}+m_{\mathcal{P}_{p_2}(c)}}\delta^{m_{\mathcal{P}_{p_1}(s)}}_{m_{\mathcal{P}_{q_2}(v)}}\delta^{m_{\mathcal{P}_{p_2}(d)}}_{m_{\mathcal{P}_{q_1}(b)}},$$

and for the quadratic terms

$$[A_{21}]^{j_a,j_b,\delta_{AB},q_1,j_u,j_v,\delta_{UV},q_2,j_x,j_y,\delta_{XY},q_3}_{j_r,j_s,\delta_{RS},p_1,j_c,j_d,\delta_{CD},p_2,j_e,j_f,\delta_{EF},p_3}(J,J',J'',J''') =$$
$$= \sum_{\mathrm{all}\,m's} D^{j_a,m_a,j_b,m_b,\delta_{AB}}_{j_r,m_r,j_s,m_s,\delta_{RS}}(J)D^{j_u,m_u,j_v,m_v,\delta_{UV}}_{j_c,m_c,j_d,m_d,\delta_{CD}}(J')D^{j_x,m_x,j_y,m_y,\delta_{XY}}_{j_e,m_e,j_f,m_d,\delta_{EF}}(J''){\times}$$
$$\times \delta^{m_{\mathcal{P}_{q_2}(v)}}_{m_{\mathcal{P}_{p_1}(r)}}\delta^{m_{\mathcal{P}_{q_3}(x)}}_{m_{\mathcal{P}_{p_1}(s)}}\delta^{m_{\mathcal{P}_{q_1}(a)}}_{m_{\mathcal{P}_{p_2}(d)}}\delta^{m_{\mathcal{P}_{q_1}(b)}}_{m_{\mathcal{P}_{p_3}(e)}}\delta^{m_{\mathcal{P}_{q_2}(u)}+m_{\mathcal{P}_{q_3}(y)}}_{m_{\mathcal{P}_{p_2}(c)}+m_{\mathcal{P}_{p_3}(f)}}{\times}$$
$$\times (j_{\mathcal{P}_{p_2}(c)},m_{\mathcal{P}_{p_2}(c)},j_{\mathcal{P}_{p_3}(f)},m_{\mathcal{P}_{p_3}(f)}|J'''){\times}$$
$$\times (j_{\mathcal{P}_{q_2}(u)},m_{\mathcal{P}_{q_2}(u)},j_{\mathcal{P}_{q_3}(y)},m_{\mathcal{P}_{q_3}(y)}|J'''),$$

$$[A_{22}]^{j_a,j_b,\delta_{AB},q_1,j_u,j_v,\delta_{UV},q_2,j_x,j_y,\delta_{XY},q_3}_{j_r,j_s,\delta_{RS},p_1,j_c,j_d,\delta_{CD},j_e,j_f,\delta_{EF}}(J,J',J'',J''') =$$
$$= \sum_{\mathrm{all}\,m's} D^{j_a,m_a,j_b,m_b,\delta_{AB}}_{j_r,m_r,j_s,m_s,\delta_{RS}}(J)D^{j_u,m_u,j_v,m_v,\delta_{UV}}_{j_c,m_c,j_d,m_d,\delta_{CD}}(J')D^{j_x,m_x,j_y,m_y,\delta_{XY}}_{j_e,m_e,j_f,m_d,\delta_{EF}}(J''){\times}$$
$$\times \delta^{m_{\mathcal{P}_{q_2}(u)}}_{m_{\mathcal{P}_{p_1}(r)}}\delta^{m_{\mathcal{P}_{q_3}(x)}}_{m_{\mathcal{P}_{p_1}(s)}}\delta^{m_{\mathcal{P}_{q_1}(a)}}_{m_c}\delta^{m_{\mathcal{P}_{q_1}(b)}}_{m_d}\delta^{m_{\mathcal{P}_{q_3}(y)}+m_{\mathcal{P}_{q_2}(v)}}_{m_e+m_f}{\times}$$
$$\times (j_e,m_e,j_f,m_f|J''')(j_{\mathcal{P}_{q_3}(y)},m_{\mathcal{P}_{q_3}(y)},j_{\mathcal{P}_{q_2}(v)},m_{\mathcal{P}_{q_2}(v)}|J'''),$$

$$[A_{23}]^{j_a,j_b,\delta_{AB},q_1,j_u,j_v,\delta_{UV},j_x,j_y,\delta_{XY}}_{j_r,j_s,\delta_{RS},p_1,j_c,j_d,\delta_{CD},p_2,j_e,j_f,\delta_{EF},p_3}(J,J',J'',J''') =$$
$$= \sum_{\text{all } m's} D^{j_a,m_a,j_b,m_b,\delta_{AB}}_{j_r,m_r,j_s,m_s,\delta_{RS}}(J) D^{j_u,m_u,j_v,m_v,\delta_{UV}}_{j_c,m_c,j_d,m_d,\delta_{CD}}(J') D^{j_x,m_x,j_y,m_y,\delta_{XY}}_{j_e,m_e,j_f,m_d,\delta_{EF}}(J'') \times$$
$$\times \delta^{m_x}_{m_{\mathcal{P}_{p_1}(r)}} \delta^{m_y}_{m_{\mathcal{P}_{p_1}(s)}} \delta^{m_{\mathcal{P}_{q_1}(a)}}_{m_{\mathcal{P}_{p_3}(e)}} \delta^{m_{\mathcal{P}_{q_1}(b)}}_{m_{\mathcal{P}_{p_2}(d)}} \delta^{m_u+m_v}_{m_{\mathcal{P}_{p_2}(c)}+m_{\mathcal{P}_{p_3}(f)}} \times$$
$$\times (j_{\mathcal{P}_{p_2}(c)}, m_{\mathcal{P}_{p_2}(c)}, j_{\mathcal{P}_{p_3}(f)}, m_{\mathcal{P}_{p_3}(f)} | J''')(j_u, m_u, j_v, m_v | J''')$$

$$[A_{24}]^{j_a,j_b,\delta_{AB},q_1,j_u,j_v,\delta_{UV},j_x,j_y,\delta_{XY}}_{j_r,j_s,\delta_{RS},p_1,j_c,j_d,\delta_{CD},j_e,j_f,\delta_{EF}}(J,J',J'',J''') =$$
$$= \sum_{\text{all } m's} D^{j_a,m_a,j_b,m_b,\delta_{AB}}_{j_r,m_r,j_s,m_s,\delta_{RS}}(J) D^{j_u,m_u,j_v,m_v,\delta_{UV}}_{j_c,m_c,j_d,m_d,\delta_{CD}}(J') D^{j_x,m_x,j_y,m_y,\delta_{XY}}_{j_e,m_e,j_f,m_d,\delta_{EF}}(J'') \times$$
$$\times \delta^{m_x}_{m_{\mathcal{P}_{p_1}(r)}} \delta^{m_y}_{m_{\mathcal{P}_{p_1}(s)}} \delta^{m_{\mathcal{P}_{q_1}(a)}}_{m_c} \delta^{m_{\mathcal{P}_{q_1}(b)}}_{m_d} \delta^{m_e+m_f}_{m_u+m_v} \times$$
$$\times (j_e, m_e, j_f, m_f | J''')(j_u, m_u, j_v, m_v | J''') \,.$$

A.2 Symmetry-Adapted Form of CI Method

The SA form of the CI method for one-electron open-shell systems reads

$$\begin{pmatrix} 1 & 0 & 0 \\ 0 & \sqrt{2!} & 0 \\ 0 & 0 & \sqrt{3!2!} \end{pmatrix} \begin{pmatrix} \mathcal{H}^{U}_{Q} & \mathcal{H}^{UV,J_{uv}}_{QD} & \mathcal{H}^{UVW,J_{vw},J_{uvw}}_{QCD,J_{cd}} \\ \mathcal{H}^{AU}_{QR,J_{qr}} & \mathcal{H}^{AUV,J_{uv}}_{QRD,J_{qr}} & \mathcal{H}^{AUVW,J_{vw},J_{uvw}}_{QRCD,J_{qr},J_{cd}} \\ \mathcal{H}^{ABU,J_{ab}}_{QRS,J_{rs},J_{qrs}} & \mathcal{H}^{ABUV,J_{ab},J_{uv}}_{QRSD,J_{rs},J_{qrs}} & \mathcal{H}^{ABUVW,J_{ab},J_{vw},J_{uvw}}_{QRSCD,J_{rs},J_{qrs},J_{cd}} \end{pmatrix} \times$$
$$\times \begin{pmatrix} 1 & 0 & 0 \\ 0 & \frac{1}{\sqrt{2!}} & 0 \\ 0 & 0 & \frac{1}{\sqrt{3!2!}} \end{pmatrix} \begin{pmatrix} C^{U} \\ C^{\overline{UV},J_{uv}}_{D} \\ C^{\overline{UVW},J_{vw},J_{uvw}}_{\overline{CD},J_{cd}} \end{pmatrix} = \Delta E \begin{pmatrix} C^{Q} \\ C^{\overline{QR},J_{qr}}_{A} \\ C^{\overline{QRS},J_{rs},J_{qrs}}_{\overline{AB},J_{ab}} \end{pmatrix},$$

where

$$\mathcal{H}^{UV,J_+}_{QD}(J) = \sum_{J'} v^{UV}_{QD}(J') [B_{13}]^{j_u,j_v,\delta_{UV}}_{J,j_d}(J_+, J', J) \,,$$

$$\mathcal{H}^{UVW,J_{vw},J_+}_{QCD,J_-}(J) = \sum_{J',q} \frac{1+\mathrm{sgn}(\mathcal{P}_q)}{2} \delta^{\mathcal{P}_q(W)}_{Q} v^{\mathcal{P}_q(U)\mathcal{P}_q(V)}_{CD}(J') \times$$
$$\times [B_{15}]^{j_u,j_v,j_w,\delta_{UV},\delta_{VW},q}_{j_c,j_d,\delta_{CD}}(J', J_{vw}, J_+, J_-, J) \,,$$

$$\mathcal{H}^{AUV,J_{uv}}_{QRD,J_{qr}}(J) = (\varepsilon_q + \varepsilon_r - \varepsilon_a)\delta^{A}_{D}\delta^{U}_{Q}\delta^{V}_{R} +$$
$$+ \sum_{J'} \delta^{A}_{D} v^{UV}_{QR}(J') [B_{33,1}]^{j_a,j_u,j_v,\delta_{UV}}_{j_d,j_q,j_r,\delta_{QR}}(J', J_{uv}, J_{qr}, J) +$$
$$+ \sum_{J',p,q} \mathrm{sgn}\mathcal{P}_p \mathrm{sgn}\mathcal{P}_q \delta^{\mathcal{P}_q(V)}_{\mathcal{P}_p(R)} v^{\mathcal{P}_q(U)A}_{D\mathcal{P}_p(Q)}(J') [B_{33,2}]^{j_a,j_u,j_v,\delta_{UV},q}_{j_d,j_q,j_r,\delta_{QR},p}(J', J_{uv}, J_{qr}, J)$$

$$\mathcal{H}^{AUVW,J_{vw},J_+}_{QRCD,J_{qr},J_-}(J) = \sum_{J',q} \mathrm{sgn}(\mathcal{P}_q)\delta^{\mathcal{P}_q(U)}_{Q}\delta^{\mathcal{P}_q(V)}_{R} v^{\mathcal{P}_q(W)A}_{CD}(J')\times$$
$$\times [B_{35,1}]^{j_a,j_u,j_v,j_w,\delta_{UV},\delta_{VW},q}_{j_q,j_r,\delta_{QR},j_c,j_d,\delta_{CD}}(J', J_{qr}, J_{vw}, J_+, J_-, J)+$$
$$+ \sum_{J',q,p_1,p_2} \frac{1+\mathrm{sgn}(\mathcal{P}_q)}{2}\prod_{i=1}^{2}\mathrm{sgn}(\mathcal{P}_{p_i})\delta^{A}_{\mathcal{P}_{p_2}(C)}\delta^{\mathcal{P}_q(W)}_{\mathcal{P}_{p_1}(Q)} v^{\mathcal{P}_q(U)\mathcal{P}_q(V)}_{\mathcal{P}_{p_2}(D)\mathcal{P}_{p_1}(R)}(J')\times$$
$$\times [B_{35,2}]^{j_a,j_u,j_v,j_w,\delta_{UV},\delta_{VW},q}_{j_q,j_r,\delta_{QR},p_1,j_c,j_d,\delta_{CD},p_2}(J', J_{qr}, J_{vw}, J_+, J_-, J)\,,$$

$$\mathcal{H}^{ABUVW,J_{ab},J_{vw},J_{uvw}}_{QRSCD,J_{rs},J_{qrs},J_{cd}}(J) = (\varepsilon_q+\varepsilon_r+\varepsilon_s-\varepsilon_a-\varepsilon_b)\delta^{A}_{C}\delta^{B}_{D}\delta^{U}_{Q}\delta^{V}_{R}\delta^{W}_{S}+$$
$$+\sum_{J'}\delta^{U}_{Q}\delta^{V}_{R}\delta^{W}_{S}v^{AB}_{CD}(J')\times$$
$$\times [B_{55,1}]^{j_a,j_b,\delta_{AB},j_u,j_v,j_w,\delta_{UV},\delta_{VW}}_{j_q,j_r,j_s,\delta_{QR},\delta_{RS},j_c,j_d,\delta_{CD}}(J', J_{qr}, J_{qrs}, J_{ab}, J_{vw}, J_{qvw}, J_{cd}, J)+$$
$$+\sum_{J',p,q}\frac{1+\mathrm{sgn}(\mathcal{P}_p)}{2}\frac{1+\mathrm{sgn}(\mathcal{P}_q)}{2}\delta^{A}_{C}\delta^{B}_{D}\delta^{\mathcal{P}_q(W)}_{\mathcal{P}_p(Q)}v^{\mathcal{P}_q(U)\mathcal{P}_q(V)}_{\mathcal{P}_p(R)\mathcal{P}_p(S)}(J')\times$$
$$\times [B_{55,2}]^{j_a,j_b,\delta_{AB},j_u,j_v,j_w,\delta_{UV},\delta_{VW},q}_{j_q,j_r,j_s,\delta_{QR},\delta_{RS},p,j_c,j_d,\delta_{CD}}(J', J_{qr}, J_{qrs}, J_{ab}, J_{vw}, J_{qvw}, J_{cd}, J)+$$
$$+\sum_{J',q_1,q_2,p_1,p_2}\frac{1+\mathrm{sgn}(\mathcal{P}_{q_2})}{2}\mathrm{sgn}(\mathcal{P}_{q_1})\prod_{i=1}^{2}\mathrm{sgn}(\mathcal{P}_{p_i})\times$$
$$\times \delta^{\mathcal{P}_{q_2}(U)}_{\mathcal{P}_{p_1}(R)}\delta^{\mathcal{P}_{q_2}(V)}_{\mathcal{P}_{p_1}(S)}\delta^{\mathcal{P}_{q_1}(A)}_{\mathcal{P}_{p_2}(C)}v^{\mathcal{P}_{q_2}(W)\mathcal{P}_{q_1}(B)}_{\mathcal{P}_{p_2}(D)\mathcal{P}_{p_1}(Q)}(J')\times$$
$$\times [B_{55,3}]^{j_a,j_b,\delta_{AB},q_1,j_u,j_v,j_w,\delta_{UV},\delta_{VW},q_2}_{j_q,j_r,j_s,\delta_{QR},\delta_{RS},p_1,j_c,j_d,\delta_{CD},p_2}(J', J_{qr}, J_{qrs}, J_{ab}, J_{vw}, J_{qvw}, J_{cd}, J)\,.$$

Here, the various spinor-angular functions B read

$$[B_{13}]^{j_u,j_v,\delta_{UV}}_{J,j_d}(J_+, J', J) = \sum_{\mathrm{all}\, m's} D^{j_u,m_u,j_v,m_v,\delta_{UV}}_{j_d,m_d}(J_+, J)\times$$
$$\times (j_u,m_u,j_v,m_v|J')(J,M,j_d,m_d|J')\delta^{m_u+m_v}_{M+m_d}\,,$$

$$[B_{15}]^{j_u,j_v,j_w,\delta_{UV},\delta_{VW},i}_{j_c,j_d,\delta_{CD}}(J', J_{vw}, J_+, J_-, J) =$$
$$= \delta^{j_{\mathcal{P}_i(w)}}_{J}\sum_{\mathrm{all}\, m's} D^{j_u,m_u,j_v,m_v,j_w,m_w,\delta_{UV},\delta_{VW}}_{j_c,m_c,j_d,m_d,\delta_{CD}}(J_{vw}, J_+, J_-, J)\times$$
$$\times (j_{\mathcal{P}_i(u)}, m_{\mathcal{P}_i(u)}, j_{\mathcal{P}_i(v)}, m_{\mathcal{P}_i(v)}|J')(j_c,m_c,j_d,m_d|J')\delta^{m_{\mathcal{P}_i(u)}+m_{\mathcal{P}_i(v)}}_{m_c+m_d}\delta^{m_{\mathcal{P}_i(w)}}_{M}\,,$$

$$[B_{33,1}]^{j_a,j_u,j_v,\delta_{UV}}_{j_d,j_q,j_r,\delta_{QR}}(J', J_{uv}, J_{qr}, J) = \delta^{j_a}_{j_d}\times$$
$$\times \sum_{\mathrm{all}\, m's} D^{j_u,m_u,j_v,m_v,\delta_{UV}}_{j_d,m_d}(J_{uv}, J)D^{j_q,m_q,j_r,m_r,\delta_{QR}}_{j_a,m_a}(J_{qr}, J)\times$$
$$\times (j_u,m_u,j_v,m_v|J')(j_q,m_q,j_r,m_r|J')\delta^{m_u+m_v}_{m_q+m_r}\delta^{m_a}_{m_d}\,,$$

$$[B_{33,2}]^{j_a,j_u,j_v,\delta_{UV},k}_{j_d,j_q,j_r,\delta_{QR},i}(J', J_{uv}, J_{qr}, J) = \delta^{j_{\mathcal{P}_k(v)}}_{j_{\mathcal{P}_i(r)}}\times$$
$$\times \sum_{\mathrm{all}\, m's} D^{j_u,m_u,j_v,m_v,\delta_{UV}}_{j_d,m_d}(J_{uv}, J)D^{j_q,m_q,j_r,m_r,\delta_{QR}}_{j_a,m_a}(J_{qr}, J)\times$$
$$\times (j_d,m_d,j_{\mathcal{P}_i(q)},m_{\mathcal{P}_i(q)}|J')(j_{\mathcal{P}_k(u)},m_{\mathcal{P}_k(u)},j_a,m_a|J')\delta^{m_{\mathcal{P}_k(u)}+m_a}_{m_d+m_{\mathcal{P}_i(q)}}\delta^{m_{\mathcal{P}_k(v)}}_{m_{\mathcal{P}_i(r)}}\,,$$

$$[B_{35,1}]^{j_a,j_u,j_v,j_w,\delta_{UV},\delta_{VW},q}_{j_q,j_r,\delta_{QR},j_c,j_d,\delta_{CD}}(J',J_{qr},J_{vw},J_+,J_-,J)=\delta^{j_{\mathcal{P}_q(u)}}_{j_q}\delta^{j_{\mathcal{P}_q(v)}}_{j_r}\times$$
$$\times\sum_{\text{all }m's}D^{j_q,m_q,j_r,m_r,\delta_{QR}}_{j_a,m_a}(J_{qr},J)D^{j_u,m_u,j_v,m_v,j_w,m_w,\delta_{UV},\delta_{VW}}_{j_c,m_c,j_d,m_d,\delta_{CD}}(J_{vw},J_+,J_-,J)\times$$
$$\times\delta^{m_{\mathcal{P}_q(u)}}_{m_q}\delta^{m_{\mathcal{P}_q(v)}}_{m_r}(j_c,m_c,j_d,m_d|J')(j_{\mathcal{P}_q(w)},m_{\mathcal{P}_q(w)},j_a,m_a|J')\delta^{m_{\mathcal{P}_q(w)}+m_a}_{m_c+m_d},$$

$$[B_{35,2}]^{j_a,j_u,j_v,j_w,\delta_{UV},\delta_{VW},q}_{j_q,j_r,\delta_{QR},p_1,j_c,j_d,\delta_{CD},p_2}(J',J_{qr},J_{vw},J_+,J_-,J)=\delta^{j_a}_{j_{\mathcal{P}_{p_2}(c)}}\delta^{j_{\mathcal{P}_q(w)}}_{j_{\mathcal{P}_{p_1}(q)}}\times$$
$$\times\sum_{\text{all }m's}D^{j_q,m_q,j_r,m_r,\delta_{QR}}_{j_a,m_a}(J_{qr},J)D^{j_u,m_u,j_v,m_v,j_w,m_w,\delta_{UV},\delta_{VW}}_{j_c,m_c,j_d,m_d,\delta_{CD}}(J_{vw},J_+,J_-,J)\times$$
$$\times\delta^{m_a}_{m_{\mathcal{P}_{p_2}(c)}}\delta^{m_{\mathcal{P}_q(w)}}_{m_{\mathcal{P}_{p_1}(q)}}(j_{\mathcal{P}_q(u)},m_{\mathcal{P}_q(u)},j_{\mathcal{P}_q(v)},m_{\mathcal{P}_q(v)}|J')\times$$
$$\times(j_{\mathcal{P}_{p_2}(d)},m_{\mathcal{P}_{p_2}(d)},j_{\mathcal{P}_{p_1}(r)},m_{\mathcal{P}_{p_1}(r)}|J')\delta^{m_{\mathcal{P}_q(u)}+m_{\mathcal{P}_q(v)}}_{m_{\mathcal{P}_{p_2}(d)}+m_{\mathcal{P}_{p_1}(r)}},$$

$$[B_{55,1}]^{j_a,j_b,\delta_{AB},j_u,j_v,j_w,\delta_{UV},\delta_{VW}}_{j_q,j_r,j_s,\delta_{QR},\delta_{RS},j_c,j_d,\delta_{CD}}(J',J_{qr},J_{qrs},J_{ab},J_{vw},J_{qvw},J_{cd},J)=\delta^{j_u}_{j_q}\delta^{j_v}_{j_r}\delta^{j_w}_{j_s}\times$$
$$\times\sum_{\text{all }m's}D^{j_q,m_q,j_r,m_r,j_s,m_s,\delta_{QR},\delta_{RS}}_{j_a,m_a,j_b,m_b,\delta_{AB}}(J_{qr},J_{qrs},J_{ab},J)\times$$
$$\times D^{j_u,m_u,j_v,m_v,j_w,m_w,\delta_{UV},\delta_{VW}}_{j_c,m_c,j_d,m_d,\delta_{CD}}(J_{vw},J_{uvw},J_{cd},J)\times$$
$$\times\delta^{m_u}_{m_q}\delta^{m_v}_{m_r}\delta^{m_w}_{m_s}(j_a,m_a,j_b,m_b|J')(j_c,m_c,j_d,m_d|J')\delta^{m_c+m_d}_{m_a+m_b},$$

$$[B_{55,2}]^{j_a,j_b,\delta_{AB},j_u,j_v,j_w,\delta_{UV},\delta_{VW},q}_{j_q,j_r,j_s,\delta_{QR},\delta_{RS},p,j_c,j_d,\delta_{CD}}(J',J_{qr},J_{qrs},J_{ab},J_{vw},J_{qvw},J_{cd},J)=\delta^{j_a}_{j_c}\delta^{j_b}_{j_d}\delta^{j_{\mathcal{P}_q(w)}}_{j_{\mathcal{P}_p(q)}}\times$$
$$\times\sum_{\text{all }m's}D^{j_q,m_q,j_r,m_r,j_s,m_s,\delta_{QR},\delta_{RS}}_{j_a,m_a,j_b,m_b,\delta_{AB}}(J_{qr},J_{qrs},J_{ab},J)\times$$
$$\times D^{j_u,m_u,j_v,m_v,j_w,m_w,\delta_{UV},\delta_{VW}}_{j_c,m_c,j_d,m_d,\delta_{CD}}(J_{vw},J_{uvw},J_{cd},J)\times$$
$$\times\delta^{m_a}_{m_c}\delta^{m_b}_{m_d}\delta^{m_{\mathcal{P}_q(w)}}_{m_{\mathcal{P}_p(q)}}(j_{\mathcal{P}_q(u)},m_{\mathcal{P}_q(u)},j_{\mathcal{P}_q(v)},m_{\mathcal{P}_q(v)}|J')\times$$
$$\times(j_{\mathcal{P}_p(r)},m_{\mathcal{P}_p(r)},j_{\mathcal{P}_p(s)},m_{\mathcal{P}_p(s)}|J')\delta^{m_{\mathcal{P}_q(u)}+m_{\mathcal{P}_q(v)}}_{m_{\mathcal{P}_p(r)}+m_{\mathcal{P}_p(s)}}$$

and

$$[B_{55,3}]^{j_a,j_b,\delta_{AB},q_1,j_u,j_v,j_w,\delta_{UV},\delta_{VW},q_2}_{j_q,j_r,j_s,\delta_{QR},\delta_{RS},p_1,j_c,j_d,\delta_{CD},p_2}(J',J_{qr},J_{qrs},J_{ab},J_{vw},J_{qvw},J_{cd},J)=$$
$$=\delta^{j_{\mathcal{P}_{q_2}(u)}}_{j_{\mathcal{P}_{p_1}(r)}}\delta^{j_{\mathcal{P}_{q_2}(v)}}_{j_{\mathcal{P}_{p_1}(s)}}\delta^{j_{\mathcal{P}_{q_1}(a)}}_{j_{\mathcal{P}_{p_2}(c)}}\times$$
$$\times\sum_{\text{all }m's}D^{j_q,m_q,j_r,m_r,j_s,m_s,\delta_{QR},\delta_{RS}}_{j_a,m_a,j_b,m_b,\delta_{AB}}(J_{qr},J_{qrs},J_{ab},J)\times$$
$$\times D^{j_u,m_u,j_v,m_v,j_w,m_w,\delta_{UV},\delta_{VW}}_{j_c,m_c,j_d,m_d,\delta_{CD}}(J_{vw},J_{uvw},J_{cd},J)\times$$
$$\times\delta^{m_{\mathcal{P}_{q_2}(u)}}_{m_{\mathcal{P}_{p_1}(r)}}\delta^{m_{\mathcal{P}_{q_2}(v)}}_{m_{\mathcal{P}_{p_1}(s)}}\delta^{m_{\mathcal{P}_{q_1}(a)}}_{m_{\mathcal{P}_{p_2}(c)}}(j_{\mathcal{P}_{q_2}(w)},m_{\mathcal{P}_{q_2}(w)},j_{\mathcal{P}_{q_1}(b)},m_{\mathcal{P}_{q_1}(b)}|J')\times$$
$$\times(j_{\mathcal{P}_{p_2}(d)},m_{\mathcal{P}_{p_2}(d)},j_{\mathcal{P}_{p_1}(q)},m_{\mathcal{P}_{p_1}(q)}|J')\delta^{m_{\mathcal{P}_{q_2}(w)}+m_{\mathcal{P}_{q_1}(b)}}_{m_{\mathcal{P}_{p_2}(d)}+m_{\mathcal{P}_{p_1}(q)}}.$$

Attachments

[3] T. Uhlířová and J. Zamastil. Stability of the closed-shell atomic configurations with respect to variations in nuclear charge. *Physical Review A*, 101:062504, 2020. Including SI.

[4] T. Uhlířová, J. Zamastil, and J. Benda. Calculation of atomic integrals between relativistic functions by means of algebraic methods. *Computer Physics Communications*, 280:108490, 2022.